CRACKING MODE AND SHEAR STRENGTH OF LIGHTWEIGHT CONCRETE BEAMS

KUM YUNG JUAN

NATIONAL UNIVERSITY OF SINGAPORE

2011

CRACKING MODE AND SHEAR STRENGTH OF LIGHTWEIGHT CONCRETE BEAMS

KUM YUNG JUAN

(B.Eng (Hons.) Malaya)

A THESIS SUBMITTED FOR
THE DEGREE OF DOCTOR OF PHILOSOPHY

DEPARTMENT OF
CIVIL AND ENVIRONMENTAL ENGINEERING

NATIONAL UNIVERSITY OF SINGAPORE

2011

Acknowledgement

The author would like to record his sincere thanks and gratitude to his late supervisor, Associate Professor Wee Tiong Huan for his invaluable guidance, advice, and encouragement throughout this study. He also wishes to thank Professor M. A. Mansur for his input on developing the research program.

The author acknowledges the support and facilities provided by the National University of Singapore to carry out this research. Special thanks are due to the staff of the Structural Engineering and Concrete Laboratory at NUS for their assistance and help in preparing and setting up the experimental part of this study. The assistance from the Building and Construction Authority in the form of a grant, which this research forms a part, is also gratefully acknowledged.

Special thanks are extended to NUS Senior Research Fellow, Dr. Tamilselvan T., for his guidance and advice as well as to NUS Senior Research Engineer, Jacob Lim L. G., and my colleague Dr. Thamaraikkannan V. T. The highest appreciation is reserved for their friendly comments, perspective, and constructive distractions that were always welcomed with good spirits.

Finally the author expresses his deepest appreciation for the patience, understanding, and unwavering support of his partner Joanne, as well as from his parents and siblings who maintained the numinous from the quotidian.

This page intentionally left blank for pagination.

Table of Contents

This page intentionally left blank for pagination.

Summary

Lightweight concrete is a high performance material with advantages for a myriad of applications. It has the potential to be used in sophisticated structures like prefabricated high-rise construction and architectural icons, to simple low-cost housing and rapidly erected semi-permanent structures.

There however remains significant lacunae in engineering knowledge with regards to shear response of reinforced concrete. This is especially true of lightweight concrete with and without aggregates which remains a maturing engineering material. While lightweight aggregate concrete has been introduced and successfully used in specialized environments, it has yet to generate mainstream acceptance as an alternative to normal weight concrete.

An experimental program including 64 lightweight concrete beams without transverse reinforcement and 22 companion normal weight concrete reference beams were tested under monotonically increasing third point loading until ultimate physical failure. The results were analyzed and compared with empirical equations in the literature as well as international reinforced concrete building codes.

Within the scope of this study, it was found that lightweight aggregate concrete beams without transverse reinforcement behaved in a similar manner to the reference normal weight concrete beams until the onset of diagonal cracking. Thereafter, while normal weight concrete beams were able to continue resisting shear until a flexural mode of physical failure occurred, lightweight aggregate concrete was unable to develop sufficient resistance and physically failed in a brittle shear mode.

Foamed concrete and lightweight aggregate-foamed concrete also responded to loads like normal weight concrete. Diagonal cracking occurred at lower

loads than both normal weight concrete and lightweight aggregate concrete due to its tensile strength being much lower than the reference concrete although having comparable compressive strengths. Nevertheless, after the onset of diagonal cracking, foamed concrete and lightweight aggregate-foamed concrete was able to continue resisting a significant amount of shear prior to physical ultimate failure. This ability was found to be due to the irregular and angular cracking plane at the macro level compared to the smooth crack surface at the micro level.

Using the diagonal cracking and ultimate shear capacity data generated from this test program and the rigorous observations recorded, a prediction equation was derived for shear strength of lightweight concrete beams without transverse shear reinforcement based on the parametric behavior model of Russo *et al.* (2005). This diagonal cracking equation was then tested against the results of a set of rectangular lightweight concrete beams as well as data from the literature and found to be in good agreement across the range of parameters tested including with and without shear reinforcement.

Comparison of the performance of these lightweight high-strength concrete beams with and without transverse reinforcement against design equations of the American Concrete Institute and the British Standards Institute show that the design equations can be used with confidence. Diagonal cracking of lightweight concrete beams only occur beyond the design loads and deflection limits imposed. However, caution should be exercised when considering the behavior of lightweight concrete beams beyond service loads as the physical shear capacity of the material may be exhausted prior to its flexural capacity.

List of Tables

This page intentionally left blank for pagination.

List of Figures

This page intentionally left blank for pagination.

List of Symbols

a	Shear span
A_s	Longitudinal tensile steel area
A_{sw}	Transverse tensile steel area
b_w, b_v	Web width
d	Effective depth
d_a	Aggregate size
D_c	Aggregate density
E_c	Modulus of elasticity of concrete
f_{cd}	Design compressive strength of concrete
f_{ck}	Characteristic concrete compressive strength – cylinder
f_{ct}	Concrete splitting tensile strength
f_{cu}	Concrete compressive strength – cube
f_t	Concrete tensile strength
f'_c	Concrete compressive strength – cylinder
f'_{yl}	Yield strength of steel reinforcement
f_{ywd}	Yield strength of transverse reinforcement
j_0	Flexural lever arm
M_u	Ultimate applied bending moment
V	Shear force
V_c	Concrete contribution shear force resistance
V_{du}	Ultimate shear resistance of dowel action
$V_{Rd,c}$	Ultimate applied shear force at cracking, without transverse reinforcement
$V_{Rd,s}$	Ultimate capacity of vertical shear reinforcement
$V_{Rd,max}$	Ultimate capacity of concrete compression strut
V_s	Transverse steel contribution shear force resistance
V_u	Ultimate applied shear force

w_c Concrete density

k, p, q, s, z, α Constant factor

z Moment lever arm

α_{cc} coefficient taking account of long term effects on the compressive strength and of unfavorable effects resulting from the way the load is applied

α_{cw} Coefficient for state of stress in compression chord

ρ_w, ρ Reinforcement ratio

γ_c Concrete material safety factor

γ_m Material safety factor

v_1 Strength reduction factor for concrete cracked in shear

v_u Ultimate applied shear stress

v_{cr} Applied shear stress at cracking

σ_{cp} Mean compressive stress in the section due to axial force and prestress

η, λ, ξ Size effect factor

θ Angle of compression strut in rotating angle truss model

Δn_u Critical crack width

Chapter 1 Introduction

Concrete is a non-homogenous solid matrix of materials that is the most widely used man made substance on the planet (Lomborg 2001). In its simplest form, concrete is made up of four basic components: cement, water, fine aggregate, and coarse aggregate. A hydration reaction between cement and water creates a hardening paste that binds the aggregates with strength of the resulting concrete found to be predominantly governed by its water-to-cement ratio. Using a small ratio, compressive strengths in excess of 100 MPa can be routinely produced on a commercial scale (ACI 363R-92).

Although concrete can develop high compressive strengths, plain concrete is unsuitable for structural applications due to a low tensile capacity, in the order of 10 percent of its compressive strength. Steel reinforcing bars are then introduced to form a composite system where tensile forces are resisted by steel and compressive forces by concrete. With both concrete and steel acting in tandem, reinforced concrete becomes an excellent construction material with many advantages over other structural media.

Nevertheless, producing concrete using rock based aggregates tends to yield concrete with heavy densities in the region of 2300 kg/m^3 to 2400 kg/m^3 regardless of strength. This gives rise to unattractive strength-to-weight ratios as compared to structural steel, especially in concretes with low strengths where a large fraction of the inherent capacity is expended to support its self-weight. Concrete structures in general thus have dead loads that exceed the imposed loads in contrast to steel structures where the dead load is usually comparable to the imposed loads.

This poor strength-to-weight ratio can be improved either by increasing the material strength or by reducing its self-weight. The former is accomplished in high

strength concretes where the development of superplaticisers made small water-to-cement ratios attainable by lowering the minimum water content required to maintain workability. Since this increase in strength is achieved without altering the self-weight, the strength-to-weight ratios of these high-strength concretes is correspondingly enhanced.

Alternatively, reducing the density, and by extension, the self-weight of concrete has similar effect. These lightweight concretes have been known to antediluvian engineers who capitalized on the advantages more than 2 millennia ago in the Mediterranean region. Some famous structures which utilized lightweight concrete were from the Roman Empire, including the dome of the Pantheon (finished in 27 B.C.) and the Coliseum (built between 75-80 A.D.), both of which are still standing today. In the case of the Pantheon, naturally occurring lightweight volcanic stones found on Mount Vesuvius were used to produce the concrete in the upper portion of the dome, without which the dome would not have been able to support its own weight (ACI 213R-03).

Today, concretes with light weights can be achieved through a variety of methods including aerated concretes, using lightweight aggregates, or producing no-fines concrete, among others. In a no-fines concrete, the fine aggregate portion is omitted to obtain a weight reduction. Although this material has deficiencies and limited structural applications (Malhotra 1976), it was successfully used for large scale public housing projects in Britain during the decade after World War II (Finnimore 1989).

Lightweight aggregates can also be used as a substitute over conventional rock based aggregates to obtain a lower density and self-weight of concrete while maintaining properties broadly similar to normal weight concrete. These lightweight

aggregates make use of an internal microstructure of air filled voids to lower its bulk densities compared to its rock based counterparts that typically have no voids.

Meanwhile, aerated concrete has density reducing air voids worked directly into the concrete microstructure rather than have them confined within the aggregates. These voids may be chemically induced as in autoclave aerated concrete. In foamed concrete, the coarse aggregate and fine aggregate component is ignored while foam is mechanically introduced into a cement paste to get an extremely light concrete with densities as low as 400 kg/m^3 (Wee 2005). A typically low compressive strength coupled with self-leveling and self-compacting properties makes foamed concrete widely used for trench reinstatement works (Jones and McCarthy 2005).

Recently, 60 MPa foamed concrete at densities of 1700 kg/m^3 have been produced by using low water-to-cement ratios (Wee 2005). Foamed concrete can thus be produced to meet the compressive strength requirements of a structural concrete although other aspects of its structural performance are as yet not well established.

Even larger improvements to the strength-to-weight ratios can be gained by increasing the strength of concrete while simultaneously reducing the self-weight as in the case of lightweight high-strength concretes. Compressive strengths up to 100 MPa (Wee 2005) have been reported in the literature. This high-performance concrete can significantly reduce the dead load of a structure allowing it to be built on locations where soil conditions would not have otherwise permitted. In many cases, the architectural expression of form combined with functional design can be achieved more readily with structural lightweight concrete than with any other medium (ACI 213R-03).

While lightweight concretes derives considerable appeal from an improved strength-to-weight ratio, this material also boasts enhanced thermal insulation, fire resistance, and acoustic insulation properties. Lightweight concrete has thermal conductivity values half that of normal weight concrete (Chandra and Berntsson 2003) due chiefly to its low density and pore structure which traps air – being a poor conductor of heat. This low value means that heat does not easily penetrate through the material thus reducing a building's interior heating and/or cooling requirements, a reduction most welcome amid rising energy costs and growing concerns on climate change.

Although lightweight concrete is able to improve some properties of normal weight concrete, inevitably, trade-offs are made with others. From a structural stand point, a lower modulus of elasticity causes member deflections to be greater than in normal weight concrete counterparts. In addition, lightweight concretes have lower tensile strengths and a subsequently reduced shear resistance (ACI 213R-03). This is in lieu of the improved interfacial transition zone in lightweight aggregate concrete. A smaller net solid area in aerated concretes may also be a contributing factor to its lower tensile strength. These limitations do not necessarily diminish the value of lightweight concrete since the weaknesses can be overcome with appropriate structural design and detailing.

A major obstacle preventing wide spread adoption of lightweight concrete is the economic consideration of elevated costs. Synthetically produced lightweight aggregates are more costly than natural aggregates while aerated concrete tend to have a large cement content. However, the higher material costs can be readily offset by savings from construction efficiency and functionality of the completed building (ACI 213R-03). Successful use of lightweight concrete as a mainstream construction

material also depends on sufficient research data and practical experience with the material (Gerritse 1981).

Already, internationally recognized building codes of practice acknowledge the role and potential of lightweight aggregate concrete by allowing the structural use of the material with associated design guidelines and equations suggested. However much of these design provisions are modified forms of normal weight concrete requirements and have remained unchanged based on research and data on lightweight concrete obtained in the 1950's. To date, research on the structural behavior of lightweight concrete, especially foamed concrete with and without aggregates, remains scarce when compared to the large pool of data available for normal weight concretes.

1.1 Research Motivation

Over the last two decades, the manufacturing sector was revolutionized by innovations such as robotic manufacturing processes, just-in-time inventory systems and total quality management philosophies. The transportation and logistics industry was also streamlined with containerization of cargo from centuries old method of break bulk cargo (Levinson 2006). While these sectors have benefited vastly from improved efficiency and productivity, the construction sector continues to be plagued with wastage and delays. Construction sites are often characterized by a seemingly organized chaos hidden behind hoardings in stark contrast to the efficient moving manufacturing lines or gleaming electronic clean rooms.

In an effort to overhaul the traditional in-situ construction method, construction related associations around the world are advocating and promoting efficient building techniques. Novel construction methods and systems such as hybrid concrete construction, industrial building systems, and prefabricated

technologies are advancing this cause with development of new high performance materials such as polymers and resins enhancing the technological leap. In Singapore, the Building and Construction Authority (BCA) has made it compulsory via legislation that a minimum buildability score must be met as a prerequisite for building approval. This requirement aims to improve the labor efficiency and the quality of construction in Singapore (Building and Construction Authority 2005).

Through the course of assessing the buildability score, adoption of precast components and prefabricated systems is heavily rewarded. This is because a higher level of quality can be maintained at the precasting yard which is often more spacious, equipped with tools, and safer when compared to the tight confines of scaffolding and working at height. An expedited erection schedule is then possible with reduced movement of materials, smaller quantity of construction debris, and less housekeeping tasks.

With an incentive to shift towards prefabricated construction systems, synergies can be obtained with lightweight concrete, itself a high-performance material. By substituting lightweight concrete for normal weight concrete, a saving on self-weight of up to 30 percent can be realized on otherwise identical segments thus allowing more components to be transported, or for larger components to be moved without exceeding vehicle loading limits. Larger segments also reduces the number of joints required between the precast elements.

On site, these lighter components translate to lower lifting requirements where smaller capacity cranes can be deployed or existing cranes being able to lift larger and/or more segments. The number of personnel required to maneuver the segments into position is also decreased since lighter segments are easier to handle. This is crucial as tower crane availability is typically on the critical path of the construction process and it can be freed for other lifting tasks quickly.

Aside from prefabricated construction systems, lightweight concrete can also contribute to improved buildability using in-situ casting methods. The smaller weight of lightweight concrete gives rise to smaller formwork pressures that require less sophisticated temporary supports and props thus reducing wastage and cost. Because lightweight concrete is produced and handled in a similar manner to normal weight concrete, existing equipment, infrastructure and skills will continue to be relevant, unlike where other high-performance materials are adopted.

Structurally, the reduced self-weight of reinforced concrete components results in smaller column loads and a correspondingly lower demand on foundation design especially in high-rise buildings where these weight savings are quickly compounded. Foundations which need to support lower loads will be smaller, less expensive, and technically less challenging to construct. Longer beam spans and expanded column bays are also possible with the higher strength-to-weight ratios of lightweight concrete. Economic benefits can then be reaped during service since these large, open, column free spaces are architecturally desirable.

Beyond the construction phase, lightweight concrete also has benefits in service. The BCA initiated Green Mark assessment for buildings promotes environmentally sound technologies for maintaining building services and preserving the comfort of tenants. Using lightweight concrete can contribute directly or indirectly to scoring points in the Green Mark assessment process. Cooling requirements can be reduced in a building due to the thermal insulating properties of lightweight concrete especially when it is used to construct walls and slabs. This energy savings can be significant even considering the increased energy requirement in lightweight aggregate manufacture since the operational energy of buildings over its design lifetime is ten times the energy embodied in their construction (Head 2001).

1.2 Research Significance

Current codes of practice including the American Concrete Institute's "Building Code Requirements for Structural Concrete, ACI 318-05", the British Standard Institute's "Structural Use of Concrete: Code of Practice for Design and Construction, BS 8110 : 1997", and Eurocode 2: "Design of Concrete Structures" provides for the design of shear in reinforced concrete sections by assuming that the total shear resistance, V, is the sum of a 'concrete contribution', V_c, and the resistance provided by transverse reinforcement, V_s (Equation 1-1). The 'concrete contribution' term in this approach is an adjusted fit of predictions by theoretical truss models to real experimental observations. Expressions for this term are empirically derived after extensive experimental campaigns and is usually taken as the shear strength of beams without stirrups/links. This semi-empirical approach may be misleading since it lacks a physical explanation (Regan 1993).

$$V = V_c + V_s \tag{1-1}$$

In the case of lightweight aggregate concrete, the 'concrete contribution' is treated by the code as a fixed fraction of normal weight concrete 'concrete contribution' at similar compressive strengths. The application of a single constant reduction factor for lightweight aggregate concrete is quite possibly an over-simplification considering the wide variety of aggregates and aggregate properties available (Regan *et al.* 2005, Wesche 1968). A comparatively smaller body of experimental data related to lightweight aggregate concrete may also compromise the reliability of these correlations (Nesbit 1966). Specifically for lightweight aggregate-foamed concrete, Regan and Arasteh (1990) indicated that development of an expression for the shear strength of the material is premature due to limited data available.

Since the current design approach is based on empirical expressions derived from normal weight concrete tests, an unconservative design may occur if these expressions are extrapolated to conditions previously untested. The equations may have omitted certain secondary factors, while what is secondary in normal weight concrete may be primary in lightweight concrete (Wesche 1968). Such unconservative designs were reported by Salandra and Ahmad (1989), and Ahmad *et al.* (1994) for slender high-strength lightweight aggregate concrete beams. Here, the code equations which were developed from normal weight concrete up to 41 MPa was extrapolated to cover high-strength lightweight concrete. This deficiency was echoed by Ramirez *et al.* (2004) who observed similarly unconservative design especially in high-strength lightweight concrete members with low to minimum transverse reinforcement.

With the current relatively limited use of lightweight concrete, code provisions have been adequate in guiding its structural design. This may be attributed to the design philosophy of the codes. Shear failures are brittle and occur with little or no advance indication of structural distress. A flexural failure mode is thus preferred as it can be made ductile with large deflections that warn of an impending collapse. As a consequence, reinforced concrete members are typically designed for flexure prior to being proportioned for shear. Empirical equations which give lower bound shear resistance values are also readily accepted sacrificing some degree of economical design for a higher level of conservatism.

Lacunae within this approach to lightweight concrete design may soon become apparent with expanding use of lightweight concrete in more environments and conditions. It has been observed by numerous researchers that lightweight concrete members exhibit significantly lower reserve shear strengths post-diagonal cracking as compared to normal weight concrete. Although diagonal cracking is

adopted as the failure criteria by codes, this lower reserve strength when compared with normal weight concrete eliminates a degree of implicit conservatism with consequences to the overall safety margins in a structure. Nesbit (1966) first observed this when lightweight aggregate concrete test beams developed diagonal cracking at 90-100% ultimate load while normal weight concrete had larger margins. More research is thus required to understand shear in lightweight concrete (Holland 1995, FIB Task Group 8.1 2000).

Through the course of an experimental program of lightweight concrete beam tests, insights into the shear failure mechanisms of reinforced concrete in general and reinforced lightweight concrete in particular can be obtained. Lightweight concrete has been known to behave in the same manner as normal weight concrete but with parameters having an expanded range values (Gerritse 1981) which can aid a generalized shear resistance mechanism to be elucidated. Several such shear failure mechanisms and models for normal weight concrete have been proposed by Taylor (1959), Kani (1966), Krefeld and Thurston (1966b), Chana (1987), Reineck (1991), and Zararis and Papadakis (2001).

Among the various factors affecting shear resistance, the aggregate interlock component of shear transfer in lightweight concrete is expected to deviate significantly from its normal weight concrete counterpart. In normal weight concrete, the aggregates tend to be the strongest component while the interfacial transition zone is the weakest. Thus for normal weight concrete under tensile stresses, cracks will propagate around the aggregate via the interfacial transition zone, leaving jagged aggregate protrusions for shear transfer.

Shear cracks in lightweight concrete meanwhile have been observed to penetrate through the weak lightweight aggregates (Nesbit 1966) indicating that the lightweight aggregate is the weakest component of the concrete matrix. Although the

jagged aggregate protrusions no longer occur, Walraven and Al-Zubi (1995) noted that the irregular shape of the crack face in lightweight aggregate concrete may still cause it to be able to continue developing shear friction as evident in local crushing of the material. Meanwhile, in foamed concrete, the loss of interface shear friction may be even more pronounced and negatively impact the shear resistance of the material.

This phenomenon of cracking through the aggregate is similar to crack formation in high-strength normal weight concretes. Due to this, lightweight aggregate concrete has better strength compatibility between the cement paste and aggregate much like normal weight high-strength concrete. This strength compatibility may then lead to similarities between the behavior of the two materials.

Another factor affecting lightweight concrete is the density of the material. Empirical equations used to compute the concrete contribution do not currently take into account the density of the material due to the narrow range of normal weight concrete densities. With lightweight concrete, the possibility arises that these equations may be generalized by including a density term. The provision of two lightweight concrete factors in the ACI 318-05 for sand-lightweight concrete and all-lightweight concrete may be interpreted as an indication of the possibility that density may play a role. While Eurocode 2 does take into account density classifications, this approach still does not have adequate performance (Regan *et al.* 2005).

For shear in reinforced concrete, there remains no general theory that is able to predict the response. Two types of approach have been developed the first being empirical in nature while the second adopts a rational direction. Current codes of practice use design equations based largely on empirical tests and decades of experience. There also exists a dichotomy between the response of members with transverse reinforcement and those without transverse reinforcement.

In this work, laboratory tests were conducted on lightweight concrete beams to examine the applicability of existing theories and design codes to lightweight concrete especially high-strength lightweight aggregate concrete and foamed concretes. Observations and results derived from these tests also create a significant data point that allow new insights and sheds more light on the mechanisms in action to resist shear in reinforced concrete.

1.3 Objectives

There is a need to establish the structural performance of lightweight concretes with or without aggregates with regionally available materials and conditions for the benefit of the construction industry and ultimately the society. In light of this, an extensive research program has been conducted at the National University of Singapore on the development and applications of structural lightweight concrete with and without aggregates. This study is part of the above mentioned research program and continues with the focus on evaluating the behavior of lightweight concrete with and without aggregates in shear.

The objectives of this study is summarized below and presented visually in Figure 1-1:

- Probe the shear transfer mechanism and failure models of lightweight concrete with and without aggregates.
- Re-evaluate and propose new design methods for lightweight concrete with and without aggregates.
- Develop a model and associated prediction equation for the shear strength of lightweight aggregate concrete with normal weight fine aggregate.

This study will consist of an experimental part and an analytical part. Three types of lightweight concrete will be considered including: lightweight aggregate

concrete, lightweight aggregate-foamed concrete and foamed concrete. Material strengths will range from 30 to 40 MPa for lightweight aggregate-foamed concrete and foamed concrete while lightweight aggregate concretes will cover a range from 30 MPa to a high-strength 80 MPa. Normal weight concretes will also be included in experimental programs as a comparative reference benchmark and for control purposes.

A series of tests will be conducted using specimens of various geometries with typical reinforcement arrangements to observe the response of the above mentioned materials. These tests focused on the structural performance of the concrete in consideration at a element level. Loads were monotonically applied until failure, i.e. the concrete ruptures. The performance of structural systems, i.e. frames, are not included in the scope of this study as is dynamic and cyclic loading.

Analysis of data generated from the experimental part allowed the shear provisions in international codes of practice to be evaluated. Empirical equations were also examined and refined with data generated from this study while reinforced concrete shear failure models and rational theories were revisited.

1.4 Organization of the Dissertation

This dissertation is divided into six chapters. Each chapter builds on the preceding one to systematically present the ideas, motivations, and methods behind this study on shear in lightweight concrete with and without aggregates.

Chapter One, of which this is a sub-section, is an introduction to the research topic. A general background of lightweight concretes and it's permutations is given together with a brief mention on shearing behavior in reinforced concrete. The motivation to pursue research and development of lightweight concrete with and without aggregates is then detailed followed by the potential significance of the

findings to human knowledge. Objectives and scope of work is presented next to define the limits and expectations of this study. Finally the layout of this dissertation is given.

Chapter Two, the literature review covers material properties of lightweight concrete and developments in the understanding of shear in reinforced concrete members. The material properties of lightweight concrete include a brief history of its development together with characteristics reported by other researchers worldwide. Known deviations from normal weight concrete behavior were compared and contrasted while phenomenon unique to lightweight concrete are listed. This chapter provides the fundamental material background on which the research work was built on. Approaches to predict shear resistance adopted by current codes of practice including empirical equations, emerging rational theories, and proposed failure mechanisms are detailed in this section. Research efforts on shear response of lightweight concretes previously attempted by others are also listed with their findings.

The experimental program and cracking modes of lightweight concrete beams without transverse reinforcement are detailed in Chapter Three. The experimental program included a comprehensive set of 48 specimens over 4 types of concrete with different compressive strengths and cross sections. Test beam preparation and test methods are also detailed in this chapter. Following that, valuable data on crack propagation, deflections, and ultimate loads that were recorded in the course of this program and are presented. A qualitative model on shear mode cracking in lightweight concrete based on known shear resistance mechanisms is proposed.

Loading and strength results obtained from the experimental program from beams without transverse reinforcement are then analyzed and compared with

prediction equations of various design codes and those found in the literature in Chapter Four. Using information derived from the test series of Chapter Three and expanded information of Chapter Four, a mathematical expression was derived to predict the shear strength of lightweight concrete. Chapter Five meanwhile covers the results and discussion of a companion series of 38 rectangular beams containing transverse reinforcement. Information obtained from this companion series is used to enhance the number of data points since the transverse reinforcement does not have significant effect until shear cracking begins. The strength of these lightweight concrete beams are also compared with the provisions of the British Standards and with the Eurocode 2.

Finally, the conclusion and a summary of significant findings from this work is contained in Chapter Six. Suggested future works to further explore and build on the results and analyses herein are also listed in the final chapter.

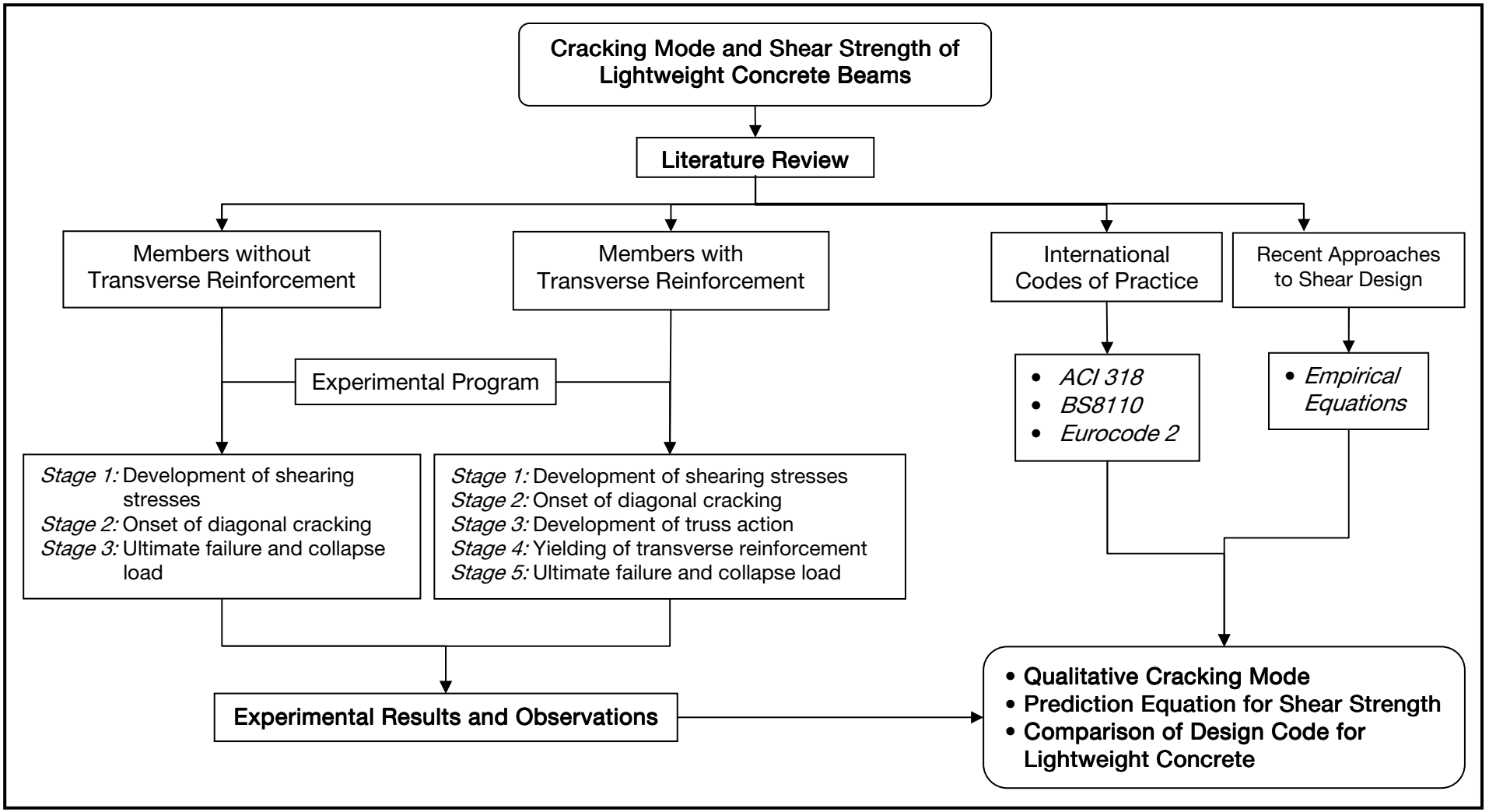

Figure 1-1 Objectives and scope of works

Chapter 2 Literature Review

This section presents some background and material characteristics of structural lightweight concrete. The topic has been discussed in-depth by Clarke (1993), and Chandra and Berntsson (2003) with the emphasis on lightweight aggregate concrete. A state-of-the-art report, “Guide for Structural Lightweight-Aggregate Concrete” compiling the research and experience gained in North American practice was published by Committee 213 of the American Concrete Institute in 2003. The International Federation for Structural Concrete (FIB), based in Lausanne, Switzerland also released a bulletin on the subject in 1999 and 2000 which focused mainly on European practice. Meanwhile, reference to UK practice and the British Codes were included in the “Guide to Structural Use of Lightweight Aggregate Concrete” published by The Institution of Structural Engineers together with the Concrete Society in 1987.

Numerous technical publications on lightweight aggregate concrete by EuroLightCon, a European research project Brite EuRam BE96-3942 based in Norway also exist. While lightweight concrete behaves in a manner largely similar to normal weight concrete, significant differences exist which require the separate treatment of lightweight concrete (Gerittse 1981). The following sections will summarize development and material properties of structural lightweight concrete. This will be followed by a review of shear design theories and methods for reinforced concrete in general and lightweight concrete in particular.

2.1 Development of Modern Lightweight Structural Concrete

The discovery of modern lightweight aggregates was made by Stephen J. Hayde who recognized the potential of ‘bloaters’ in the brick making industry to be utilized

in this manner. A rapid expansion of the feed material causes a microstructure of air filled voids to form resulting in aggregates that have low bulk densities. Lightweight aggregates manufactured from shale, clay, or slate via a rotary kiln process was patented by Hayde in 1918, while commercial production of expanded slag began in 1928 followed by the production of the first structural quality sintered-shale aggregate in 1948.

One of the earliest modern day uses of lightweight concrete was for constructing ships and barges circa 1918. The adoption of this material in construction was given a boost in the late 1940's when a National Housing Agency survey was conducted on the potential use of lightweight concrete for home construction. This was followed by extensive studies on concrete made from lightweight aggregates to determine their properties. The focus on potential structural use of this material spurred an interest in constructing building frames, bridge decks and pre-cast members from it. The Tacoma Narrows Bridge is one such example where the bridge deck was expanded after the first collapse without requiring the piers to be replaced (ACI 213R-03).

During the 1950's, many multi-storey structures and bridges were designed to be constructed from lightweight concrete capitalizing on the reduced self weight of the material. Case studies of many such projects have been compiled in ACI 213R-03 and Bulletin 8 of the FIB (1999). Some more notable buildings include the Guggenheim Museum, in Bilbao, Spain, the TWA Terminal at Kennedy Airport, New York, and the Nordhordland Floating Bridge in Norway.

The success of these structures galvanized further investigations into lightweight concrete for offshore floating structures. These investigations were lead by oil companies who were keen to explore this material to improve their offshore operations. Research and development work was conducted in the 1980's with

results made available in 1990's. The Heidrun tension leg platform and the BP Harding Field gravity base tank are some offshore structures built from high-strength lightweight concrete.

Synthetic lightweight aggregates are now manufactured around the world and sold under trade names such as Leca, Lytag, and Liapor among others. These modern aggregates can be used for structural applications and are found with a wide range of properties each suited to a particular use. Through the last century, continued research and practical experience has seen this material used successfully. Nevertheless, in-depth knowledge of lightweight concrete is still maturing and has not approached the vast reservoir of experience with normal weight concrete.

2.2 Classification of Lightweight Concrete

Lightweight concretes can be classified according to compressive strength – which has structural implications, density – which quantifies the reduction in self weight, and constituent materials – which affect concrete properties. ACI 213R-03 defines a structural lightweight concrete as a concrete with an equilibrium density to ASTM C567 between 1120 kg/m^3 and 1920 kg/m^3 with a minimum 28 day compressive strength of 17 MPa. The lower density limit is given since compressive strengths of lightweight concretes are often related to the density of the material and is of importance for structural use. Structural lightweight concretes are then a subset of specified density concrete which are defined in ACI 213R-03 as concretes with equilibrium densities lying between 800 kg/m^3 and 2240 kg/m^3. No strength limits are prescribed for this classification since specified density concrete may be used for non-structural applications, e.g. as an insulation material. On the other hand, ACI 213R-03 defines high-strength lightweight concrete as a structural lightweight concrete with a 28 day compressive strength in excess of 40 MPa.

Eurocode 2 meanwhile does not specify a lower limit for densities, but defines lightweight concrete as having an oven dry density not exceeding 2000 kg/m^3. Elsewhere, FIB recommendations to Model Code 90 proposes that structural lightweight concrete grades be limited within a range of 12 MPa to 80 MPa.

Besides compressive strengths and density classifications, concrete produced using both fine and coarse lightweight aggregates are classified as "all-lightweight concrete", while "sand-lightweight" concrete is used if only the coarse aggregate portion is made up of lightweight aggregates. These classifications based on constituent materials are made as certain material properties of structural lightweight concrete has been observed to differ. In general, using lightweight fine aggregate reduces the structural performance of the concrete and increases the sensitivity of mix proportioning due to absorption of mix water by the lightweight fine aggregates. In contrast, using normal weight fine aggregates does not significantly compromise the weight savings of lightweight concrete.

Foamed concrete is a potential structural material currently being widely used as a controlled low strength material. It is of interest to note that by strict definition, foamed concrete is not a concrete since the aggregate portion is commonly omitted but the term is used to convey engineering and durability properties that are closer to concrete than of cement paste. While the method of creating foamed concrete is well known (McCormick 1967, Tam *et al.* 1987, Grutzeck 2005), different researchers have referred to foamed concrete alternatively as aerated concrete, cellular concrete, and gassed concrete. Although foamed concrete has a similar physical microstructure to autoclave aerated concrete (AAC), the latter is produced in a manner distinct from foamed concrete. The chemical reactions in the production of AAC also means that it develops strong chemical bonds that result in properties and behavior different from mechanically produced foamed concrete (Grutzeck 2005). Lightweight aggregate-

foamed concrete meanwhile has also been known to be referred to as hybrid concrete.

2.3 Lightweight Aggregates

Lightweight aggregates derive their low particle relative density from a cellular pore system. This pore system is typically formed as a result of a thermal process which may be natural, such as volcanic action, or artificially applied with the resulting aggregates classified as such. Being of a volcanic origin, natural lightweight aggregates like pumice and scoria are not found in most parts of the globe. These volcanic aggregates develop their cellular pore structure when gas bubbles in the molten lava become trapped due to the rapid cooling of ejected lava. With no control over the production process, natural lightweight aggregates are used ‘as is’, at most with some mechanical treatment e.g. crushing and sieving.

Synthetic lightweight aggregates meanwhile are formed by pyroprocessing of some argillaceous material. Two main types of thermal treatment are widely used including agglomeration and expansion techniques. Agglomeration takes place when some of the materials melt at temperatures above 1100°C and the particles that make up the finished aggregate are bonded together by fusion. Alternatively, a cellular pore structure can also be developed by heating certain raw materials to incipient fusion. At this temperature, gasses are evolved within the pyroplastic mass, causing expansion, which bloats the aggregate who’s internal structure is retained upon cooling.

Unlike natural lightweight aggregates, synthetic lightweight aggregate can be designed and manufactured to suit different concrete requirements including adjustments to the particle density. A smooth, non-vesicular surface more adaptable for use in structural concrete can also be appropriately produced. This ability to

control the manufacturing process and constituent materials give greater versatility to the application of synthetic lightweight aggregate (Owens 1993) while maintaining consistent quality (Neville 1999).

Strong durable synthetic lightweight aggregates contain a uniformly distributed system of pores that have a size range of approximately 5 μm to 300 μm. The pore system is developed in a continuous, relatively crack-free, high-strength vitreous phase. Upon exposure to moisture, pores close to the surface are readily permeable and fill with water within the first few hours. Interior pores, however, fill extremely slowly, requiring many months of submersion to approach saturation. A small fraction of interior pores are essentially non-interconnected and will continue to remain unfilled even after years of immersion (ACI 213R-03).

These features of the pore system in combination should not increase the density of the compacted concrete either by significant water permeation (absorption) or cement paste pervasion into the body of the aggregate particle when the aggregate is mixed into concrete. The absorption of free mixing water by the aggregates is undesirable and they are typically soaked in water prior to concrete production either by submerging or by sprinkling. Since the pores of the aggregate is saturated, no mixing water is absorbed. This situation has beneficial effects because the free water within the aggregate pores may be released into the cement matrix upon self desiccation as a method of internal curing (Philleo 1991, Weber and Reinhardt 1995).

The interfacial transition zone between the mortar matrix and the aggregate also shows improved properties compared to normal weight aggregate (Neville 1999). As the cement paste hydrates, the matrix is able to form inside the pores of the lightweight aggregate thus ‘gripping’ the aggregate and producing good bond between the phases. Friable lightweight aggregate notwithstanding, this improved

bond allows cracking to propagate through the aggregate rather than around the aggregate at the interfacial transition zone.

Bulk density of lightweight aggregates is measured by weighing a container of known volume filled with the aggregate. The method is prescribed by BS EN 1097 Part 3 (1998) and can be loose or compacted. Two aggregates made of the same material may have different bulk densities depending on the efficiency of particle packing. BS EN 1097 Part 6 (2000) and BS EN 1097 Part 7 (2008) meanwhile provides the specification for determining the particle density of the aggregates. The codes detail the wire basket method and pyknometer method respectively. Two aggregates made of the same material will have the same particle density regardless of particle size.

2.4 Properties of Lightweight Concrete

The properties of lightweight aggregates have some bearing on the properties of the fresh and hardened concrete (Wesche 1968). It should, however, be recognized that properties of lightweight concrete are greatly influenced by the quality of the cementitious matrix, in common with those of normal weight concrete. Specific properties of aggregates that may affect the properties of the concrete are: particle shape and surface texture, relative density, bulk density, strength of lightweight aggregates, strength ceiling, total porosity, grading, moisture content and absorption, and modulus of elasticity of lightweight aggregate particles (ACI 213R-03).

2.4.1 Compressive Strength of Lightweight Concrete

The strength of aggregate particles varies with type and source of the material and is measurable only in a qualitative way. Some particles may be strong and hard while others may be weak and friable. For compressive strengths up to approximately

35 MPa, ACI 213R-03 notes that there is no reliable correlation between aggregate strength and concrete strength indicating that strength is more dependent on the cementitious matrix.

Structural lightweight aggregates used in producing structural lightweight concretes are prescribed by ACI 213R-03 to meet the requirements of ASTM C330 with bulk density less than 1120 kg/m^3 for fine aggregate and less than 880 kg/m^3 for coarse aggregate. A practical relative density range for coarse lightweight aggregate is from 1/3 to 2/3 that of normal weight aggregates. Particle densities below this range may require more cement to achieve a required strength and may thereby fail to meet the density requirements of the concrete. This leads to the concept of a 'strength ceiling' where any continued increase in the concrete compressive strength is not practically achievable.

The strength ceiling is influenced predominantly by the coarse aggregate and may be quite high for certain lightweight aggregates, approaching that of some normal weight aggregates. This ceiling can be increased appreciably by reducing the maximum size of the coarse aggregate for most lightweight aggregates, especially the weaker and more friable ones (ACI 213R-03). This reduction of particle size reduces the stress concentration around the aggregate and also allows for a more homogenous concrete matrix to be produced.

The hypothetical air bubble 'aggregates' of a foamed concrete results in a essentially homogenous matrix which is able to develop compressive strengths in excess of 25 MPa with densities as low as 1400 kg/m^3 (Jones and McCarthy 2005). The strength of foamed concrete is derived from the strength of the cement matrix itself and its microstructure. As such significant improvement in compressive strengths are possible with the use of a pozzolan such as fly ash.

2.4.2 Modulus of Elasticity and Poisson's Ratio

The modulus of elasticity depends on the relative amounts of paste and aggregate and the modulus of each constituent (LaRue 1946, Pauw 1960). Generally, the modulus of elasticity for lightweight concrete is considered to vary between 50% and 75% that of normal weight sand and gravel concrete of the same strength (IStructE 1987). Variations in lightweight aggregate grading usually have little effect on modulus of elasticity provided the relative volumes of cement paste and aggregate remain fairly constant.

ACI 213R-03 recommends that equation 2-1 below given in ACI 318 may be used for values of concrete density, w_c between 1440 kg/m^3 and 2480 kg/m^3 and strength levels of between 21 and 35 MPa. This equation is derived from Pauw's formula. The report also notes that concretes in service may deviate from this formula by up to 20%.

$$E_c = {w_c}^{1.5} 0.043 \sqrt{f'_c} \text{ N/mm}^2 \quad (2\text{-}1)$$

The IStructE (1987) guide similarly gives the elastic modulus as given in BS8110 shown below as equation 2-2. However, there is generally a separate relation between cube strengths and E-values for different types of aggregates together with a concomitant upper bound limiting value. Nevertheless, it was noted that reduced density of the material and a larger water content which retards time dependent deformations tend to counter balance the reduced elastic modulus value.

$$E_c = {D_c}^2 \sqrt{f_{cu}} \times 10^{-6} \text{ kN/mm}^2 \quad (2\text{-}2)$$

Where D_c is the nominal density of the aggregate.

The Poisson ratio meanwhile varies slightly with age, test conditions and physical properties of the concrete. A value of 0.20 may be usually assumed for practical design purposes (ACI 213R-03).

2.4.3 Tensile Strength of Lightweight Concrete

The tensile strength of concrete is only a fraction of its compressive strength and is dependent on the tensile strength of the coarse aggregate and mortar phases, and the degree to which the two phases are securely bonded. Traditionally, this value has been defined as a function of compressive strength. This should only be taken as a first approximation since it does not reflect aggregate particle strength, surface characteristics of the aggregates or the concrete's moisture content and distribution (ACI 213R-03). For a given lightweight aggregate, the tensile strength may also not increase in a manner comparable to the increase in compressive strength. Increases in tensile strength tend to occur at a lower rate relative to increases in compressive strength. This becomes more pronounced as compressive strength increases beyond 35 MPa with tensile strengths being over-predicted. Replacing lightweight fine aggregate with normal weight fine aggregate will also normally increase tensile strength.

Concrete tensile strengths can be measured through direct tensile tests or indirectly via splitting tensile tests or flexural tensile tests. Due to the weak and brittle nature of concrete under tension, indirect tensile tests are easier to perform and tensile splitting strengths and/or modulus of rupture values from flexural tensile tests are preferred. However, these values are influenced by moisture content and specimen storage conditions prior to the test as well as the different stress distributions within the specimen as the test is carried out (FIP 1983).

The splitting tensile strength of concrete cylinders to ASTM C496 is an effective method of measuring tensile strength and is useful in estimating the diagonal tensile resistance of a concrete element. Splitting tensile strengths show a narrow range of this property for continuously moist-cured lightweight concrete (ACI 213R-03). Nevertheless, splitting tensile strength of lightweight aggregate concrete has a larger scatter than that of normal weight concrete due to the influence of the aggregate and the influence of curing method (FIP 1983).

When test specimens are subjected to air drying, stability of these results begin to fluctuate. During drying of the concrete, moisture loss progresses at a slow rate into the interior of concrete members, resulting in the development of tensile stresses at the exterior faces and balancing compressive stresses in the still moist interior zones. Furthermore, if the lightweight aggregates are not saturated, they will absorb water from the mortar surrounding the aggregate creates tensile shrinkage stresses that will diminish the stress the concrete is able to balance (FIP1983). Thus the tensile resistance to external loading of drying lightweight concrete will be reduced from that indicated by continuously moist-cured concrete (Hanson 1961, Pfeifer 1967). For the former type of curing condition, the splitting tensile strength of lightweight concrete varies from approximately 70 to 100% that of the normal weight reference concrete when comparisons are made at equal compressive strength (Evans and Dongre 1963, FIP 1983, ACI 213R-03). FIP (1983) gives a median value correlation, which is also near the lower bound value, to lightweight concrete compressive strength as:

$$f_{ct} = 0.23 {f_{cu}}^{2/3} \tag{2-3}$$

The values of modulus of rupture from tests on high-strength lightweight concrete yield inconsistent correlation with code requirements. While Huffington (2000) reported that the tensile splitting and modulus of rupture tests results

generally met AASHTO requirements for high-strength lightweight concrete, Nassar (2002) found that in his investigation, the modulus of rupture levels were about 60 to 85% of ACI 318 code requirements where the material factor for sand lightweight concrete is recommended to be 0.85.

Similar to tensile splitting strengths, studies have indicated the modulus of rupture of concrete undergoing drying are extremely sensitive to the transient moisture content (FIP 1983). Under these conditions modulus of rupture tests may not furnish reliable results that are reproducible (Hanson 1961) or have satisfactory correlation to compressive strengths (Slate *et al*. 1986).

Tensile strength of lightweight concrete that undergoes drying is more relevant in respect to the shear strength behavior of concrete in structures. Shear is related to the tensile strength of concrete and tests have shown that diagonal tensile strength of beams and slabs correlate closely with the tensile splitting strengths (Hanson 1958 and 1961). A minimum tensile splitting strength of 2.0 MPa (290 psi) is required for structural lightweight aggregates conforming to the requirements of ASTM C330 to ensure adequate performance of the material (ACI 318-05).

The different formulae found in code and standards are similar, and a better approximation is hardly possible without distinguishing between types of aggregates, moisture conditions, lightweight fine and coarse aggregate, normal weight fine and lightweight coarse aggregate, and normal weight fine and coarse aggregates (FIB Bulletin 8).

2.5 Analysis of Reinforced Concrete Members in Shear

Probably more research has been carried out into shear behavior than into any other mode of failure for reinforced concrete. Despite this, there remains considerable areas of uncertainty and disagreement with respect to a rational theory to unify the

approach towards shear design. This is evident in the numerous papers and discussions on the topic found in the literature (Reineck 1991, Ramirez 1998, Mander 1998) including during the 1987 IABSE Symposium in Delft. Regan (1993) in his presentation to the Institution of Structural Engineers in London retraced 100 years of developments in reinforced concrete shear theory and design while the Joint ASCE-ACI Committee 445 (1998) provided further clarity by reporting some recent developments and the state-of-the-art in shear design.

As it stands, reinforced concrete shear is approached with classification into either members without transverse reinforcement or members where transverse reinforcement is provided. In case of the former, models predicting the shear failure mechanism relies on the material itself with some contribution from the longitudinal reinforcement. Failure models for the latter meanwhile take into account the ability of the transverse reinforcement bars to carry tensile stresses.

None of the rational models proposed to date completely satisfies the three fundamental requirements of force equilibrium, strain compatibility, and the material laws simultaneously (Hsu 1993). Of these requirements, the material laws governing the behavior of reinforced concrete is the most vexing partly due to the non-homogenous nature of reinforced concrete and a bi-axial tension-compression state of stress in slender beams subjected to shearing stresses.

While these rational models continue to be refined, shear design continues to be carried out with confidence for all normal members. The empirical design methods given in codes of practice have had the advantage of being tested against, and being adjusted to fit a very large body of experimental data (Narayanan and Beeby 2005).

2.6 Reinforced Concrete Members Without Transverse Reinforcement

This area is probably of limited importance for beams where some shear reinforcement will always be provided but is of major importance for slabs where it is often very inconvenient to provide shear reinforcement. This has been the most researched area of shear performance, but, as yet, no generally accepted theory describing the ultimate behavior of a member without shear reinforcement has been developed. The formulae given in codes should therefore be considered to be basically empirical. Because of the amount of testing that has been carried out, the effect of the major variables can be clearly established, and the resulting formulae can be considered as highly reliable for normal types of element (Narayanan and Beeby 2005).

The simplest method of predicting the shear capacity of a reinforced concrete section without transverse reinforcement is to relate the average shear stress at failure to the tensile strength of concrete. This approach to determining the shear capacity was proposed almost a century ago by Mörsch and continues to be the basis of the ACI Building Code and several other international codes of practice (ASCE-ACI 445). While this relationship can provide acceptable empirical equations from sound statistical regression, it is of interest that the average principal tensile stresses to cause secondary diagonal (flexure-shear) cracking is usually much less than concrete tensile strength. This may possibly be due to stress concentration at the tip of initial crack and/or reduction of cracking stress due to coexisting transverse compression (Kupfer and Gerstle 1973). A non-uniform shear stress distribution at the outermost flexural crack as a result of a concentration of bond stresses and a reduction of the internal lever arm due to arch action in the flexurally cracked zone may also contribute to the phenomenon (Kim and White 1991).

2.6.1 Mechanisms for Shear Transfer

For members without transverse reinforcement, shearing stresses are resisted by the concrete itself. Diagonal cracking was observed to be the predominant mode of ultimate failure in beams of this type with many behavior models proposed (Taylor 1960, Chana 1987, Reineck 1991). The state of stress in the web of a reinforced concrete member differs considerably from what is predicted by the theory of linear elasticity with the complexity of the problem compounded when the concrete cracks. For such sections, ASCE-ACI Committee 445 on Shear and Torsion lists five known mechanisms of shear transfer, four of which were previously identified by ASCE-ACI Committee 426. These mechanisms include shear stresses in uncracked concrete of the flexural compression zone, interface shear transfer across crack surfaces, dowel action of longitudinal reinforcing bars, and arching action. A fifth mechanism was identified since 1973 where residual tensile stresses which are transmitted across cracks exist. Figure 2-1 illustrates these shear transfer mechanisms. Although these mechanisms are known, the issue of shear resistance remains a highly complicated system influenced by various parameters to indeterminate degrees.

In slender members without axial compression, shear stresses in the compression zone do not contribute significantly to the shear capacity because the depth of the compression zone is relatively small (Taylor 1959, Reineck 1991). However at locations of maximum moment, the compression zone may resist much of the shear especially after significant yielding of the longitudinal reinforcement. This reversal can be attributed to the increased crack widths which reduce the ability of the other shear transfer mechanisms to provide resistance.

Interface shear transfer meanwhile transmits shearing stress across the crack surface when both sides of the crack slip past each other. This mechanism of shear resistance is sometimes known as aggregate interlock or crack friction. The ideas

involved were clearly presented in the 1973 ASCE-ACI Committee 426 report based on work by Fenwick and Paulay (1968), Mattock and Hawkins (1972) and Taylor (1960). Significant progress in further exploring this mechanism was accomplished by Gambarova (1981), Walraven (1981), and Millard and Johnson (1984). Most notably, Walraven developed a model that considered the probability that aggregate particles idealized as spheres will project from the crack surface.

In this model, relationships between stresses and displacements are taken as a function of the concrete compressive strength. However, these relationships were developed for a range of normal compressive stresses beyond the range that is relevant for shear transfer in beams with stirrups. Vecchio and Collins (1986) then extended Walraven's ideas in which Vecchio and Collins assumed that the shear that can be transferred is a function of the square root of compressive strength, $\sqrt{f'_c}$. Four parameters have also been identified in the literature that affect the amount of interface shear transfer. These parameters include crack interface shear stress, crack width, normal stresses, and crack slip.

Even with large differences between the constitutive laws applied by different researchers, interface shear transfer plays an important role in the redistribution of diagonal compression fields in beams with stirrups (Collins 1978, Kupfer *et al.* 1983, Dei Poli *et al.* 1990). This is implicitly taken into account within the diagonal 'crushing' strength of compression field approaches and is explicit in members without stirrups as the ability of the diagonal cracks to transfer shear which determines the capacity.

Although much work by numerous researchers have supported this mechanism (Taylor 1959, Sherwood *et al.* 2007), Zararis and Papadakis (2001) have proposed that interface shear transfer and dowel action have no appreciable effect on resisting shear. The basis of this argument is the hypothesis that any slippage along the crack – which is required to develop interface shear transfer – is prevented

by an intact compression zone. Tests and analysis of steel fiber reinforced concrete beams yields results that are in agreement (Choi *et al.* 2007) since the fiber reinforcement is able to transmit tensile stresses across the cracks.

The dowel action of longitudinal reinforcement is also known to be one of the shear resistance mechanisms in reinforced concrete beams (Krefeld and Thurston 1966a, Vintzeleou and Tassios 1986). However, there remains disagreement over the importance of its contribution to the total shear resistance. On the one hand, Chana (1987) postulated that dowel action is the limiting mechanism that governs the shear strength of a section without transverse reinforcement. Joint ASCE-ACI Committee 445 (1998) meanwhile reports that the contribution of dowel action is insignificant since the strength of the dowel is limited by the tensile strength of the concrete cover. The abrupt nature of a shear failure makes it difficult to establish if the failure of dowel action causes the failure to precipitate (Chana 1987) or that failure of other mechanisms results in the redistribution of stress to be resisted which instantly leads to the failure of dowel action.

While Joint ASCE-ACI Committee 445 is unconvinced of the contributions, it does concede that dowel action may play an appreciable role when welded wire fabric is used (Mansur *et al.* 1986) as the tensile stresses are distributed to an enlarged area. Similarly, this action may also be significant in members with large amounts of longitudinal reinforcement especially if they are placed in more than one layer.

Residual tensile stresses across cracks have been recently shown to contribute to the resistance of shearing actions. When the concrete first cracks, a clean break does not occur with small pieces of concrete still bridging the crack. These pieces may continue transmitting the tensile stresses up to crack widths of 0.05 mm to 0.15 mm. This action can be observed from a significant decreasing

(softening) branch after the peak tensile stress. Gopalaratnam and Shah (1985) and Reinhardt *et al*. (1986) have more recently developed a reliable measurement of this softening branch. The residual tensile stresses occur across deformations that are localized in a very small region. Thus the response is given in terms of stress-crack opening relationships and not strain as is usually the case. This resistance mechanism is the cornerstone of fracture mechanics approach based on the assumption that it is the primary shear transfer mechanism. Similarly, Reineck's tooth model (1991) provide that residual tensile stresses provide significant portion of shear resistance of very shallow members (<100mm) where the width of flexural and diagonal cracks are small.

2.6.2 Empirical Methods of Shear Analysis and Design

Derived by statistical regression, empirical equations are affected by the methods with which the underlying data is obtained, analyzed, and interpreted. If included, inappropriate test results may cause a large scatter of points that then influence the coefficients of regression (Bazant and Kim 1984, Kim and Park 1996, Bae *et al.* 2006). When properly derived, empirical equations can model the expected behavior within the range of values observed and parameters tested in the underlying data. However, the sometimes simple empirical equations for shear design belies the uncertainty in assessing influences and interactions of complex parameters governing its behavior.

Poor representation of certain parameters can and do exist in the source data while extrapolating to conditions beyond the model limits may give rise to risky un-conservative designs or wasteful uneconomical requirements (Mphonde and Frantz 1984, Regan 1993). Nevertheless, for most commonly encountered situations, sufficient experience has been obtained such that these equations are robust and satisfactorily used in codes of practice (MacGregor and Wight 2005).

An example of a flawed empirical equation is Equation 11-5 of the ACI Building Code shown here as Equation 2-4 below. This equation is given by the code as an alternative to Equation 11-3 of the same code (Equation 2-5 here) to be used to calculate the shear resistance separately for each point being considered via a $\frac{V_u d}{M_u}$ term. This term – restricted to values below unity – takes into account the ratio of moments, that cause flexural cracking, to the shear that has to be resisted there. The amount of longitudinal reinforcement, ρ is also considered with shear strength increasing with ρ. As the available reinforcement is increased and the moment decreased, narrower flexural cracks form thus leaving a larger area of intact concrete in the flexural compression zone to resist shear. Smaller crack widths also mean closer contact between two sides of the concrete improving resistance through interface shear friction (ASCE-ACI 445 1998).

$$V_c = \left(1.9\sqrt{f'_c} + 2500\rho_w \frac{V_u d}{M_u}\right)\frac{b_w d}{7} \qquad (2\text{-}4)$$

Although Equation 2-4 considers more parameters, Joint ASCE-ACI Committee 445 (1998) views it as inappropriate and strongly suggests that it not be used. The constants in that equation was derived from a data pool that includes results from both short beams and slender beam tests, thereby mixing data from two different behavior types: arching action and beam action. Furthermore, most of the beams from that data pool had high reinforcement ratios which skew the representation for that parameter. Flaws in the derivation of Equation 2.1 also leads to it underestimating the effect of longitudinal reinforcement, ρ for beams without web reinforcement while its treatment of the shear span-to-depth ratio, $\frac{a}{d}$ expressed as $\frac{V_u d}{M_u}$ is also not entirely correct (MacGregor and Wight 2005).

While Equation 11-5 of the ACI Building Code (Equation 2-4 above) may be flawed, Equation 11-3 of the same code (Equation 2-5 below) provides a lower bound

average shear stress value at diagonal cracking. This equation is used for design to the ACI Building Code and gives reasonable lower bound values for small, slender beams not subjected to axial loads, and with at least 1% of longitudinal reinforcement. Beam tests have shown that the nominal shear strength varies with the occurrence of cracks at different average shear stress values. Where large moments occur even though appropriate longitudinal steel has been selected, extensive flexural cracks will be evident. As a result, the uncracked area of the beam cross section will be greatly reduced and the nominal shear strength, V_c can be as low as $1.9\sqrt{f'_c}b_w d$ (U.S. Customary Units). On the other hand, in regions where the moment is small, the cross section will only be slightly cracked with a large portion of the cross section available to resist shear. For such a case, tests show that V_c of about $3.5\sqrt{f'_c}b_w d$ (U.S. Customary Units) can be developed prior to shear failure (ACI-ASCE 326). Based on this information, the code suggests that conservatively, V_c can be taken to be as high as $2.0\sqrt{f'_c}b_w d$ (U.S. Customary Units) (MacGregor and Wight 2005).

$$V_c = 2\sqrt{f'_c}b_w d \tag{2-5}$$

Zsutty (1971) proposed another equation which is a significant improvement over Equation 11-5 of the ACI Building Code (Equation 2-4 above). Like the latter equation, additional consideration for reinforcement ratio and the shear span-to-depth ratio is present. However, Zsutty separates the short beams from the slender beams at a shear span-to-depth ratio of 2.5 prior to performing statistical regression. Mphonde and Frantz (1984) improved Zsutty's regression after testing both short and slender high strength and low strength concrete beams. The addition of high strength concretes into the data set increases confidence in applying the design equations to this material which was not available in Zsutty's time.

Bazant and Kim (1984) later introduced an empirical equation for design which takes into consideration size effect in members of different dimensions, the maximum aggregate size and fracture mechanics approaches. This equation also differs from the other equations here in that it was derived for the ultimate shear capacity first before being appropriately scaled to predict the onset of diagonal cracking which has been adopted as the shear failure load. The variable d_a is the maximum aggregate size while the variable, α accounts for the load configuration, i.e. shear span-to-depth ratio. This equation was then extended and improved by Kim and Park (1996) and Bae *et al.* (2006). Another equation was proposed by Okamura and Higai (1980) and further recalibrated by Niwa et al (1986). This equation is a more reliable empirical formula since it includes test results for large beams for size effect.

Using a differential equation of a beam lever arm, Russo *et al.* (2005) analytically developed a model for computing the internal shear force in a beam. This model was then parametrically fitted to a large body of experimental data to obtain a prediction equation. A design formula was also proposed with conservative results and the advantage that it is continuous over shear span-to-effective depth ratios and is shown to be more conservative than major design codes.

Tureyen and Forsch (2003) developed a semi rational model of concrete shear strength after testing concrete beams reinforced with fiber-reinforced polymer (FRP) bars. It was observed from their tests that the shear capacity of beams reinforced with FRP bars was noticeably lower than steel reinforced equivalents. The reduced stiffness of the FRP bars was thought to contribute to this reduction in shear carrying capacity. The traditional shear resistance model was then relooked at and a new model developed taking into account a modified shear stress distribution through the

intact zone of concrete. This development was brought about due to the higher neutral axis caused by using FRP bars that are less stiff than steel.

The empirical formula given in the British Code BS8110 (Equation 2-6) meanwhile takes into account the major parameters known to affect shearing strengths. Reinforcement ratios are considered by the term in the first parenthesis, while shear span-to-depth ratios are simplified into the term in the second parenthesis. For values of f_{cu} above 25 MPa, the term in the third parenthesis comes into effect up to a maximum of 40 MPa. For design purposes, a material safety factor cast as γ_m is included in the equation.

$$V_c = 0.79\left(\frac{100A_s}{b_v d}\right)^{1/3}\left(\frac{400}{d}\right)^{1/4}\left(\frac{f_{cu}}{25}\right)^{1/3} \quad (2\text{-}6)$$

Eurocode 2 which is the code of practice adopted throughout the European Union also proposes a semi-empirical equation for members that do not require transverse reinforcement. This is applicable to members with a depth smaller than 200 mm such as slabs and lintels. A general equation shown as equation 2-7 below is given with values $C_{Rd,c}$, k, and k_1 subject to variations prescribed in national annexes of nations within the CEN. Values for these two parameters are recommended in the code and have been adopted without change in the UK national annex (refer to Table 2-1).

$$V_{Rd,c} = \left[C_{Rd,c}k(100\rho f_{ck})^{1/3} + k_1\sigma_{cp}\right]b_w d \quad (2\text{-}7)$$

While the formulas given in the American code and Bazant and Kim correlate the tensile strength of concrete to the square root of compressive strength, equations by Niwa *et al*, Zsutty, the British Code and Eurocode 2 use a cube root relationship. All empirical equations presented in this section are listed summarized in Table 2-1.

2.7 Reinforced Concrete Members With Transverse Reinforcement

Design of reinforced concrete structures has remained semi-empirical in nature due to the complex nature of shear response. Currently, there are no complete and accepted rational theory to describe the behavior of reinforced concrete members, not through lack of attempts. Regan (1993) in a paper presented to the Institution of Structural Engineers in London chronologically detailed the efforts of scientists and researchers over a century to elucidate a mathematical expression that is able logically predict shear response while fulfilling the laws of equilibrium, compatibility and material properties.

Since the structural collapse of Wilkins Air Force Depot in Ohio which occurred in 1955, deficiencies in available shear design methods were dramatically exposed (Ramirez 1998). The American Concrete Institute and the American Society of Civil Engineers then established joint ACI-ASCE Committee 326 to study shear and diagonal tension in reinforced concrete. A landmark report was published by this committee in 1962 which serves as the basis of the ACI building code until today. Work by ACI-ASCE Committee 326 was continued by joint ASCE-ACI Task Committee 426 who published their report in 1973 containing new information on the response of various reinforced concrete members to shear. Most recently, ASCE-ACI Committee 445 (1998) on Shear and Torsion released a state of the art report on recent approaches to shear design.

Two leading rational theories under development are the compression field theory (Collins 1978) and its subseq uent modified compression field theory (Vecchio and Collins 1986) and the rotating-angle softened-truss model (Belarbi and Hsu 1994, 1995; Hsu 1993; Pang and Hsu 1995). The basis of these theories is the truss model that postulates that the shearing stresses are resisted in a member by developing truss action with the longitudinal and transverse reinforcement in tension

and the diagonally cracked concrete forming diagonal compression struts. The main difference in these two theories is the manner with which the material response and concomitantly the inclination of the diagonal tension strut is treated. This arises from the manner that new cracks form while preexisting cracks spread and change inclination as the load is increased.

The approach adopted by the compression field theory was based on an analogous tension field theory developed by H. A. Wagner (ACI445 1998). While the compression field theory was a breakthrough in the rational understanding of shear behaviour of reinforced concrete, it assumes that after cracking, there will be no tensile stresses in the concrete. As this assumption does not agree with experimental observations, Vecchio and Collins (1986) proposed a modification where in establishing the angle of inclined strut, the concrete strains are averaged over lengths greater than the crack spacing.

Meanwhile, the rotating angle – softened truss model uses a slightly different approach to the modified compression field theory to account for the tensile capacity of the diagonally cracked concrete. As its' name suggests, the rotating angle – softened truss model assumes that the angle of strut inclination changes as the load is increased. In addition, instead of checking the stress conditions at a crack, as is done by the modified compression field theory, the rotating angle – softened truss model adjusts the stress-strain relationship to take into consideration the possibility of local yielding at the vicinity of the crack. This gives rise to the softened stress-strain relationships used in the model.

Rational truss approaches with concrete contributions have been adopted by the Eurocode 2. The use of a variable angle truss model allows for a more economic design as compared to the conservative fixed 45° truss models. Selecting a lower angle of incline results in less transverse steel being required to maintain vertical

equilibrium. In order to avoid very flat angles and potential under-reinforced sections, Eurocode 2 limits allowable angles of incline.

The continued research and development of such a rational theory is not only of academic importance but will also facilitate the confident design of non-typical reinforced concrete elements such as deep beams and corbels without resorting to strut and tie models and engineering judgment. Nevertheless empirical equations used in current design approaches are supported by an overwhelming body of research data and may be simpler to apply than to understand and adopt methods proposed by rational theories (Mander 1998).

The shear strength being able to be developed by a reinforced concrete section also depends on the manner and position of loading. If the loads are applied to the top of the beam while the support is at the bottom, the section is able to develop its full shear strengths. However, if the loads are applied at the soffit of the beam, such as in half-through girders, the beam element is unable to develop its shear strength (Taylor 1960).

2.8 Shear in Reinforced Lightweight Concrete

The availability and proven performance of lightweight aggregates has led to the improved functionality and economical design of buildings, bridges and marine structures for more than 80 years. During much of this period, designs were based on properties of normal weight concrete, properly adjusted by engineers but without adequate guidance of recommended practices specifically pertaining to lightweight concrete. Today, all major international codes of practice accept lightweight aggregate concrete as a structural medium with general guidelines for engineers.

Lightweight concrete members have been shown by test and performance to behave in fundamentally the same manner as its normal weight counterpart with

differences in performance those of degree (Taylor and Brewer 1963, Gerittse 1981). From a shear and diagonal tension perspective, these properties are sufficiently different to require design modifications. Codes of practice generally approach this issue by introducing reduction factors to normal weight concrete equations. This is because although lightweight concrete has higher material tensile strength, under air drying which is the case in practice, it will generally have a lower tensile strength that normal weight concrete of equal compressive strength (Hanson 1968).

In the United States, the empirical derivation of shear strengths from a large number of lightweight concrete beams test until failure (Hanson 1961, Hognestad *et al.* 1964, Ivey and Buth 1967) forms the basis of the ACI design code, ACI318 (ACI213R-03). Meanwhile, the provisions in the British and European codes relating to lightweight concrete was similarly derived from test result of large scale experimental campaigns (Hamadi and Regan 1980, Clarke 1987, Evans and Dongre 1963).

Developments in theory of reinforced concrete, evolution of design philosophy from working loads to limit state design, and advances in cement and lightweight aggregate material technology since the 1960s spurred renewed research into the shear performance of lightweight aggregate concrete. Numerous papers on the subject of shear in lightweight concrete beams was presented at the International Symposium on Structural Lightweight Aggregate Concrete in 1995.

Shear friction is thought to have a major contribution to the overall shear capacity of a reinforced concrete beam. Early interest in lightweight reinforced concrete beams focused on this area since tensile cracks were observed to propagate through the aggregates resulting in smoother crack interfaces (Hamadi and Regan 1980, Bardhan-Roy and Swami 1995, Thorenfeldt and Stemland 2000). While the crack interface was indeed found to be smoother, nevertheless, cracks

themselves propagated in an angular fashion allowing the section to continue resisting shear through alternative displacements of the shear contact area (Walraven and Al-Zubi 1995). Foamed concretes that do not contain aggregates of any type was also found to develop shear capacities that agree well with predictions given by the British Standard BS8110 (Regan and Arasteh 1990).

Shear tests on lightweight aggregate concrete remain scarce compared to their normal weight concrete counterpart. Lack of experimental data from sand-lightweight concrete to all-lightweight concrete through foamed concrete hampers development of safe economical designs with the material. In the case of foamed concrete, Jones and McCarthy (2005) most recently carried out a series of pilot load/deflection tests on full scale beams to exlore its use as a structural material. A summary of investigations of shear in lightweight aggregate concrete from literature is summarized in Table 2-2 below.

2.8.1 ACI 318 Treatment of Lightweight Concrete Shear

The American Concrete Institute's Building Code ACI318-05 addresses the shear design of lightweight aggregate concrete by reducing the concrete contribution component through one of two methods. The first method involves replacing the square root relationship between compressive and tensile strengths with cylinder splitting values, *i.e.* substituting f_{cu} with $f_{ct}/6.7$. The coefficient 6.7 was derived from tests by Hanson (1961) which relate the aforementioned values. There are some draw backs of using this method in that cylinder splitting strengths are not usually specified and not suitable for field concrete. A large scatter of results also occur when test specimens are subjected to air drying conditions, a condition more representative of actual structures (Holm and Bremner 2000).

A second, generally more conservative approach in calculating the permissible shear may be used if an engineer is unable or hesitant to specify cylinder splitting values. Reduction factors are available that determine the shear capacity of lightweight concrete as a fixed percentage of normal weight concrete shear. Two separate factors, 0.85 for sand-lightweight concrete and 0.75 for all-lightweight concrete is provided because research on splitting tensile strength of lightweight concrete shows an improvement in tensile strength when natural sand is used in place of lightweight fine aggregates (Pfeifer 1967, Ivey and Buth 1967).

Most research addressing tensile strength and shear strength of structural lightweight concrete that formed the basis for existing ACI 318 building code requirements were limited to concrete with a compressive strength of less than 41 MPa. For some lightweight aggregates, the tensile strength ceiling may be reached earlier than the compressive strength ceiling.

In view of this lack of information, Ramirez et. al (2004) carried out a comprehensive investigation into the shear strength of high strength reinforced and prestressed lightweight concrete beams with compressive strengths between 41 MPa to 69 MPa. While the tests showed that the shear capacities of test beam exceeded requirements of ACI 318 and AASHTO LRFD methods, the degree of conservatism was greater for the normal weight concrete when considering the margin between onset of critical cracking and ultimate shear failure. Ramirez *et al.* also cautioned that the 0.85 factor for sand-lightweight concrete does not adequately account for the reduction in shear capacity compared to companion normal weight concrete beams. This is especially important for the case of beams with low to minimum amounts of shear reinforcement where the concrete contribution is the larger fraction of total shear. Salandra and Ahmad (1989) and Ahmad *et al.* (1994)

further concluded that this is unconservative for high-strength beams with shear depth-to-span ratios larger than 3.0.

2.8.2 BS 8110 Treatment of Lightweight Concrete Shear

Unlike the American ACI 318, the British Standard BS8110 only prescribes a factor of 0.8 for lightweight concrete with no distinction between sand-lightweight or all-lightweight concrete. This factor is also imposed on the maximum limit of shear stress that a section can be subjected to; $0.63f_{cu}$ or 4 Mpa whichever is lower even when shear reinforcement is provided (IStructE 1987). It also limits the maximum allowable compressive strength to 40 MPa with an alternative table used for values of compressive strength below 25 MPa that depends only on the amount of longitudinal steel provided: by implication, no account is taken of the depth of the member. Ahmad *et al.* (1994) concluded that allowing the concrete strength to exceed 40 MPa in the equation for the computation of shear strength still provides an adequate margin of safety. The factor can also be increased to 0.85 simultaneously. Clarke (1987) suggested that for beams without links, the factor can be increased as high as 0.9.

2.8.3 Eurocode 2 Treatment of Lightweight Concrete Shear

Eurocode 2 treatment of lightweight concrete is also based on the corresponding rules for normal density concrete. The first term in parenthesis of Equation 2-7 is multiplied by a coefficient for determining tensile strength with no change to the second term which accounts for axial compression in the member. Values of $C_{Rd,c}$ for lightweight concrete is also reduced from $^{0.18}/_{\gamma_c}$ for normal weight concrete to $C_{lRd,c} = {}^{0.15}/_{\gamma_c}$for lightweight concrete.

Unlike the ACI design code or the British Standard that adopt a fixed fraction of the normal weight concrete equation, Eurocode 2 has both a fixed reduction in the

$C_{lRd,c}$ term as well as a variable reduction coefficient , η_1 that considers the density of the lightweight aggregate used by classifiying the aggregate into density classes. The coefficient is then computed by reducing 60 percent of the normal weight concrete contribution by the ratio of the upper limit of the appropriate density class to the density of normal weight aggregates (2200 kg/m^3) as shown in equation 2-8 below.

$$\eta_1 = 0.40 + 0.60\rho/2200 \tag{2-8}$$

The final equation for the shear strength of lightweight aggregate concrete applied by Eurocode 2 for beams not requiring transverse reinforcement and not subject to axial loads is shown in equation 2-9 below with recommended values and lightweight concrete adjustments. The code also explicitly states that the provisions for lightweight concrete given therein does is not applicable to foamed and aerated concretes as the concrete must have a closed structure.

$$V_{lRd,c} = \left[{}^{0.15}/_{\gamma_c}\, k(0.40 + 0.60\rho/2200)(100\rho f_{ck})^{1/3}\right] b_w d \tag{2-9}$$

2.9 Conclusion

It is clear that lightweight concrete brings many advantages as a structural medium both in practice and as a medium for research to further unravel the mechanisms of shear resistance. The information presented in the following chapters build on the information of lightweight concrete, reinforced concrete theory, lightweight concrete subjected to shearing action, and of code provisions on the design of reinforced concrete using lightweight concrete.

Table 2-1 List of normal weight concrete shear strength empirical equations

Name	Equation	Units	Comments
Equation 11-3 of the ACI318-05 building code	$V_c = 2\sqrt{f'_c}\,b_w d$	U.S. Customary	
	$V_c = \frac{\sqrt{f'_c}}{6} b_w d$	SI	
Equation 11-5 of the ACI318-05 building code	$V_c = \left(1.9\sqrt{f'_c} + 2500\rho_w \frac{V_u d}{M_u}\right)\frac{b_w d}{7} \leq 3.5\sqrt{f'_c}\,b_w d$	U.S. Customary	Suggested that this equation be avoided.
	$V_c = \left(\sqrt{f'_c} + 120\rho_w \frac{V_u d}{M_u}\right)\frac{b_w d}{7} \leq 0.3\sqrt{f'_c}\,b_w d$	SI	
Eurocode 2	$V_{Rd,c} = \left[C_{Rd,c} k \left(100\rho \quad f_{ck}\right)^{1/3} + k_1 \sigma_{cp}\right] b_w d$	SI	Code equation
	$V_{Rd,c} = \left[\frac{0.18}{\gamma_c} k \left(100\rho\ f_{ck}\right)^{1/3} + 0.15\sigma_{cp}\right] b_w d$		Recommended Values (also UK national annex)
BS8110-97	$v_c = 0.79\left(\frac{100A_s}{b_v d}\right)^{1/3}\left(\frac{400}{d}\right)^{1/4}\left(\frac{f_{cu}}{25}\right)^{1/3}\frac{1}{\gamma_m}$	SI	
Niwa *et al.* (1986)	$V_c = 0.20\frac{\rho^{1/3}}{d^{1/4}}\left(f'_c\right)^{1/3}\left(0.75 + \frac{1.40}{a/d}\right) b_w d$	SI	
Zsutty (1971)	$v_c = 59\left(f'_c\,\rho\frac{d}{a}\right)^{1/3}$	U.S. Customary	Only for a/d > 2.5

Name	Equation	Units	Comments
Mphonde and Frantz (1984)	$v_u = 10.10 {f'_c}^{1/3} + 71$	U.S. Customary	Limited to compressive strength 21-103 MPa and a/d 3.6
	$v_u = 0.366 {f'_c}^{1/3} + 0.49$	SI	
Bazant and Kim (1984)	$v = \frac{8\rho^{1/3}}{\sqrt{1+\frac{d}{25d_a}}}\left(\sqrt{f'_c} + 3000\sqrt{\frac{\rho}{\alpha^5}}\right)$	U.S. Customary	$\alpha = a/d$ for point load
			$\alpha = l/4d$ for uniform load
Ahmad *et al.* (1986)	$v_u = \eta[50(f'_c \rho\, d/a)]^{0.333}$	U.S. Customary	For high-strength normal weight concrete.
	$\eta = 1 - 0.0414[(d-5.35)^{0.85}/(a/d)^{0.63}]$		
	for $3 \le (a/d) \le 6$		
Reineck (1991)	$V_c = \frac{0.4 b_w d f_{ct} + V_{du}}{\left[1 + 0.16\frac{f_{ct}}{f_c}\lambda\left(\frac{a}{d}-1\right)\right]}$	SI	
	$\lambda = \frac{f_c}{E_s \rho}\frac{d}{\Delta n_u}$		
Kim and Park (1996)	$v_u = 3.5 {f'_c}^{\alpha/3}\rho^{3/8}(0.4 + d/a)\lambda(d)$		$\alpha = 1$ for $a/d \ge 3$
	$\lambda(d) = \frac{1}{\sqrt{1+0.008d}} + 0.18$		$\alpha = 2 - \frac{(a/d)}{3}$ for $1 \le a/d < 3$
Rebeiz (1999)	$v_{cr} = 0.4 + \sqrt{f'_c \rho(d/a)}[2.7 - 0.4\alpha]$	SI	Cracking shear strength
	$v_u = 0.4 + \sqrt{f'_c \rho(d/a)}[10 - 3\alpha]$		Ultimate shear strength
			$\alpha = 2.5$

Name	Equation	Units	Comments
			for $a/d \geq 2.5$
			$\alpha = a/d$ for $1 \leq a/d < 2.5$
Tureyen and Forsch (2003)	$V_c = \frac{2}{3} b_w c \sqrt{{f_t}^2 + f_t \frac{\sigma_m}{2}}$	U.S. Customary	
Russo *et al.* (2005)	$v_{uc} = 1.13\xi \left[\rho^{0.4} {f'_c}^{0.39} + 0.5\rho^{0.83} {f'_{yl}}^{0.89} \left(\frac{a}{d}\right)^{-1.2-0.45a/d} \right]$ $\xi = \frac{1 + \sqrt{5.08/d_a}}{\sqrt{1 + d/(25d_a)}}$	SI	
Bae *et al.* (2006)	$v = 4.65 \left(5.5 - 1.5\frac{a}{d}\right)^{\lambda} \frac{\sqrt{f'_c}\, p^{0.5}}{(1+d)^{0.4}}$		$\lambda = 1$ for $a/d \leq 2.5$ $\lambda = 0$ for $a/d > 2.5$

Table 2-2 Summary of literature on shear tests of lightweight concrete

Investigator	Concrete Types	Aggregate Type	Concrete Compressive Strengths (MPa)	Transverse Reinforcement	No. of Lightweight Concrete Specimens	Specimen Type	Comments
Taylor and Brewer (1963)	SLWC	Expanded Clay, Pulverised Fuel Ash	23.4 – 36.9 *Cube 100 mm*	Without	36	Rectangular Beam	
Hognestad *et al.* (1964)	ALWC	Expanded Clay, Expanded Shale	30.0 *Cylinder 150 mm x 300 mm*	Without	6	Slab Plate	Punching shear tests
Ivey and Buth (1967)	SLWC	Expanded Shale, Expanded Slate (Angular and Rounded)	19.2 – 32.3 *Cylinder Dimension unspecified*	Without	26	Rectangular Beam	
Hamadi and Regan (1980)	NWC, ALWC	Leca	23.0 – 26.3 *Cube Dimension unspecified*	With	5	T-Beam	Companion push off specimens
Clarke (1987)	SLWC	Pellite, Pumice Lytag	23.6 – 60.4 *Cube Dimension unspecified*	With	40	Rectangular Beam	

Investigator	Concrete Types	Aggregate Type	Concrete Compressive Strengths (MPa)	Transverse Reinforcement	No. of Lightweight Concrete Specimens	Specimen Type	Comments
Salandra and Ahmad (1989)	SLWC	Expanded Slate	54.7 – 72.4 *Cylinder 100 mm x 200 mm*	With and without	8	Rectangular Beam	Silica Fume added
Ahmad *et al.* (1994)	SLWC	Expanded Slate	30.5 – 89.3 *Cylinder 100 mm x 200 mm*	With and without	15	Rectangular Beam	Silica Fume
Bardhan-Roy and Swami (1995)	SLWC	Pulverised Fuel Ash (Lytag)	23.5 – 47 *Cube Dimension unspecified*	Without	30	T-Beam	
Thorenfeldt *et al.* (1995)	NWC, SLWC	Leca	32.2 – 39.7 *Cylinder 150 mm x 300 mm*	With	4	Large I-beam	Self Flowing Concrete
Walraven and Al-Zubi (1995)	NWC, SLWC	Lytag, Liapor, Aardelite	23.9 – 57.9 *Cube Dimension unspecified*	With	12	I-Beam	
Thorenfeldt and Stemland (2000)	ALWC	Leca	42.7 *Cylinder 150 mm x 300 mm*	Without	16	Rectangular Beam	11 small and 5 large scale
Ramirez *et al.* (2004)	NWC, SLWC	Expanded Shale (Haydite)	46.2 – 75.2 *Cylinder Dimension unspecified*	With	7	Rectangular Beam	

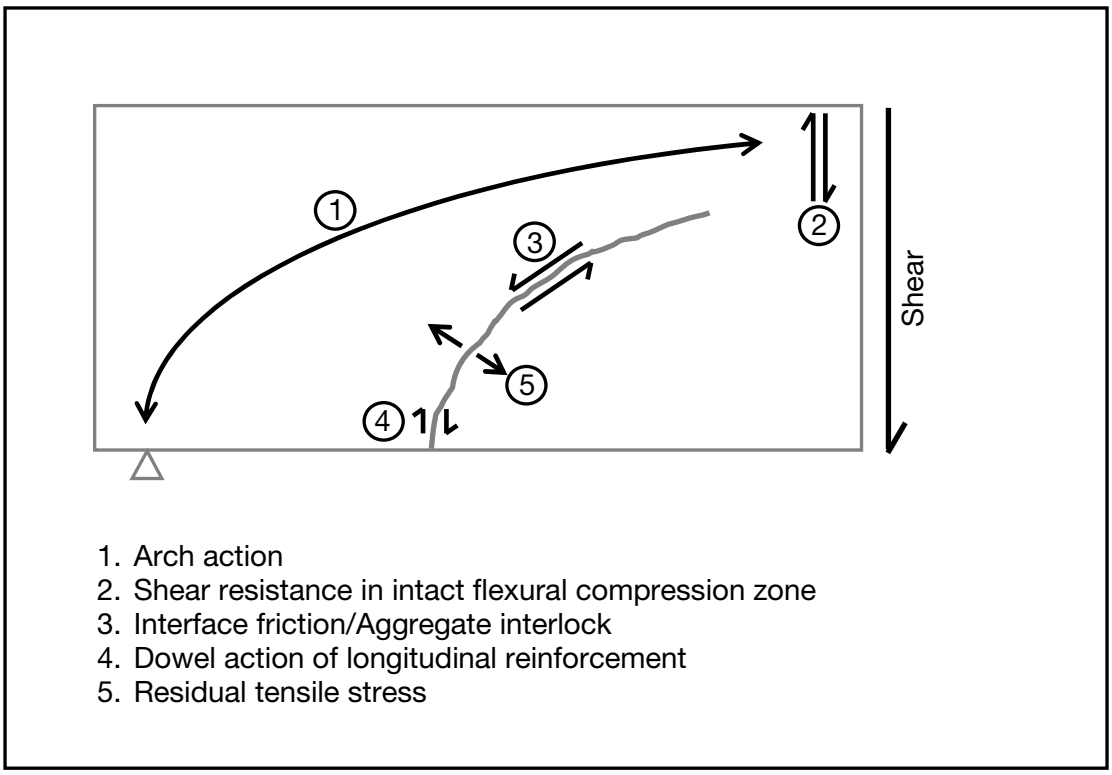

1. Arch action
2. Shear resistance in intact flexural compression zone
3. Interface friction/Aggregate interlock
4. Dowel action of longitudinal reinforcement
5. Residual tensile stress

Figure 2-1 Shear Resistance Mechanisms

Chapter 3 Cracking Modes of Lightweight Concrete Beams without Transverse Reinforcement

Extensive research has been carried out on shear resistance mechanisms of reinforced concrete members without transverse reinforcement. The five mechanisms involved have been identified as the shear resistance of the intact concrete in the flexural compression zone, dowel action of the longitudinal reinforcement bars, shear friction across the inclined crack interface, arching action especially in zones near to the support, and residual tensile capacity across the crack interface. The individual contribution of each mechanism vary through the loading history of a member and is governed by propagation and pattern of the cracks. Physical failure of the member occurs when the stresses are no longer able to be redistributed across the cracks to alternative mechanisms. As the ability of the redistribution depends on the crack pattern and crack propagation, design codes define ultimate failure as the onset of diagonal cracking which will significantly disrupt the ability of shear stresses to be redistributed.

The relative contributions of individual shear resistance mechanisms and their interactions are not clear. A novel approach of Zararis and Papadakis (2001) suggests that the intact concrete above a critical shear crack prevents any slippage across the crack interface which opens orthogonally. As such the resistance model is postulated to be from the intact concrete of the flexural compression zone with insignificant contribution from interface friction, and shear deformation of the longitudinal reinforcement steel bars rather than dowel action. An analytical model based on these assumptions was derived therein and shows good correlation with experimental data from the literature. This is in contrast with the widely accepted view that interface friction plays an important role in shear resistance (ASCE-ACI 445 1998).

An experimental program was thus designed to investigate the structural behavior of lightweight concrete beams with the focus on its shear response. This program included a series of laboratory tests which were carried out at the National University of Singapore. Reinforced lightweight concrete beams with two different cross section geometries were tested under a range of parameters known to influence it's behavior in shear. These parameters include steel reinforcement ratios, concrete compressive strengths, shear-span-to-depth ratios, *et cetera*. Monotonically increasing third point loading was applied until physical failure of the test beams.

With the results from lightweight concrete tests in this study, an additional data point was added to the body of experimental information available in the literature. Cracking from lightweight concrete occurs through the friable lightweight aggregate rather than around the aggregate as in normal weight concrete. This leads to a smoother interface and by extension reduced interface friction. Lightweight concrete has thus been observed to behave in broadly similar way to normal weight concrete with differences a matter of degree rather than mechanism. However, changes to the degree can impact the sequence of crack development, which in certain situations, significantly alter the underlying mechanism of shear resistance.

3.1 Experimental Program

The experimental program was carried out using test beams of different cross section geometries including 32 beams from the S-series and 16 beams from the R-series, all cast without transverse reinforcement. All beams in the S-series had rectangular cross sections, 300 mm wide by 125 mm deep, with an overall length of 1350 mm (*see Figure 3-1*). The beams are designed to behave in a manner similar to one-way spanning slabs. Performance of this type of member is of value as slabs account for a significant volume of structural concrete poured in a reinforced

concrete building. This leads to real reductions in self-weight of the structure even when slabs are the only major element cast with lightweight concrete. In steel structures, the advantages of light weight concrete floor plates is even more significant.

Placement of meaningful transverse shear reinforcement within the limited depth and large area of these slab members is non-trivial, thus shearing forces are frequently resisted by the concrete itself. This reliance on the shear strength of concrete renders testing lightweight concrete for its shear performance of interest. The beams tested in this phase were designed to be shear critical, *i.e.* the test beams have a calculated shear capacity that is lower than the shear force caused by the loads at calculated ultimate flexure.

This experimental program also involved testing rectangular beams which is the most common beam shape. The R-series beams were 125 mm wide by 200 mm deep, with a 2000 mm overall length (*see Figure 3-1*). Unlike the beams of the S-series – which are exempt, beams in the R-series are required by design codes to contain a minimum prescribed amount of transverse reinforcement. Shearing forces are then resisted by both the transverse steel and concrete. In this section, transverse steel was NOT added to the shear spans of the R-series beams. As such, the shear behavior of the beams are similar to the S-series and distinct from the shear resistance mechanisms of beams with transverse reinforcement. These experimental beams were added to the program as design codes of practice were largely developed based on information obtained from beams test without transverse reinforcement.

Details of the experimental program are shown in Table 3-1 and Table 3-2 for S-series and R-series respectively. The beam reference numbers are given in the form of "XY C*aa* P*b.bb* T*c.cc* AD*d.dd*" where X denotes the test series and cross

sectional geometry and Y denotes the type of coarse aggregate used in the concrete as listed in Table 3-3. Longitudinal reinforcement ratios of the test specimens are reflected in the P values where *b.bb* represents the percentage of longitudinal reinforcement. Similarly, the transverse reinforcement ratio is prefaced with T in the beam reference. The X and Y components occur for every beam in this experimental program while the other values appear where appropriate. If no property is specified, the default values for that particular test series is applied. For instance, all S-series beams are 40 MPa, have longitudinal reinforcement ratio of 0.63% and no transverse reinforcement unless noted otherwise. R-series beams meanwhile omit AD values since all the test beams were loaded with shear span-to-depth ratios of 3.0.

S-series beam reference has additional C value and AD values where *aa* is the compressive strength of the concrete in MPa and *d.dd* is the shear span-to-depth ratio. If no C*aa* value is given, the compressive strength is 40 MPa. Only S-series of beams have these designations since these two particular properties were kept constant in the R-series. Similarly, S-series of test beams do not carry the T*c.cc* component in the beam reference as they do not contain any transverse reinforcement.

For example, beam SB C50 P0.63 is a lightweight aggregate concrete beam with a 50 MPa compressive strength and 0.63% longitudinal reinforcement ratio while SXB AD3.5 is a lightweight aggregate-foamed concrete beam with 40 MPa compressive strength, longitudinal reinforcement ratio of 0.63% and shear span-to-depth ratio of 3.5.

Parametric comparison groups are then denoted by roman numerals in Table 3-1 and Table 3-2. A roman numeral is assigned to each group within which all other parameters are constant and the effect of that parameter can be compared,

e.g. All specimens with the roman numeral III in the a/d column have varying a/d ratios while all other parameters are constant.

3.1.1 Concrete Types

Four types of concrete were tested in this experimental program including a normal weight concrete, lightweight aggregate concrete, lightweight aggregate-foamed concrete, and foamed concrete. Normal weight concrete containing rock-based coarse aggregates were cast as a control material for both the S-series and R-series. The behavioral understanding of this type of concrete is well established. Reinforced concrete codes of practice were developed from extensive experimental campaigns and the vast experience gained from using normal weight concrete.

The main focus of the experimental program was on lightweight aggregate concrete. A lower concrete density is achieved by substituting the heavy rock-based aggregates with lightweight equivalents. Numerous types of these lightweight aggregates are available for use, each with different physical properties that affect the material properties of the resulting concrete. In this program, 6 types of lightweight coarse aggregate was used.

In order to round out the structural study, foamed concrete was also included in the S-series of the experimental program. While previously used as a flowable, self-compacting, low-strength material, recent developments have seen the production of a foamed concrete with compressive strengths in excess of 30 MPa. At this strength value, foamed concrete is within the compressive strength range of a structural concrete (Jones and McCarthy 2005). This concrete does not contain any physical aggregates except hypothetical air bubble ‘aggregates’ which translate to densities even lower than lightweight aggregate concrete.

An amalgamation of foamed concrete and lightweight aggregate concrete was also tested as a preliminary step towards development of these materials for structural applications. Lightweight aggregate-foamed concrete is formed by introducing a small proportion of lightweight aggregates into foamed concrete. These aggregates then contribute to higher strengths, as well as provide restraint and internal curing that can resist drying shrinkage cracking. The self-compacting properties of the foamed concrete remain and are not compromised with the introduction of lightweight aggregates into the mix.

3.1.2 Mix Proportions

Ordinary Portland Cement was used as the binder for all test beams. Blast furnace slag was also incorporated into the mix for SXB and SX1 series of foamed concrete test beams. Normal weight concrete and lightweight aggregate concrete used washed river sand of suitable grading as fine aggregate. A superplasticiser was also employed where required to ensure adequate workability of fresh concrete during casting.

Manufactured lightweight aggregates were used as coarse aggregates in producing lightweight aggregate concrete including six varieties of expanded clay aggregates each with different shapes, sizes, surface texture and particle density as shown in Figure 3-2 through to Figure 3-5. Meanwhile, crushed granite was selected as coarse aggregate for the normal weight concrete. A summary of coarse aggregate tested in this study is shown in Table 3-3.

The mix proportions and target strengths of concrete prepared throughout the experimental program is shown in Table 3-4. A normal weight sand-lightweight coarse aggregate mix was used for lightweight aggregate concrete as it allows for better workability and strength when compared with an ‘all lightweight aggregate’

mix. Normal weight sand replacement will typically increase the equilibrium concrete density from about 60 kg/m^3 to 80 kg/m^3 compared to using lightweight fine aggregates. However, diminishing returns on weight savings occur with normal weight sand replacement since larger amounts of cement will then be required to maintain strength which in itself will increase the density from 32 kg/m^3 to 96 kg/m^3 (ACI213R). A large part of weight savings can be realized by substituting just the coarse aggregate portion with lightweight coarse aggregates that have lower bulk densities compared to lightweight fine aggregates. The coarse aggregates tend to have larger particle sizes which to developed a porous structure. For comparison, lightweight fines are typically 1120kg/m^3 which is 35% less than a typical 1760kg/m^3 for normal weight fines while lightweight coarse aggregates have a typical density of 880kg/m^3 which is half that of a normal weight coarse aggregate's typical value of 1650kg/m^3 (ACI 213R).

Blast furnace slag was included in the mix for the SX1 foamed concrete series and the SXB lightweight aggregate-foamed concrete series to boost the amount of fine particles in the mix. This was not repeated for the SX2 foamed concrete series which used only ordinary Portland cement. Superplasticiser was also added to the concretes where required to maintain an acceptable level of workability. When used, the dosage of the chemical admixture did not exceed 0.2% of the cement content by weight.

Concrete material properties for the nine types of concrete tested in the S-series are summarized in Table 3-5. Actual compressive strength of lightweight aggregate concretes in this test series ranged from 42.6 MPa to 69.8 MPa while lightweight aggregate foamed concrete and foamed concrete had compressive strengths between 25.0 and 40.7 MPa. All the specimens were compared against a

reference normal weight concrete developing 28-day cube compressive strength of 39.3 MPa.

R-series concrete material properties meanwhile are shown in Table 3-6. The lightweight concrete tested ranged from 20.8 MPa for the very friable lightweight aggregate D to 49.5 MPa for lightweight aggregate E. Normal weight concrete beams from the R-series developed an average cube compressive strength of 51.5 MPa. Only 5 cubes were tested for RD and RF lightweight concrete, and 21 cubes for RN normal weight concrete all crushed after 28 days. The average cube strength, the characteristic cube strength – of which 95% of cubes exceed, and total number of cubes tested for that particular type are shown in Table 3-6. Characteristic cube strengths are only calculated for RE and RN that have at least 20 cubes tested.

Besides compressive strengths, splitting tensile strengths obtained from tests were found to be appreciably low for foamed concrete. Lightweight aggregate concrete meanwhile had similar tensile splitting values to normal weight concrete for mixes of comparable compressive strength. As the compressive strength of lightweight aggregate concrete increases, its splitting tensile strength also increases exceeding that of the reference normal weight concrete which had a lower compressive strength. Nevertheless normal weight concrete still outperformed lightweight concrete in shear even though the former had lower tensile splitting values. Other values of material properties such as equivalent cylinder strength, modulus of rupture, Young's modulus values, and density are also presented in Table 3-5.

For the R-series, tensile splitting values were measured only for RE lightweight concrete by splitting 100 mm diameter cylinders to the method specified in BS1881-117. A total of 26 cylinders were split giving on average tensile splitting value of 3.14 MPa.

Comparisons between the concrete types investigated in this beam test program were carried out on specimens with target cube strengths of 40 MPa. This strength of concrete is able to be produced comfortably for all four types of concrete tested while keeping the densities of each concrete within its expected range. The workability of all concrete at this strength is good and surface finishing is easily completed. Being above the 25 MPa compressive strength specified by design codes for structural use, this strength of concrete is selected as a base to compare difference concrete types. As this test is also interested in high-strength lightweight concrete, 40 MPa is also the highest allowable grade of concrete for design to BS8110, and will thus make the lower bound for this test.

For lightweight aggregate concrete, test beams were also cast to achieve 50 MPa and 70 MPa compressive strength, both high-strength lightweight concretes, to explore their response. This is especially pertinent considering that normal weight concretes and high-strength normal weight concrete do have significant differences that require alternative treatment of the latter.

An intermediate strength of 50 MPa cube compressive strength is selected next since the definition of high-strength lightweight concrete is given as 48 MPa in ACI213R-03. The main parameters will be varied within this grade of concrete to provide an insight into the behavior of high-strength lightweight concrete. At this strength, lightweight aggregate concrete can still be comfortably produced with the addition of a super plasticizer into the mix. Good workability is maintained and surface finishing remains easy to accomplish.

As a further comparison, 70 MPa cube compressive strength concrete was tested. This strength of concrete is well within the range of high-strength concrete be it lightweight or normal weight concrete and is in excess of the recommended maximum strength of concrete in Eurocode 2. At this magnitude, the aggregate

strength ceiling is approached with any further increase in compressive strength due solely to the cement matrix. Tests conducted using normal weight concrete has shown that shear strength prediction in codes of practice begin to be unconservative as the concrete compressive strengths exceed 50 MPa. An investigation into the behavior of lightweight aggregate concrete at these high strengths is in order to ensure adequate design.

During the initial test phase, a disproportionate amount of super plasticizer had to be added in order to achieve the desired workability. However, while slump was reasonable, the mix was extremely stiff thus making it difficult to place. Attempts at surface finishing was ultimately abandoned. Nevertheless, the desired cube compressive strengths were able to be achieved.

3.1.3 Steel Reinforcement

Flexural tension reinforcement for the S-series beams was provided by longitudinally embedding three wires of a welded wire mesh to obtain a longitudinal reinforcement ratio of 0.63%. The mesh was made from smooth 10 mm diameter hard drawn wires arranged in two layers in 100 mm square grids. A smaller reinforcement ratio of 0.28% was obtained by substituting the 10 mm wire mesh with 6 mm wire mesh of otherwise similar properties. The larger 0.97% longitudinal reinforcement ratio was then tested by embedding two 6 mm and three 10 mm wires of two interlocking meshes. No transverse reinforcement was provided for the S series test beams. To provide sufficient tension anchorage at the end of the specimens, the wire mesh was placed such that 2 welded transverse wires are located in the length beyond the support (Mansur *et al.* 1986). The 10 mm diameter wires were tested to a yield strength of 590 MPa, while the 6 mm diameter wires yield at 675 MPa.

Steel reinforcement cages for R-series rectangular beams were fabricated by tack welding. High-tensile deformed bars were used as longitudinal tensile reinforcement with nominal bar diameters of 13 m, 16 mm, 20 mm, and 25 mm. The reinforcement was arranged in a single layer of two bars for the R-series test beams. 10 mm diameter deformed bars were provided in the flexural compression zone to function as hanger bars.

In order to provide sufficient anchorage to the longitudinal tensile reinforcement, a 5 mm thick steel plate was welded to the ends of the longitudinal bars. A 20 mm clear concrete cover to the links was also enforced using plastic seats. Steel hooks were cast into the beams to allow for easy handling of the test beams with lifting apparatus. These hooks were cast in the anchorage zone beyond the supports which is outside of the test zone.

3.1.4 Test Beam Preparation

Lightweight aggregates used in this experimental program were submerged in water overnight prior to use. The aggregates were removed from the soaking tank and allowed to stand in porous gunny sacks for at least an hour to allow excess water to drain. This was done to facilitate batching of the lightweight aggregates at saturated surface dry conditions. Alternatively the aggregates were fed into a continuous vibrating screen which removed the excess water quickly. Batching of concrete making materials were carried out by weight.

Plywood formwork was coated with a layer of de-bonding oil prior to pouring concrete. A set of 4 S-series beam moulds and 8 R-series beam moulds were re-used to prepare the test beams. Lightweight aggregate concrete was mixed in a drum mixer as was normal weight concrete. Test beams were cast 4 S-series beams or 4 R-series beams at a time with concrete being poured in 2 lifts. Foamed concrete

was cast using ordinary Portland cement and pre-formed foam from a foam generator. Foamed concrete was then prepared in a twin shaft mixer prior to being poured in 3 lifts.

Internal vibration was applied to the normal weight and lightweight aggregate concrete test beams after each lift using a needle vibrator to ensure adequate compaction. Care was taken so as not to over apply vibration that may cause segregation, especially when very low density lightweight aggregates are used. Foamed concrete and lightweight aggregate-foamed concrete is self-consolidating, as such no mechanical vibration was applied. However, the formwork was tapped several times with a hammer to ensure that the foamed concrete was able to completely fill the voids in between the steel reinforcement cage.

A prerequisite number of 100 mm cubes, 100 mm diameter by 200 mm high cylinders, and 300 mm prisms with 100 mm square cross sections were also prepared in steel moulds on a vibrating table. These cubes, cylinders and prisms are used to determine the material properties of the concrete in the test beams. Surface finishing of all the test beams, cubes, cylinders and prisms was completed by hand.

Test beams were de-molded 24 hours after casting and cured under wet burlap for 3 days. Thereafter, S-series beams were kept air dry indoors while R-series beams were stored outdoors and shaded from direct sunlight. Cubes, cylinders, and prisms cast from the same concrete as the test beams were placed adjacent to the test specimens in similar conditions. The specimens were then moved indoors and left in air dry conditions at least 7 days prior to testing which was carried out after 28 days. All material property values used in analyses below are measure from tests on these specimens. No specimens were water cured or store in a fog room.

3.1.5 Test Setup

The beams were simply supported inside a stiff steel frame with one end seated on a rocker while the other end rested on rollers (*see Figure 3-6 and Figure 3-7*). Loads were applied by a hydraulic actuator to the top surface of the test beam with contact through steel rockers that extend the width of the beam. A thin layer of plaster of Paris was spread between the contact surfaces of the test beam and steel rockers to ensure a level surface and even distribution of load.

A third point loading configuration was obtained by distributing the load from the hydraulic actuator to two load point rockers via a steel spreader beam. This spreader beam had sufficient bending capacity and stiffness to avoid excessive deformation and yielding prior to failure of the test specimens. A ball seat was also placed between the spreader beam and actuator crosshead to eliminate any eccentricity within the system. The ball seat, spreader beam, and rockers were weighed and measured to have self weight of 1.09 kN. This weight is subsequently added to the total load applied on the test beams since they are not suspended from the actuator and are supported by the test beam itself.

Span lengths for each test series was maintained and kept constant for each beam geometry. The shear span-to-depth ratios were then varied by adjusting the distance of the loading point from the support. By doing this, the shear span-to-depth ratios between 1.5 and 3.5 in the experimental program was obtained. Finally, the observed side of the beam was white washed to facilitate easy detection and observation of structural cracks as loads are applied.

3.1.6 Instrumentation

Tensile strains of the longitudinal reinforcement bars caused by flexural stresses were monitored by two 20 mm electrical resistance strain gauges that were attached

near the mid-span of each longitudinal bar. The placement of the strain gauges in the pure flexure zone was staggered by at least 50mm such that flexural cracks that may distort the strain reading will not simultaneously intersect with the gage length of both strain gages.

Compressive strains of the concrete meanwhile was monitored by a single 60 mm electrical resistance strain gauge attached to the extreme compression fiber of the concrete in the flexural zone. This strain gauge was bonded to the concrete surface using an epoxy resin.

Vertical displacements of the beam specimens at mid-span was measured continuously by linear variable displacement transducers supported on the floor. Displacement of the steel frame under the beam specimen supports was also monitored by linear variable displacement transducers to control for deflections of the steel frame under load. These support settlement values measured relative to the floor (assumed as datum) was subsequently deducted from the beam displacement values to obtain the absolute deflection of the beams under load (*see Figure 3-6*).

Readings from the linear variable displacement transducers, electrical strain gauges, and hydraulic actuator load cells were recorded by a data acquisition system. The system was programmed to record measurements from all the instrumentation at a fixed time interval or when the load changes by a preset value from the previous reading, whichever is smaller.

3.1.7 Test Method

A hydraulic actuator under crosshead displacement control was used to apply two symmetrical point loads on the test beams until ultimate failure. After the beam was set up on the steel test frame, a preload of between 1 kN and 2 kN was applied to ensure adequate contact of all the steel rockers and ball seats as well as to eliminate

settlement. Instrumentation was also checked that readings were being captured by the data acquisition system. All data channels were initialized once the preload was removed and loading proper commenced.

At the beginning stages of the test, the crosshead was set to extend at a rate of 0.1 mm/minute to avoid any sudden shocks or impulse loading. This loading rate was gradually increased in 0.05 mm/minute increments once flexure cracks had developed to a maximum of 0.5 mm/minute after the steel longitudinal reinforcement bars have yielded. Loading of the beam specimen was also paused at selected intervals to observe cracks. Where ever possible, the loading rate was adjusted such that failure was achieved within a 2 hour loading window.

Observations of cracking was performed visually while the crack propagation and crack pattern were marked by hand. Selected crack widths were also measured using a scaled handheld microscope. All observations were taken from only one face of the beam. After failure of the beam, the crack patterns were photographed, prior to the actuator crosshead being withdrawn. Initiation of both flexural cracks and shear cracks was closely observed and recorded with the corresponding applied loads.

3.2 Crack Propagation and Patterns

Beams subjected to flexure-shear loading develop structural cracks that can be classified into six types depending on the cracking mechanism. These cracks in order of formation through the loading history are: flexure tension cracks, flexure-shear cracks, diagonal tension shear cracks, dowel cracks, shear compression cracks, and flexural compression cracks. The last four types of cracks appear at loads well beyond service while the final two cracks are symptomatic of ultimate physical failure.

The cracking pattern meanwhile is influenced by the loading configuration used, which in the case of this experimental program, was a third point loading. As such, only flexure compression and flexure tension cracks occur in the flexural zone. The other five of the six types, flexure compression being the exception, may occur within the shear zone (*see Figure 3-8*).

The propagation of cracks and the cracking pattern developed by a reinforced concrete member disrupts stress redistribution paths within the section and has implications on the shear resistance mechanisms as well as the ultimate capacity of a section. Cracking was observed to be more extensive in lightweight concrete than in normal weight concrete although lightweight concrete cylinder splitting values were higher than normal weight concrete. This extensive cracking and the concomitant disruption to the stress redistribution ultimately causes a reduction in the shear capacity of lightweight concrete more so than the smoothness of the crack interface.

3.2.1 Flexure Tension Cracks

Flexural tension cracks begin from the extreme flexural tension fiber at the soffit of the beam, propagating vertically upward as the load increases. They first appear in the flexural zone where the greatest bending moment for a given load occurs. Comparatively shorter cracks then gradually develop in the shear zone as the load increases. Flexure tension cracks occur first as the flexural tensile stresses increase such that they exceed the concrete tensile capacity before the principle tensile stresses of combined shear and normal stresses at mid depth exceed.

In this aspect, lightweight aggregate concrete behaves in a manner similar to normal weight concrete except that the onset of flexure cracking occurs earlier. This can be easily observed in Figures 3-9 to 3-13 where the change in slope of the load

deflection curve, characteristic of the reduced stiffness of the cracked section, begins at a higher load for normal weight concrete compared to lightweight aggregate concrete after normalizing for compressive strengths. Foamed concrete does not show similar change in the slope since there were numerous pre-existing shrinkage cracks. Although lightweight aggregate-foamed concrete did not exhibit signs of shrinkage cracking, a change in the slope also did not occur or occurred at a very low load.

All the test beams in the series developed flexure tension cracks first with other cracks forming as the loading progressed except slab SB3.0 C50 P0.23 that had a low reinforcement ratio. This particular specimen did not develop visible cracks beyond flexural tension cracks as the low ultimate load was attained when its tension steel entered the plastic range.

While flexure cracks are caused by bending moments, their development has implications to shear. Prior to cracking, normal weight concrete beams behaves as a homogenous elastic beam. Lightweight aggregate concrete was observed to behave in a similar manner with the difference directly related to the lower elastic modulus of lightweight concrete. This is shown by the stiffness of the uncracked sections that correspond to the reduction of Young's modulus.

At a fundamental level, these vertical cracks disrupt the shear flow from the loads at the top of the beam to the supports at the soffit of the beam which leads to failure when the stresses are unable to develop alternative load paths. The larger the zone of intact concrete above the crack tip, the larger the zone available for redistribution of stresses. As the bending moments are increased, flexure cracks lengthen reducing the uncracked area of a section causing increasing disruption to the shear flow.

Control of flexure crack propagation is important in maintaining the shear capacity of a section especially in the shear zone. When more flexural tensile reinforcement is used, in addition to additional dowel resistance, these reinforcing bars also restrain the extent and width of flexural cracks which in turn causes less disruption to the shear flows. This is manifested in the size effect where larger beams have reduced shear capacities since the cracks in this type of beams tend to be wider and propagate higher into the beams (MacGregor and Wight 2005, ASCE-ACI 445 1998).

3.2.2 Flexure-Shear Cracks

Within the shear zone, the combination of flexure and shearing action leads to the formation of flexure-shear cracks. This crack is identified by a curved profile starting out as a vertically oriented flexure crack from the extreme flexure tension fiber which then gradually curves and continues propagating toward the load application point at the top of the beam. The curved trajectory of the flexure-shear crack is close to the interaction of flexure and shear stresses of a homogenous uncracked elastic beam that vary along the length and the height of the member as given by Mohr's circle of stresses. Cracking occurs along the principle tension plane since concrete is much weaker in tension than compression.

However, flexure-shear cracking cannot be predicted by calculating the principle stresses in an uncracked beam necessitating the use of empirical equations to determine the cracking value (MacGregor and Wight 2005). This is due to the presence of flexural cracks in the section prior to the principle tensile stresses at mid height becoming critical. As tensile stresses cannot be transferred perpendicularly across a crack, redistribution of stresses are necessary to maintain equilibrium resulting in a highly indeterminate system.

Up until this stage, lightweight aggregate concrete maintains similarity with normal weight concrete in crack propagation. From Figure 3-14, normal weight concrete cracking can be seen to be dominated by flexure tension cracks. While flexure-shear cracks occur, they tend to be small and only begin to develop significant inclination above the mid depth of the section. No cracking of any sort was observed to occur near the supports at shear span-to-depth ratios 3.0 and above.

This is in contrast to foamed concrete and lightweight aggregate-foamed concrete where diagonal tension cracks form with few flexure-shear cracks occurring. When they do develop, flexure-shear cracks in foamed concrete and lightweight aggregate-foamed concrete begin to incline from above the level of the longitudinal reinforcement rather than above mid height of the beam.

3.2.3 Diagonal Tension Cracks

In members where the concrete is weak or where the section is heavily reinforced, stresses within the section may increase sufficiently such that diagonal tension shear cracks precipitate. These cracks appear suddenly and without warning, simultaneously extending from the neutral axis towards the loading point and the support in a straight line. Onset of these diagonal cracks indicate that the shear flow has been interrupted by the flexure cracks and beam action gives way to tied arch action.

This manner of diagonal tension cracking was observed in beams tested at short shear span-to-depth ratios of 1.5 and 2.0 with the trend persisting through the entire SX-series and SXB-series of foamed concrete even at larger ratios. The inclined angle of these diagonal tension cracks ranged between 30° and 60° from

horizontal with steeper inclines occurring when the diagonal cracking loads are higher.

Meanwhile, the mode in which diagonal tension cracks form was different in beams from the SN-series, SB-series, SB C50 series, and SB C70 series tested at longer shear-span to depth ratios. In these beams, diagonal tension cracks evolved preferentially from prior existing flexure-shear cracks where the inclined portion extends linearly down toward the soffit. This downward crack propagation happens because the arch compression strut forms in the intact concrete above the flexure-shear inclined crack forcing the shear stresses in the bottom wedge to increase quickly and precipitate the diagonal crack. While flexure cracks tend to elongate progressively as the load is increased, diagonal tension cracks appear quickly and are long and wide regardless of the manner with which they form.

Thereafter, the residual shear capacity is largely dependent on the location of the random crack that occurred. If the crack developed near to the face of support, the residual shear capacity until ultimate was small. However if the diagonal tension crack was steep and terminated further from the face of supports, residual shear capacity developed was large. This is consistent with the loss of tension anchorage of the bottom bars that destroys the tied arch action for simply supported beams (Keown *et al*. 2006).

After the stresses redistribute to arch action, shear forces are continued to be resisted. However, when the shear span is large, the compression strut required to develop arch action is shallow thus reducing its effectiveness in resisting shear. This compression strut nevertheless can continue to transmit shear across cracks since the force in the strut is in compression.

The appearance of diagonal tension cracks is taken by design codes to be the ultimate shear capacity of the section. This event is defined as the design ultimate capacity since the formation of diagonal tension cracks only occur after significant disruption to the shear flow. In addition, the formation of the diagonal tension crack itself is a disruption that severely limits the redistribution of stresses to remaining mechanisms. This is confirmed in the behavior of lightweight aggregate concrete beams that experienced ultimate physical failures shortly after diagonal cracks initially form especially at larger shear span-to-depth ratios where arching action is not effective.

Ultimate physical failure of all cases of lightweight aggregate foamed concrete (SXB- series) and foamed concrete (SX-series) meanwhile occurred with the material rupturing along a fresh diagonal crack parallel to an earlier one. It was observed that initial diagonal tension cracking occurred at a low load which was related to the low splitting tensile strength of the foamed concrete. Nevertheless, even with the presence of the diagonal tension crack, foamed concrete and lightweight aggregate-foamed concrete was able to develop sufficient shear capacity from other mechanisms to continue resisting increasing load. Ultimate physical failure only occurred at loads in excess of 2.5 times that required to form the initial crack for small shear span-to-depth ratios.

This shows that concrete tensile strengths play an important role in shear resistance before the development of diagonal cracking. After diagonal cracks form, the shear resistance mechanism changes to one dependant on interface friction. At smaller shear span-to-depth ratios, the inclined cracks are steeper allowing shear slip to be controlled by the flexural compression stresses pressing the interface together. As the shear span-to-depth ratio increases, the slope of the inclined crack

becomes shallow resulting in reduced compression component across the crack and larger component perpendicular to the crack.

Foamed concrete beams where opened up after ultimate physical failure, and while the surface was relatively smooth, the cracking plane was random with numerous angular ridges occurring that form large shear keys. This is in contrast to lightweight aggregate concretes. The crack surface for lightweight aggregate concrete was slightly rougher by inspection due to the sand particles and cracking through the lightweight aggregates. However, the actual shearing plane was smooth and did not have the ridges and angular shear keys as observed in formed concrete and lightweight aggregate-foamed concrete. In opening up the beams, considerable manual prying force had to be exerted to remove the wedge of concrete above the diagonal crack. This verifies that a small amount of residual tensile capacity can be generated across a crack plane from the irregularity of the crack surface.

While all specimens developed diagonal tension cracks, not all lead to a shear mode of ultimate failure. Only slab SN3.5 and SB3.0 C50 P0.23 did not develop diagonal tension cracks prior to ultimate load. Both failed with flexural modes, the former dominated by a large shear span-to-depth ratios and the latter governed by a low reinforcement ratio. Specimens in the SB C70 series at large shear span-to-depth ratios developed new critical diagonal cracks leading to ultimate failure after the formation of curving flexure-shear cracks. However, at lower shear span-to-depth ratio, SB C70 test beams mimicked normal weight concrete including continually resisting shear forces post diagonal tension cracking until the flexural steel yields.

3.2.4 Dowel Crack

As flexure-shear cracking and diagonal tension shear cracks become more severe, dowel cracks may form as shearing is redistributed to a dowel mechanism. This type

of crack is characterized by a horizontal crack running parallel to the longitudinal bar at a similar level as the bar splits the concrete cover. Dowel cracking was frequently observed close to or at failure of beams.

These dowel cracks only develop in beams loaded at large shear span-to-depth ratios and appear at the instance of ultimate physical failure. Overwhelmingly, dowel cracks form after the inclined flexure shear stress develop into diagonal tension cracks. At the instance of failure, the diagonal crack ruptures losing all means of shear transfer through the intact concrete and through interface friction. As such the entire shear stress is transferred to dowel action prompting the concrete to form dowel cracks. These dowel cracks then destroy the anchorage of longitudinal steel ties thus precipitating an ultimate physical failure as tied arch action is no longer able to develop.

3.2.5 Shear Compression Crack and Flexure Compression Crack

A fourth type of crack that was observed is the shear compression crack. This type of crack occurs in the region where the interaction of flexural and shear stresses cause maximum principle compression. Local crushing of the concrete occurs which is frequently accompanied by spalling of the concrete cover. From the loading configuration used in this test, shear compression cracks occur near the load application point in the shear zone. The confined section is able to continue carrying load even after the unconfined concrete cover has spalled indicating that the section has considerable residual strength after failure.

Finally, if the bending moment increases such that the compression capacity of the concrete is exhausted, the material will crush leading to flexure compression cracks at the ultimate load.

3.2.6 Cracking Patterns

Cracking was more extensive in SX-series and SXB-series where a larger number of closely spaced cracks appeared as compared to the SN-series and SB series (*see Figure 3-14 to 3-23*). This can be attributed to the lower tensile strengths available to lightweight aggregate foamed concrete and foamed concrete as indicated by their cylinder splitting and modulus of rupture values shown in Table 3-5. It was also observed that no significant cracks occurred within a length equal to the effective depth, d, from the face of support in the SN-series unlike in the three lightweight concrete series. Although shrinkage cracking developed in the foamed concrete specimens, these non-structural cracks did not appear to alter the cracking pattern with the diagonal tension cracks propagating across shrinkage cracks with negligible discontinuity.

3.2.7 Effect of Longitudinal Reinforcement on Diagonal Cracking

Diagonal tension cracks that are caused by shearing action developed in all the R-series beams tested prior to reaching ultimate failure. The onset of this inclined crack within the shear zone was keenly observed with the corresponding cracking loads recorded. In beams without transverse reinforcement, the applied shear stress to initiate diagonal cracking increases with longitudinal reinforcement ratios. The increase in shear stress required is caused by the ability of the larger reinforcement bar to control flexural cracking which disrupts the shear flow as discussed earlier. This trend is illustrated in Figure 3-24 below.

After normalizing for compressive strength by dividing by the square root of cube compressive strength, it was found that lightweight aggregate concrete initiates diagonal cracking at 75% of the shear stress required for normal weight concrete. This ratio then approaches 95% as the reinforcement ratio increases to 2.96%. The

narrowing of difference between lightweight aggregate concrete and normal weight concrete shows the importance of controlling the extent of flexural cracking and its effect on reducing shear carrying capacity especially in lightweight concrete. This is because a similar increase in longitudinal steel ratios results in a larger increase in diagonal cracking loads of lightweight concrete compared to its normal weight concrete counterpart. In other words, lightweight concrete shear strength is more sensitive to flexural cracking than in normal weight concrete which leads to a higher rate of increase of diagonal cracking load with longitudinal reinforcement ratio. The lower modulus of elasticity and modular ratio of lightweight aggregate concrete contribute to this as more load is shed to the stiffer steel as the member deforms more. This can be clearly seen from the trend lines shown in Figure 3-20. The line for lightweight aggregate concrete is approximately twice as steep as the line for normal weight concrete.

Ultimate shear stress likewise increases with longitudinal reinforcement. The ultimate shear stress of lightweight aggregate concrete exceeds 90% that of normal weight concrete for 1.23% longitudinal reinforcement, increasing to parity as the reinforcement ratio increases. Compared to diagonal cracking ratios earlier, the margin to ultimate failure is larger for lightweight aggregate concrete than for normal weight concrete. That means lightweight aggregate concrete starts diagonal cracking before normal weight concrete although their ultimate strengths may be similar. Over all types of concrete tested without transverse steel, the margin between diagonal cracking and ultimate ranged between 1.1 to 1.9 times the cracking load.

From Figure 3-25, the observed value of shear cracking for each specimen was plot against its longitudinal reinforcement ratio. It is assumed that the initial shear cracking load is not influenced by the transverse reinforcement ratio since the links do not resist tension until cracks form (Elzanaty *et al.* 1986, Chung and Ahmad

1994). The influence of dowel action of these links is also neglected. It can be seen from this figure that the diagonal cracking loads appear to be linearly related to the reinforcement ratio which may be characteristic of the influence of dowel action of these longitudinal bars.

3.3 Ultimate Failure Modes

Ultimate physical failure of the test beams occurred in one of three ways. All beams in the SN-series experienced a flexural failure mode with the longitudinal tensile reinforcement elongating into the plastic region after yielding. This was however, not before diagonal tension cracks appeared except in SN3.5 mentioned earlier. Flexural failure modes were also observed for beams tested at small shear span-to-depth ratios in SB-series, SB C50-series, SB C70-series, and SX1-series. Although diagonal tension cracks had formed in the beams, sufficient shear resistance from arching action to the support leads to their bending capacity being exhausted first.

All other specimens developed either diagonal tension failure or shear compression failure. In the former, a critical diagonal crack forms that causes the concrete to rupture. This occurs when the crack is sufficiently wide that stress redistribution to other shear resistance mechanisms is no longer possible. As such, diagonal tension failure does not occur immediately after appearance of diagonal tension cracks. Some level of tension force can still be transferred across the crack once they form via interface shear. These cracks then widen until a stage where complete shearing through or crushing of concrete at the compression tip will cause ultimate failure. For specimens in the SN-series of normal weight concrete, sufficient reserve shear strength exists after cracking for flexural failure to precipitate. These beams maintain ductility and display large deflections before flexural crushing of concrete in the flexural zone due to bending action.

From this test series, as expected, all the test specimens without transverse reinforcement failed via diagonal tension. The ultimate failure load occurred shortly after the appearance of diagonal cracks indicating that the ability of the section to redistribute stresses after the formation of these cracks is limited. Failure was sudden and occurred without warning. Shear capacity of these sections was also reached well before the flexural section reached service loads indicating premature shear failure.

The beams may also fail in shear compression where the flexural compression zone is reduced by the inclined flexure-shear crack to an extent where the concrete in this zone crushes. In this failure mode, localized crushing occurs with the possibility of a concrete wedge spalling off the compression surface. The reduced cross section of remaining concrete will then quickly rupture along a critical diagonal crack.

In both diagonal tension failure and shear compression failure, a clean smooth crack through the slab is observed with the beam held together by the wire reinforcement that remains intact. Besides preventing complete rupture of the beam, dowel action and tied arch action of the longitudinal reinforcement allows the beam to have some residual load bearing capacity.

This is supported by experimental observation of crack behavior during the loading. Flexure-shear crack widths where observed to increase with loading until diagonal tension cracking formed. The flexure-shear crack then developed translational displacement where the inclined branch slipped while the crack width at inflection point closed. Just prior to ultimate failure, the diagonal tension crack opened up rapidly before shear failure when interface friction was exceeded (*see Figure 3-26*).

3.4 Qualitative Model for Shear Resistance of Lightweight Concrete

From the experimental observations from this test program, a qualitative model illustrated in Figure 3-27 below on the development of cracking in a reinforced lightweight concrete beam is presented. Based on known shear transfer mechanisms, this model describes the changes in the active shear resistance mechanism through the loading history and the difference in normal weight concrete and lightweight concrete including foamed concrete.

An uncracked reinforced concrete beam subjected to loading will behave in the similar manner to a homogenous elastic beam. The onset of cracking in the concrete is governed by the tensile strength of the material itself and the load patterns applied. Typically, tensile stresses caused by bending moments will exceed the tensile capacity of the concrete first leading to flexure cracks. Once these cracks form, the beam no longer responds to loads as an elastic beam but is now softened. Shear is then transferred via the intact concrete above the flexure cracks. If the shear span-to-depth ratio is small, arching action and a compression strut may also develop to carry part of the shear.

As the loading increases, flexure-shear cracks form due to the interaction between the shearing stress and the flexure compression resulting in an incline. Once the crack inclines, the remaining intact concrete above the tip of the crack has reduced significantly. The shear is then resisted by tied arch action in combination with the flexural reinforcement. Shear friction also plays a part in resisting the shear especially in the inclined portion of the crack as the concrete tends to slip past. Up until this stage, normal weight concrete, lightweight concrete, and foamed concretes behave in similar fashion with differences directly related to the material properties of the types of concrete i.e. Elastic modulus, tensile capacity, and compression capacity. Once diagonal tension cracks form, the differences in behavior of normal

weight concrete and lightweight concrete begin to manifest resulting in a lower ultimate physical failure of lightweight concrete compared to normal weight concrete.

This is reflected in the experimental results where the flexural cracking of concrete is directly proportional to the elastic modulus and tensile strength of the concrete, and diagonal cracking loads appear at load thresholds lower than normal weight concrete after normalizing for material properties.

Once diagonal tension cracks form, shear is carried largely by tied arch action. At larger shear span-to-depth ratio, the compression strut of the tied arch is shallow thus requiring a larger contribution of interface friction to maintain equilibrium. The smoother crack surface of lightweight aggregate concrete is able to develop the required friction, however, this friction is lost at a lower crack level of crack width compared to normal weight concrete. Foamed concrete while having a crack interface that is even smoother than lightweight aggregate concrete managed to develop significant shear friction due to the irregular angular crack plane.

As this shear friction and tied arch action is lost, physical failure will precipitate. Tied arch action can be disrupted by the loss of tension anchorage of the longitudinal reinforcement bars. If the random crack occurs in such a way that the anchorage is compromised, the section will have a reduced shear capacity. Alternatively, the vertical component of the compression strut may also cause dowel splitting failure in the zone beyond which the hypothetical compression strut form.

3.5 Conclusion

32 S-series reinforced concrete beams and 16 R-series reinforced concrete beams of lightweight aggregate concrete with coarse lightweight aggregates and normal weight sand, foamed concrete, and lightweight coarse aggregate foamed concrete were tested until physical failure. The propagation of cracks and cracking patterns

was carefully observed and a qualitative model presented to explain the results obtained.

Lightweight aggregate concrete beams behaved in similar manner to the reference normal weight concrete beams until onset of diagonal cracking. Thereafter, while normal weight concrete beams were able to continue resisting shear until a flexural mode of physical failure occurred, lightweight aggregate concrete was unable to develop sufficient resistance and physically failed in a brittle shear mode.

Foamed concrete and lightweight aggregate-foamed concrete also responded to loads like normal weight concrete. Diagonal cracking occurred at lower loads than both normal weight concrete and lightweight aggregate concrete due to its tensile strength being much lower than the reference concrete although having comparable compressive strengths. Nevertheless, after the onset of diagonal cracking, foamed concrete and lightweight aggregate-foamed concrete was able to continue resisting significant amount of shear prior to physical ultimate failure. This is due to the irregular and angular cracking plane at macro level compared to the smooth crack surface at the micro level.

Table 3-1 Experimental program S-series

No.	Ref. Number	Target Compressive Strength	Longitudinal Reinforcement		Transverse Reinforcement			Shear span to Effective Depth Ratio	Parameters					
			Ratio (bh) %	*Bars*	*Ratio*	*Spacing*	*Spacing (multiples of effective depth)*		*f'c*	*CT*	*ρL*	*ρT*	*a/d*	*agg*
1	SN AD1.5	40	0.63	3 A10	nil	nil	nil	1.5		I			I	
2	SN AD2.0	40	0.63	3 A10	nil	nil	nil	2.0		II			I	
3	SN AD3.0	40	0.63	3 A10	nil	nil	nil	3.0		III			I	I
4	SN AD3.5	40	0.63	3 A10	nil	nil	nil	3.5		IV			I	
5	SB AD1.5	40	0.63	3 A10	nil	nil	nil	1.5	I	I			II	
6	SB AD2.0	40	0.63	3 A10	nil	nil	nil	2.0	II	II			II	
7	SB AD3.0	40	0.63	3 A10	nil	nil	nil	3.0	III	III			II	
8	SB AD3.5	40	0.63	3 A10	nil	nil	nil	3.5	IV	IV			II	
9	SB C50 AD1.5	50	0.63	3 A10	nil	nil	nil	1.5	I				III	
10	SB C50 AD2.0	50	0.63	3 A10	nil	nil	nil	2.0	II				III	
11	SB C50 AD3.0	50	0.63	3 A10	nil	nil	nil	3.0	III		I		III	I
12	SB C50 AD3.5	50	0.63	3 A10	nil	nil	nil	3.5	IV				III	
13	SB C50 AD3.0 P0.23	50	0.23	3 A6	nil	nil	nil	3.0			I			
14	SB C50 AD3.0 P0.78	50	0.78	2 A6 + 3 A10	nil	nil	nil	3.0			I			
15	SB C70 AD1.5	70	0.63	3 A10	nil	nil	nil	1.5	I				IV	
16	SB C70 AD2.0	70	0.63	3 A10	nil	nil	nil	2.0	II				IV	
17	SB C70 AD3.0	70	0.63	3 A10	nil	nil	nil	3.0	III				IV	
18	SB C70 AD3.5	70	0.63	3 A10	nil	nil	nil	3.5	IV				IV	
19	SA C50 AD3.0	50	0.63	3 A10	nil	nil	nil	3.0						I
20	SG C50 AD3.0	50	0.63	3 A10	nil	nil	nil	3.0						I
21	SXB AD1.5	40	0.63	3 A10	nil	nil	nil	1.5		I			V	
22	SXB AD2.0	40	0.63	3 A10	nil	nil	nil	2.0		II			V	
23	SXB AD3.0	40	0.63	3 A10	nil	nil	nil	3.0		III			V	I
24	SXB AD3.5	40	0.63	3 A10	nil	nil	nil	3.5		IV			V	
25	SX1 AD1.5	40	0.63	3 A10	nil	nil	nil	1.5		I			VI	
26	SX1 AD2.0	40	0.63	3 A10	nil	nil	nil	2.0		II			VI	
27	SX1 AD3.0	40	0.63	3 A10	nil	nil	nil	3.0		III			VI	I
28	SX1 AD3.5	40	0.63	3 A10	nil	nil	nil	3.5		IV			VI	
29	SX2 AD1.5	40	0.63	3 A10	nil	nil	nil	1.5		I			VII	
30	SX2 AD2.0	40	0.63	3 A10	nil	nil	nil	2.0		II			VII	
31	SX2 AD3.0	40	0.63	3 A10	nil	nil	nil	3.0		III			VII	I
32	SX2 AD3.5	40	0.63	3 A10	nil	nil	nil	3.5		IV			VII	

Table 3-2 Experimental program R-series (without transverse reinforcement)

No.	Ref. Number	Target Compressive Strength	Longitudinal Reinforcement		Transverse Reinforcement			Shear span to Effective Depth Ratio	Parameters				
			Ratio (bh) %	Bars	Ratio	Spacing	Spacing (multiples of effective depth)		*f'c*	*agg*	ρL	ρT	*a/d*
1	RD P1.06 T0.00	40	1.06	2 T13	nil	nil	nil	3.0		I	I	I	
2	RD P1.61 T0.00	40	1.61	2 T16	nil	nil	nil	3.0		II	I	II	
3	RD P2.51 T0.00	40	2.51	2 T20	nil	nil	nil	3.0		III	I	III	
4	RE P1.06 T0.00	40	1.06	2 T13	nil	nil	nil	3.0		I	IV	IV	
5	RE P1.61 T0.00	40	1.61	2 T16	nil	nil	nil	3.0		II	IV	V	
6	RE P2.51 T0.00	40	2.51	2 T20	nil	nil	nil	3.0		III	IV	VI	
7	RE P3.93 T0.00	40	3.93	2 T25	nil	nil	nil	3.0			IV	VII	
8	RF P1.06 T0.00	40	1.06	2 T13	nil	nil	nil	3.0		I	VI	VIII	
9	RF P1.61 T0.00	40	1.61	2 T16	nil	nil	nil	3.0		II	VI	IX	
10	RF P2.51 T0.00	40	2.51	2 T20	nil	nil	nil	3.0		III	VI	X	
11	RN P1.06 T0.00	40	1.06	2 T13	nil	nil	nil	3.0		I	IX	XI	
12	RN P1.61 T0.00	40	1.61	2 T16	nil	nil	nil	3.0		II	IX	XII	
13	RN P2.51 T0.00	40	2.51	2 T20	nil	nil	nil	3.0		III	IX	XIII	

Table 3-3 Coarse aggregates

Designation	Shape	Surface Texture	Bulk Density *(kg/m³)*	Nominal Diameter *(mm)*	Type	Comments
A	Spherical	Smooth	853	9	Expanded Clay (A)	Lightweight Aggregate
B	Spherical	Smooth	767	8	Expanded Clay (A)	Lightweight Aggregate
D	Spherical	Smooth	286	8	Expanded Clay (A)	Lightweight Aggregate
E	Elliptical	Rough	574	12	Expanded Clay (A)	Lightweight Aggregate
F	Angular	Rough	727	12	Expanded Clay (A)	Lightweight Aggregate
G	Spherical	Smooth	818	5	Expanded Clay (B)	Lightweight Aggregate
N	Angular	Rough	N/A	12	Granite	Rock Based Aggregate
X	Spherical	Smooth	-	-	Air Bubble	Hypothetical Aggregate

(A) Leca (B) Liapor

Note: - All lightweight aggregates are manufactured unless otherwise stated.
- Bulk density measured to BS EN 1097 Part 3 (1998).
- N/A = not available

Table 3-4 Concrete mix proportions

Concrete Type	Target Strength	OPC	Water	Sand	Coarse Aggregates	GGBFS	Foam
	MPa	kg/m^3	kg/m^3	kg/m^3	kg/m^3	kg/m^3	kg/m^3
SN	40	350	175	764	1040	-	-
SB	40	350	193	719	600	-	-
SB	50	500	160	679	600	-	-
SA	50	500	175	640	600	-	-
SG	50	450	171	692	580	-	-
SB	70	550	121	869	525	-	-
SXB	40	466	139.8	-	370	466	10.68
SX1	40	589	176.7	-	-	589	17.93
SX2	40	1097	384	-	-	-	18.9
RE	40	430	163	728	600	-	-
RF	40	430	163	728	412.5	-	-
RD	40	430	163	728	225	-	-
RN	40	415	208	730	1006	-	-

OPC: Ordinary Portland Cement
GGBFS: Ground Granulated Blast Furnace Slag

Table 3-5 Concrete material properties

Concrete Type	Cube Compressive Strength, f_{cu} MPa	Equivalent Cylinder Strength * MPa	Splitting Tensile Strength, f_{ct} MPa	Modulus of Rupture, f_r MPa	Young's Modulus, E MPa	Density kg/m^3
SN	39.3	36.5	2.91	3.77	25.12	2315
SB	42.6	39.6	3.00	2.73	22.15	1880
SB C50	47.0	43.8	3.76	3.74	23.40	1930
SB C50 P0.23 SB C50 P0.78	50.5	46.9	3.39	3.98	24.01	1930
SA	53.3	49.6	2.94	3.17	23.22	1950
SG	57.0	53.0	3.38	2.77	21.90	1900
SB C70	69.8	64.9	3.81	3.82	31.55	2020
SXB	40.7	38.3	2.42	2.19	14.07	1500
SX1	36.2	34.0	1.63	0.66	9.61	1400
SX2	25.0	23.5	2.15	-	-	1500

* 0.93 f_{cu} except 0.94 f_{cu} for SX1, SX2, and SXB (Wee 2005)

Table 3-6 Material properties of R-series

Concrete Type	Average Cube Compressive Strength MPa	Characteristic Cube Compressive Strength[(a)] MPa	Range of Compressive Strength MPa	Nos. of Cubes Tested
RD	20.8	-	17.5 – 23.3	5
RE	49.5	34.5	21.1 - 62.6	52
RF	37.3	-	32.2 – 41.3	5
RN	51.5	47.6	47.6 – 58.8	21

Note:

(a) 95% of cubes have compression strength higher than the characteristic cube strength.

Table 3-7 S-series test results

Specimen Number	a/d	Shear at diagonal cracking V_{cr}, kN	Shear at failure V_u, kN	Ultimate Mode of Failure
SN 1.5	1.5	63.0	73.5	F
SN 2.0	2.0	30.0	58.3	F
SN 3.0	3.0	33.0	40.0	F
SN 3.5	3.5	27.5	35.2	F
SB 1.5	1.5	37.5	67.0	S-F
SB 2.0	2.0	33.5	43.7	S-C
SB 3.0	3.0	34.3	36.1	S-C
SB 3.5	3.5	27.5	28.3	S-C
SB C50 1.5	1.5	65.0	74.0	S-F
SB C50 2.0	2.0	37.0	56.7	S-C
SB C50 3.0	3.0	30.0	30.3	S-C
SB C50 3.5	3.5	31.5	34.1	S-C
SB C50 P0.23 3.0	3.0	-	17.8	F
SB C50 P0.78 3.0	3.0	32.5	37.8	S
SA C50 3.0	3.0	35.0	35.3	S-C
SG C50 3.0	3.0	30.0	30.9	S-C
SB C70 1.5	1.5	67.5	72.5	F
SB C70 2.0	2.0	40.0	57.2	F
SB C70 3.0	3.0	33.0	39.4	S-C
SB C70 3.5	3.5	31.3	31.4	S-C
SX1 1.5	1.5	18.8	52.5	S
SX1 2.0	2.0	14.4	40.0	S-C
SX1 3.0	3.0	11.0	29.0	S-C
SX1 3.5	3.5	14.9	19.2	S-C
SXB 1.5	1.5	21.0	68.6	S-C
SXB 2.0	2.0	21.0	49.7	S-C
SXB 3.0	3.0	19.2	25.2	S-C
SXB 3.5	3.5	17.0	19.3	S-C
SX2 1.5	1.5	13.3	40.3	S
SX2 2.0	2.0	13.0	36.9	S
SX2 3.0	3.0	16.5	20.8	S
SX2 3.5	3.5	12.3	12.6	S

F : Flexural
S : Shear
S-F : Shear-Flexure
S-C : Shear-Compression

Table 3-8 R-series test results

Specimen Number	ρ	f_{cu}	Shear at diagonal cracking V_{cr}, kN	Shear at failure V_u, kN	Ultimate Mode of Failure
RD P1.06 T0.00	1.06	20.8	15.9	17.2	Shear
RD P1.61 T0.00	1.61	20.8	15.5	20.7	Shear
RD P2.51 T0.00	2.51	20.8	18.2	25.7	Shear
RE P1.06 T0.00	1.06	34.5	12.5	23.6	Shear
RE P1.61 T0.00	1.61	34.5	14.3	26.6	Shear
RE P2.51 T0.00	2.51	34.5	20.5	28.2	Shear
RE P3.93 T0.00	3.93	34.5	30.0	48.2	Shear
RF P1.06 T0.00	1.06	37.3	17.0	21.2	Shear
RF P1.61 T0.00	1.61	37.3	12.5	24.3	Shear
RF P2.51 T0.00	2.51	37.3	22.5	41.0	Shear
RN P1.06 T0.00 A	1.06	51.5	25.8	30.8	Shear
RN P1.61 T0.00 A	1.61	51.5	25.4	28.8	Shear
RN P2.51 T0.00 A	2.51	51.5	*unrecorded*	35.2	Shear
RN P1.06 T0.00 B	1.06	51.5	19.9	33.4	Shear
RN P1.61 T0.00 B	1.61	51.5	27.0	37.6	Shear
RN P2.51 T0.00 B	2.51	51.5	31.1	36.7	Shear

Note: RN series test beams while tested in duplicate, are treated individually in analyses herein

S-series Beam. Scale 1:20

Clear Concrete Cover 20mm

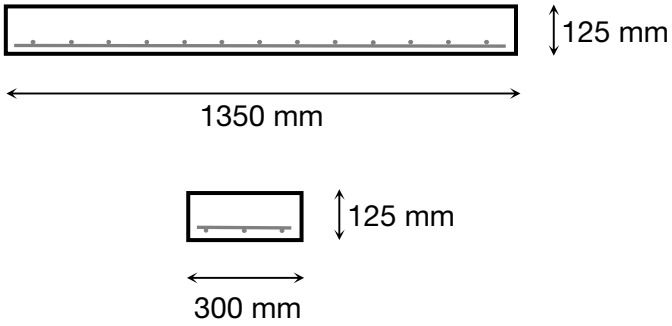

R-series Beam. Scale 1:20

Clear Concrete Cover 20mm

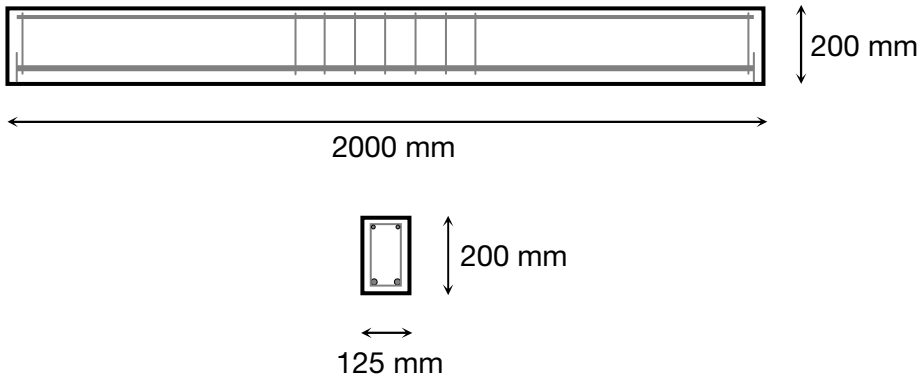

Figure 3-1 Specimen geometry

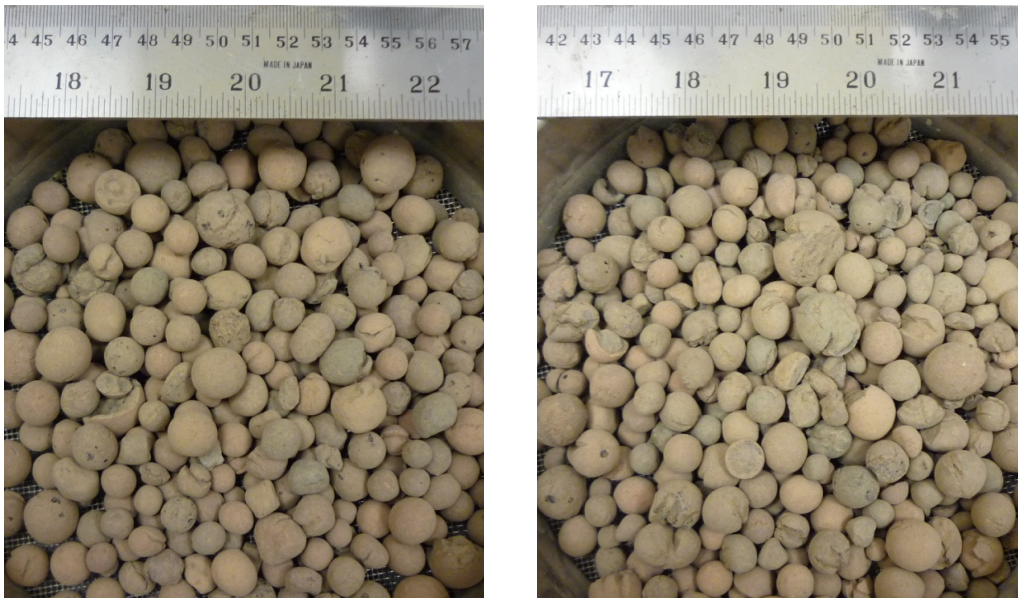

Figure 3-2 Type A lightweight aggregate (left) and Type B lightweight aggregate (right)

Figure 3-3 Type D lightweight aggregate (left) and Type E lightweight aggregate (right)

Figure 3-4 Type F lightweight aggregate (left) and Type N aggregate (right)

Figure 3-5 Type G lightweight aggregate

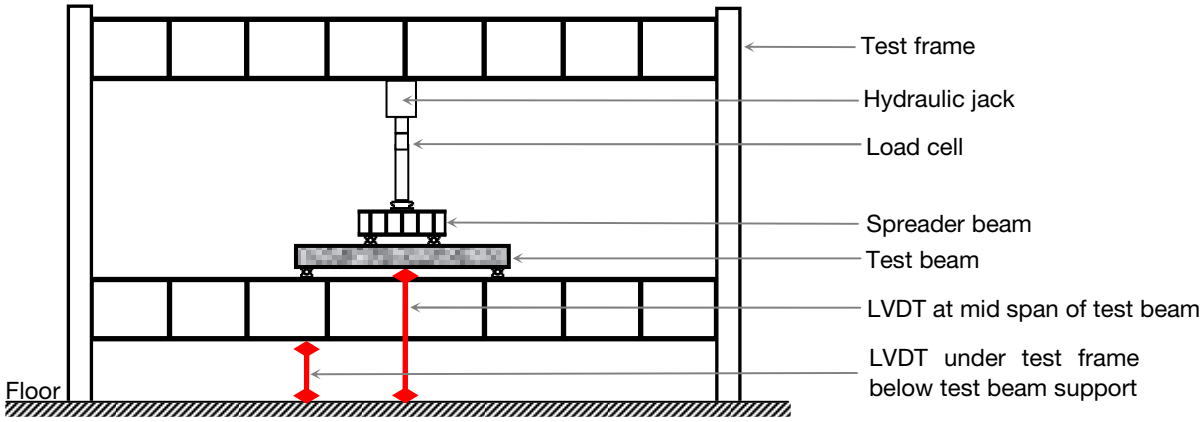

Illustrative Test Setup

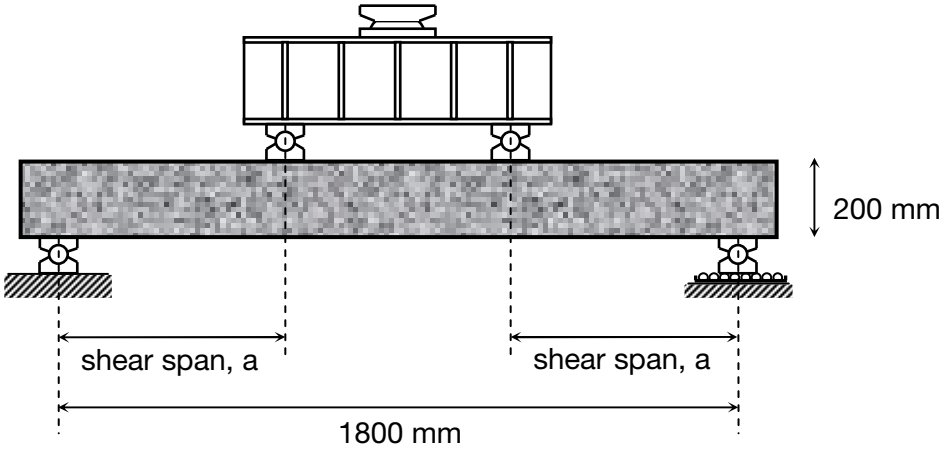

R-series Beam Test Setup

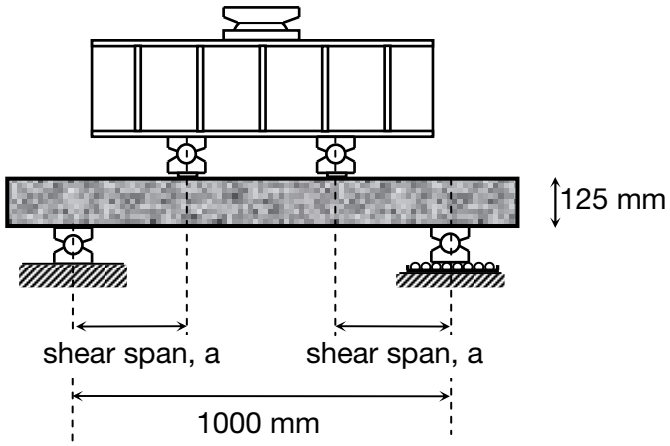

S-series Beam Test Setup

Figure 3-6 Experimental setup

Figure 3-7 Test beam ready for testing

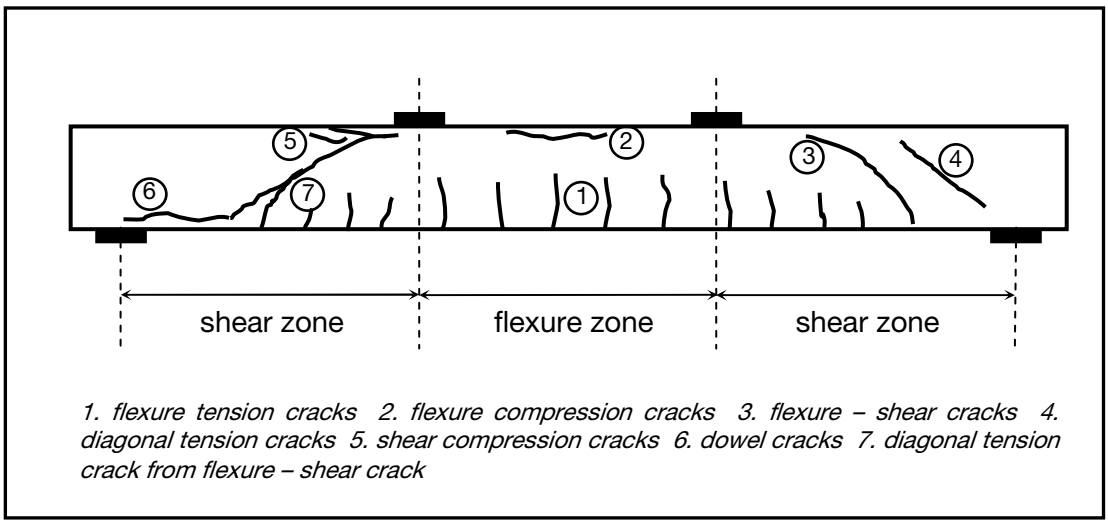

1. flexure tension cracks 2. flexure compression cracks 3. flexure – shear cracks 4. diagonal tension cracks 5. shear compression cracks 6. dowel cracks 7. diagonal tension crack from flexure – shear crack

Figure 3-8 Types of cracks

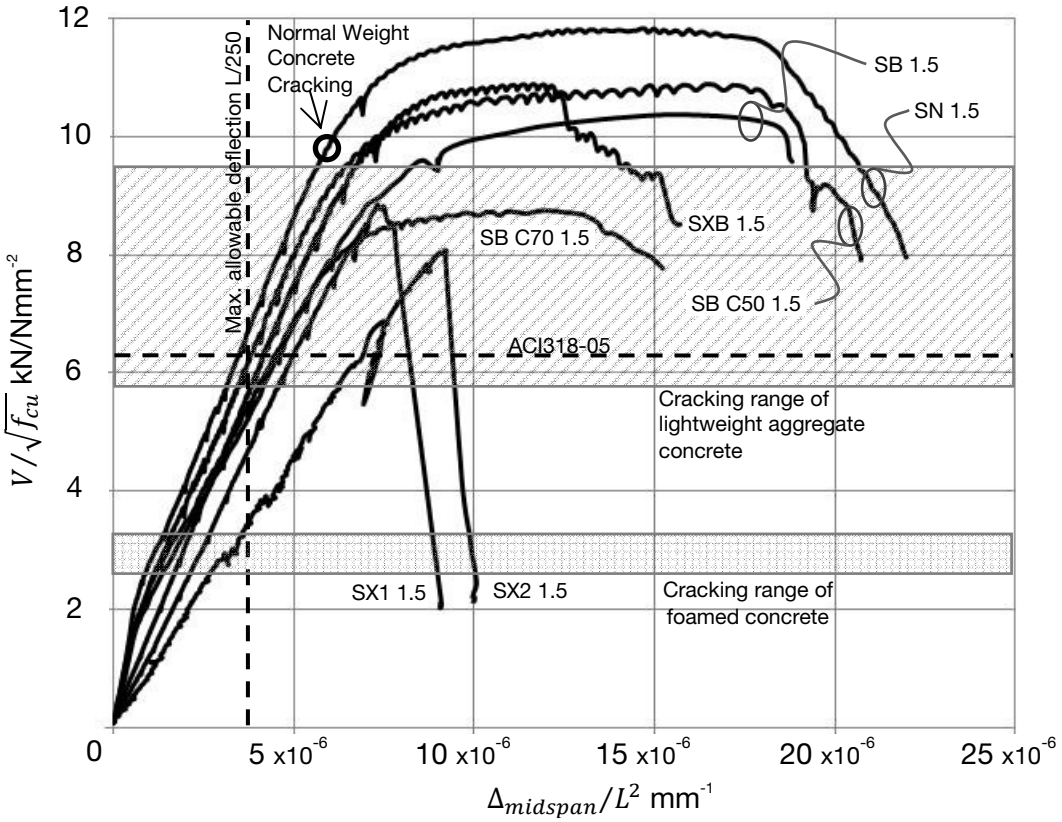

Figure 3-9 Normalised shear force - displacement curve for a/d 1.5

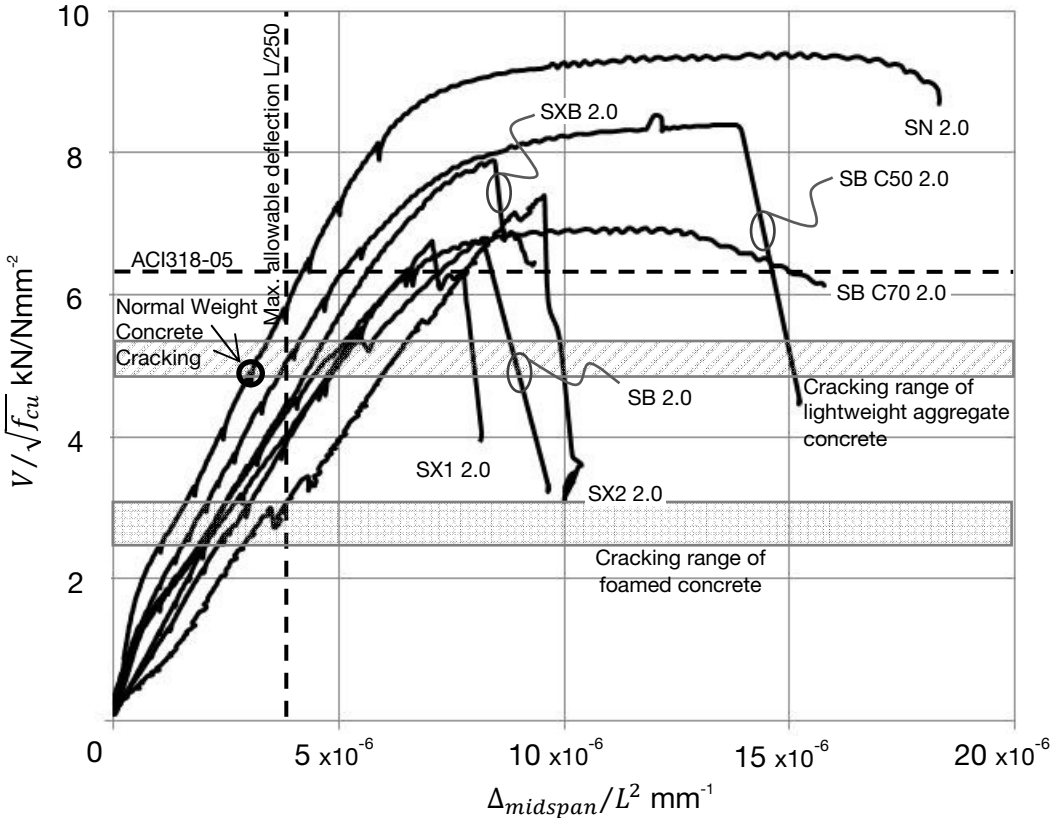

Figure 3-10 Normalised shear force - displacement curve for a/d 2.0

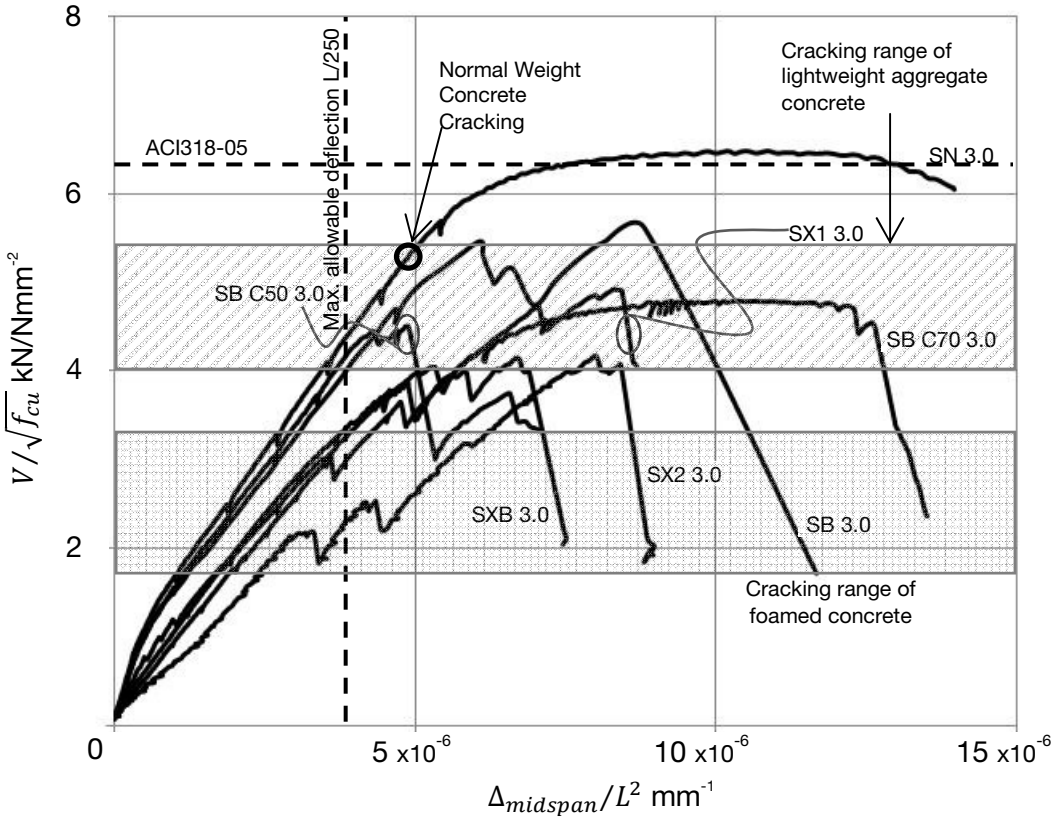

Figure 3-11 Normalised shear force - displacement curve for a/d 3.0

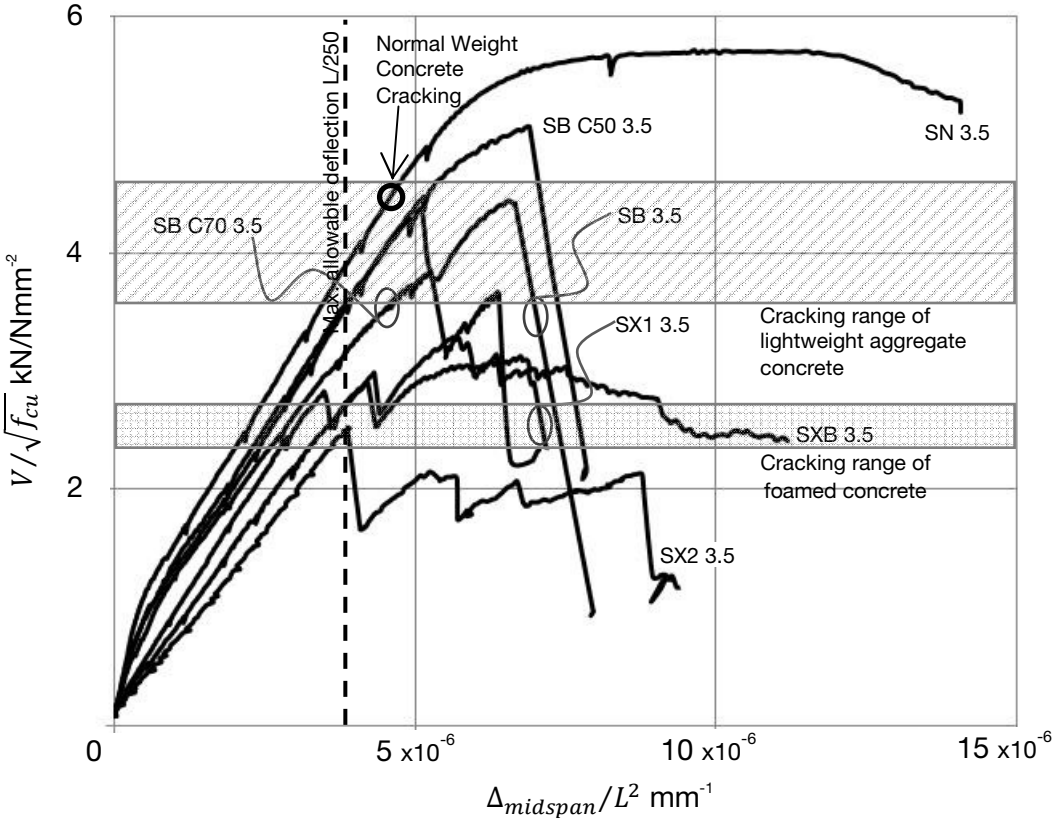

Figure 3-12 Normalised shear force - displacement curve for a/d 3.5

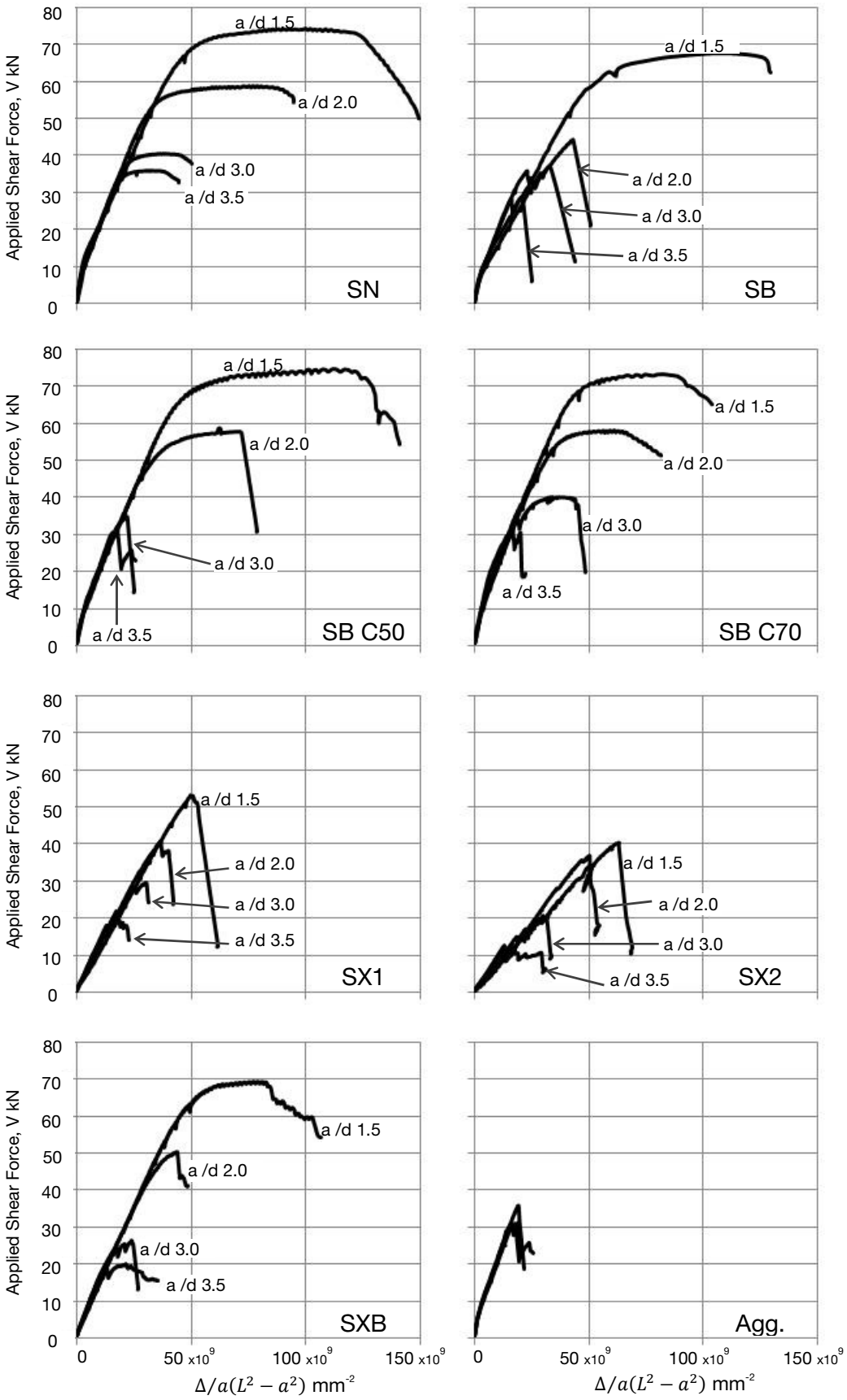

Figure 3-13 Applied shear force – normalised deflection curves

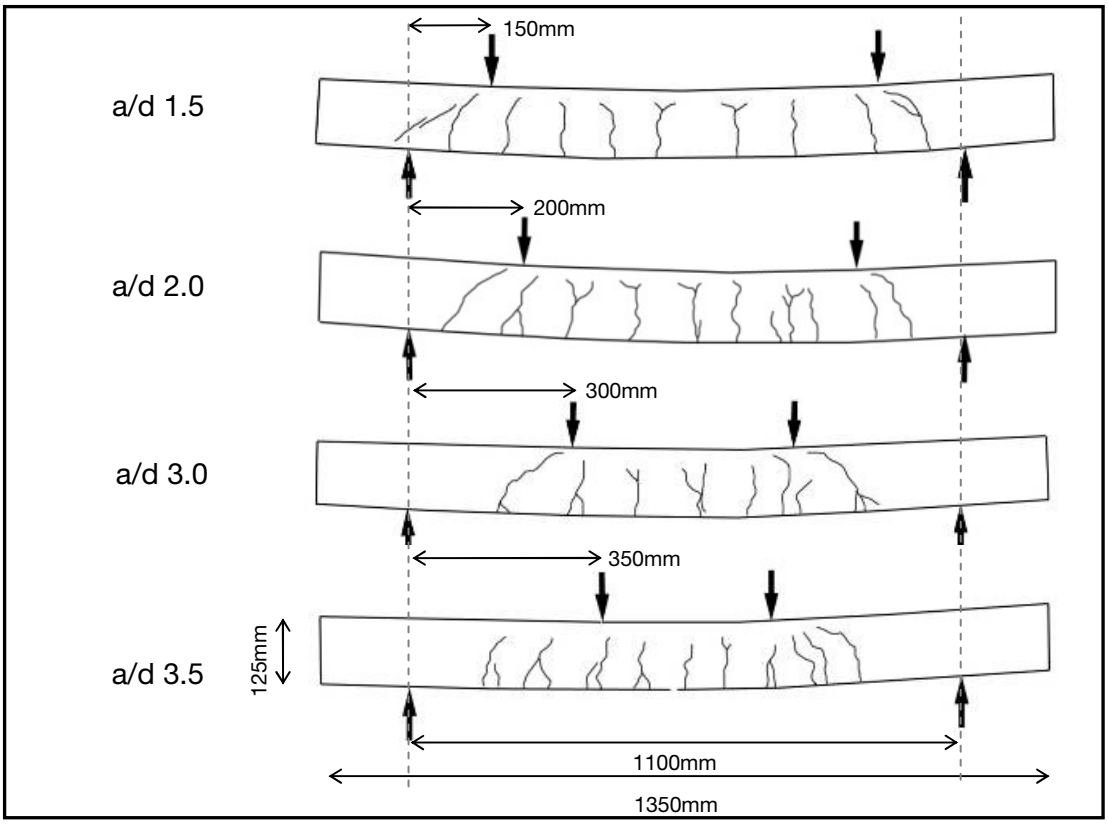

Figure 3-14 Crack pattern of SN-series

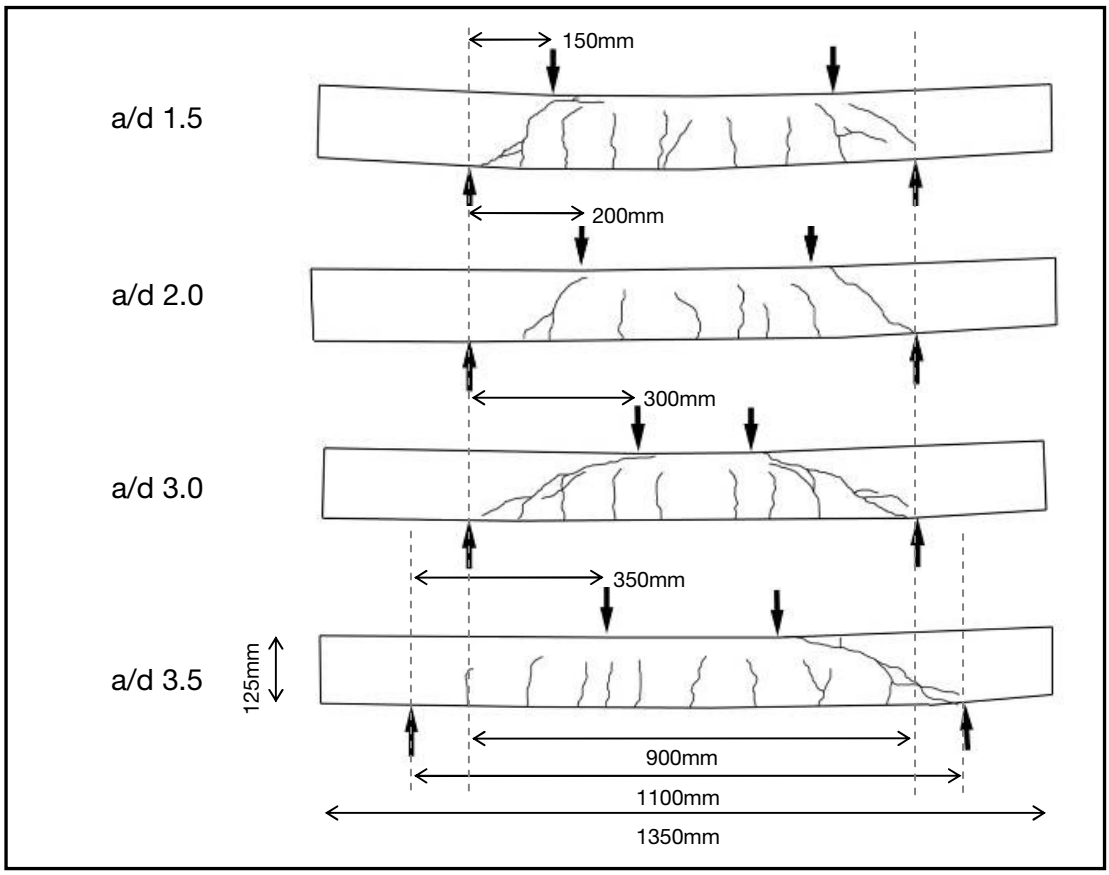

Figure 3-15 Crack pattern of SB-series

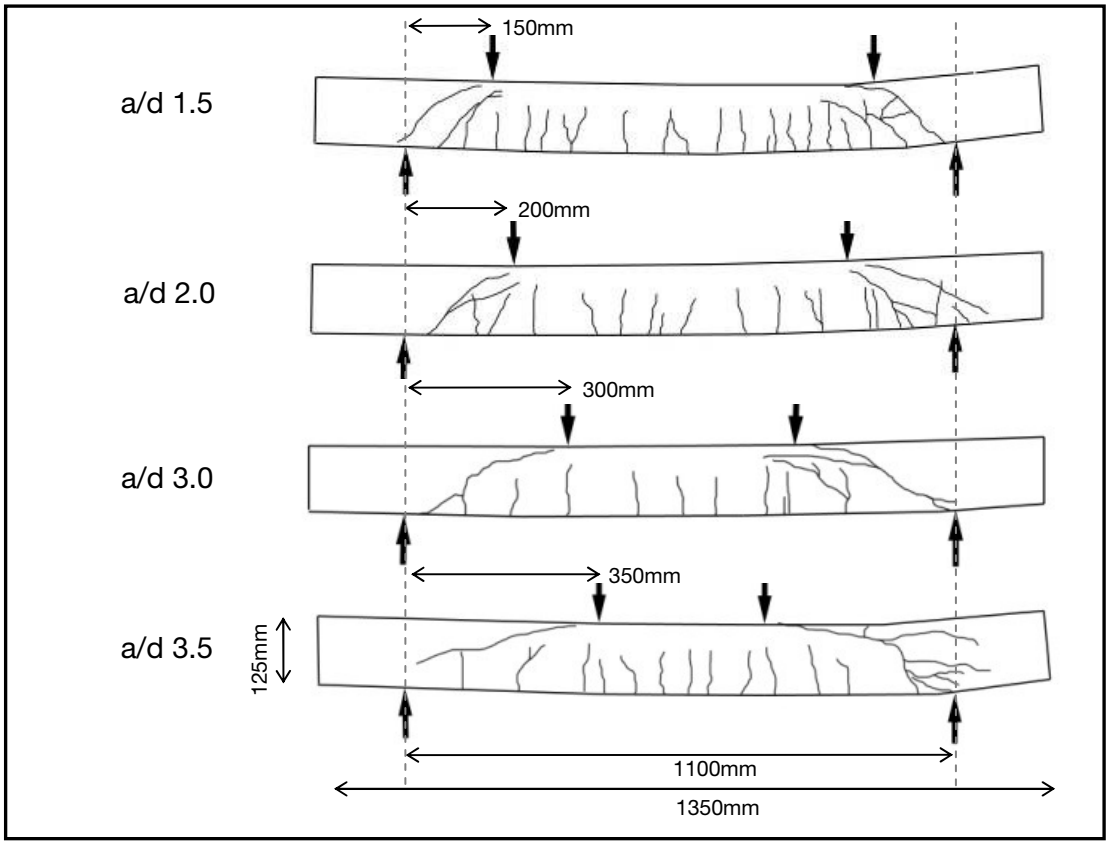

Figure 3-16 Crack pattern of SXB-series

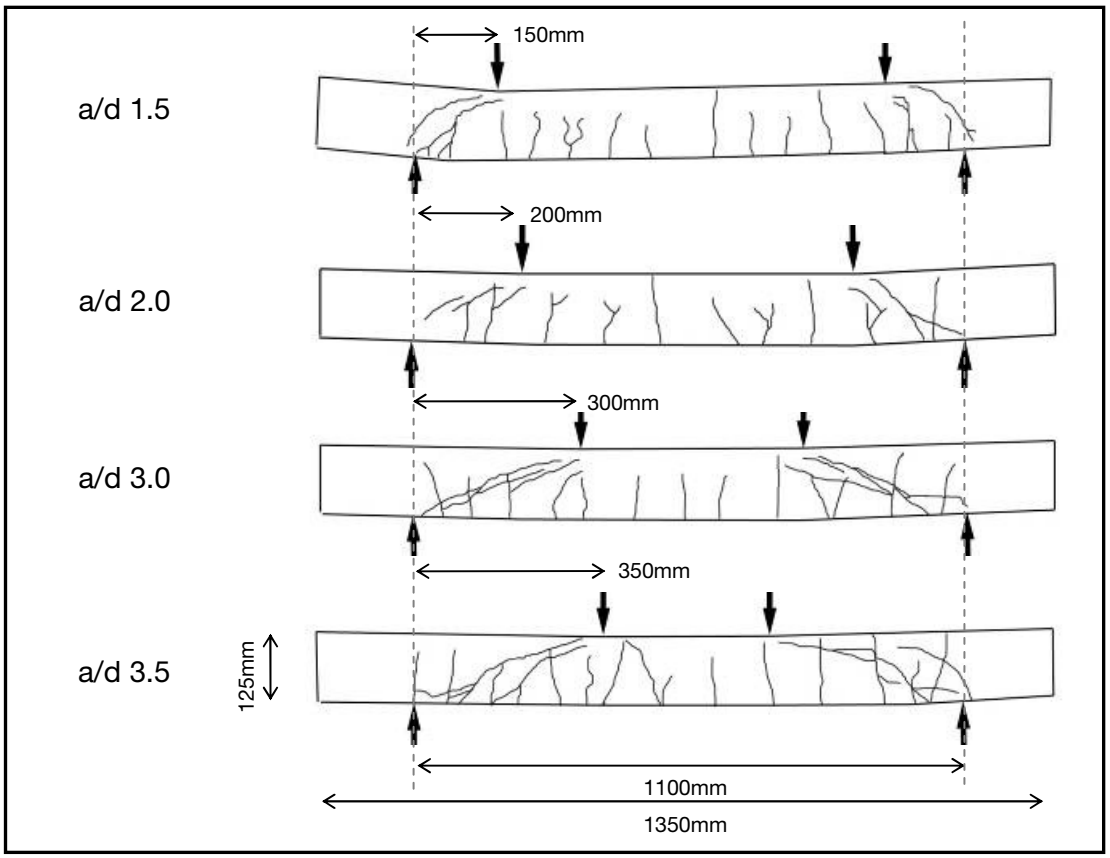

Figure 3-17 Crack pattern of SX1-series

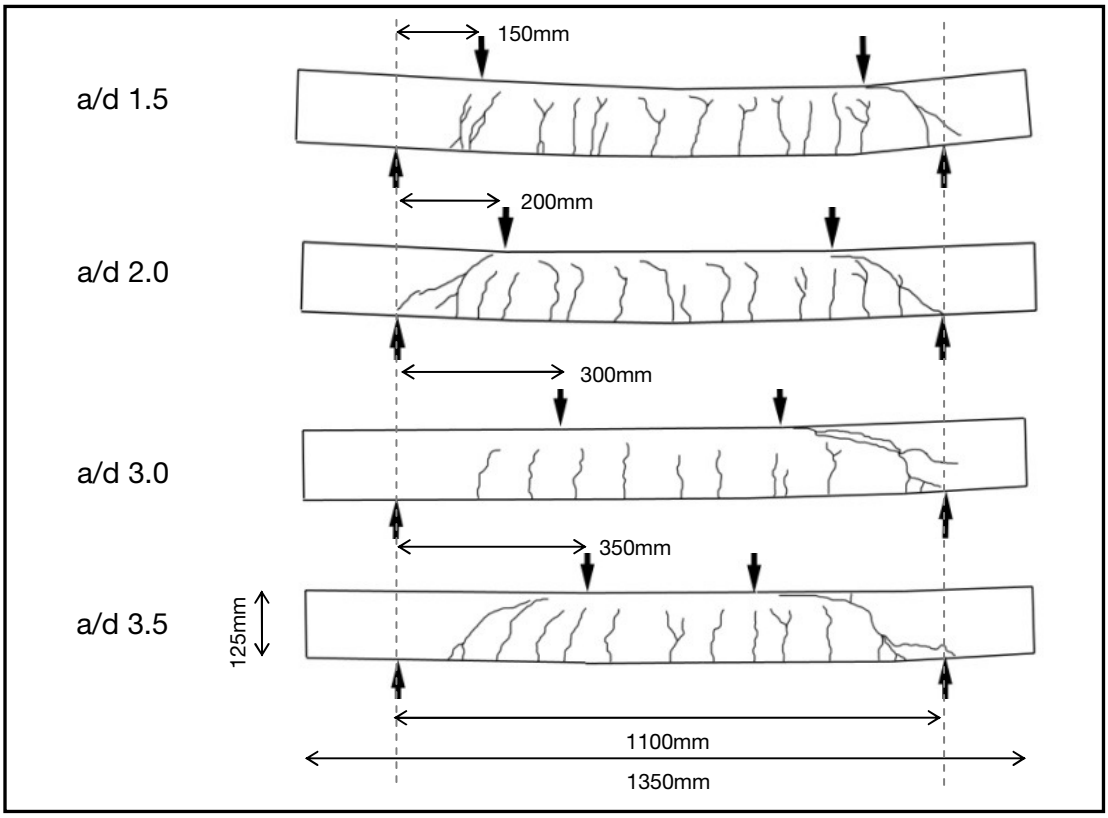

Figure 3-18 Crack pattern of SB C50-series

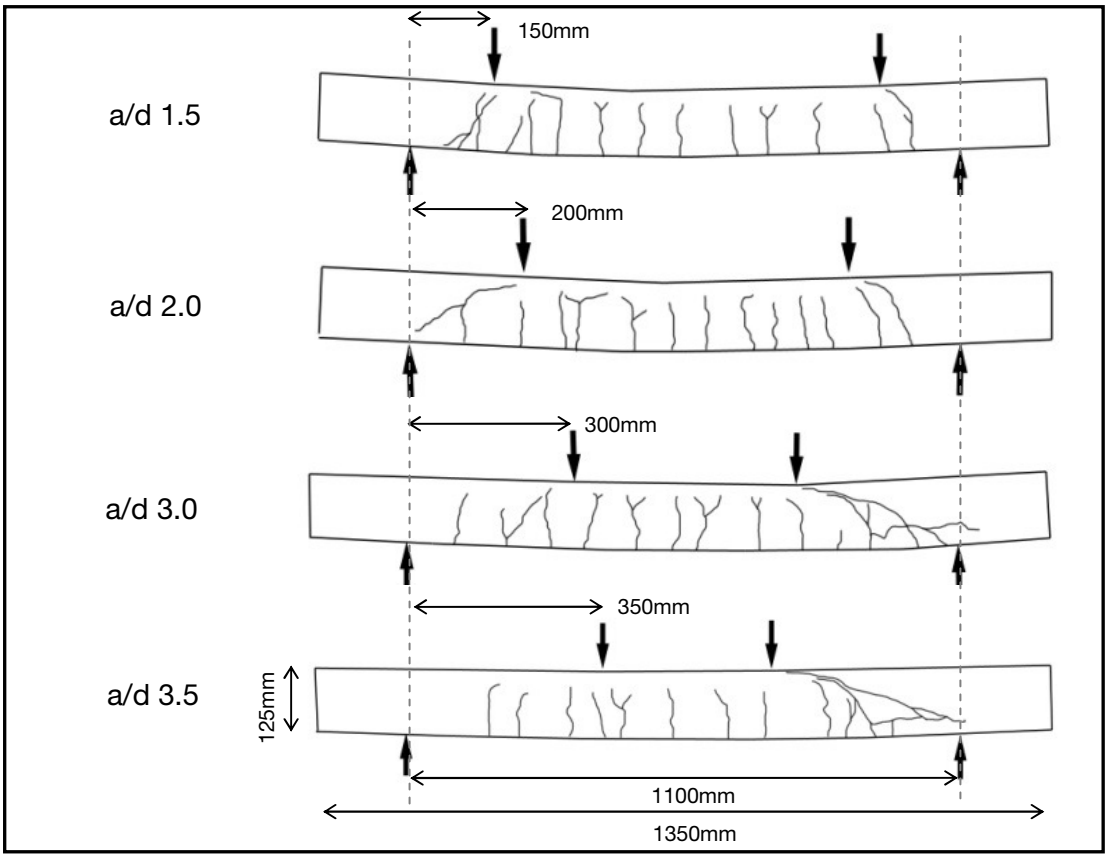

Figure 3-19 Crack pattern of SB C70-series

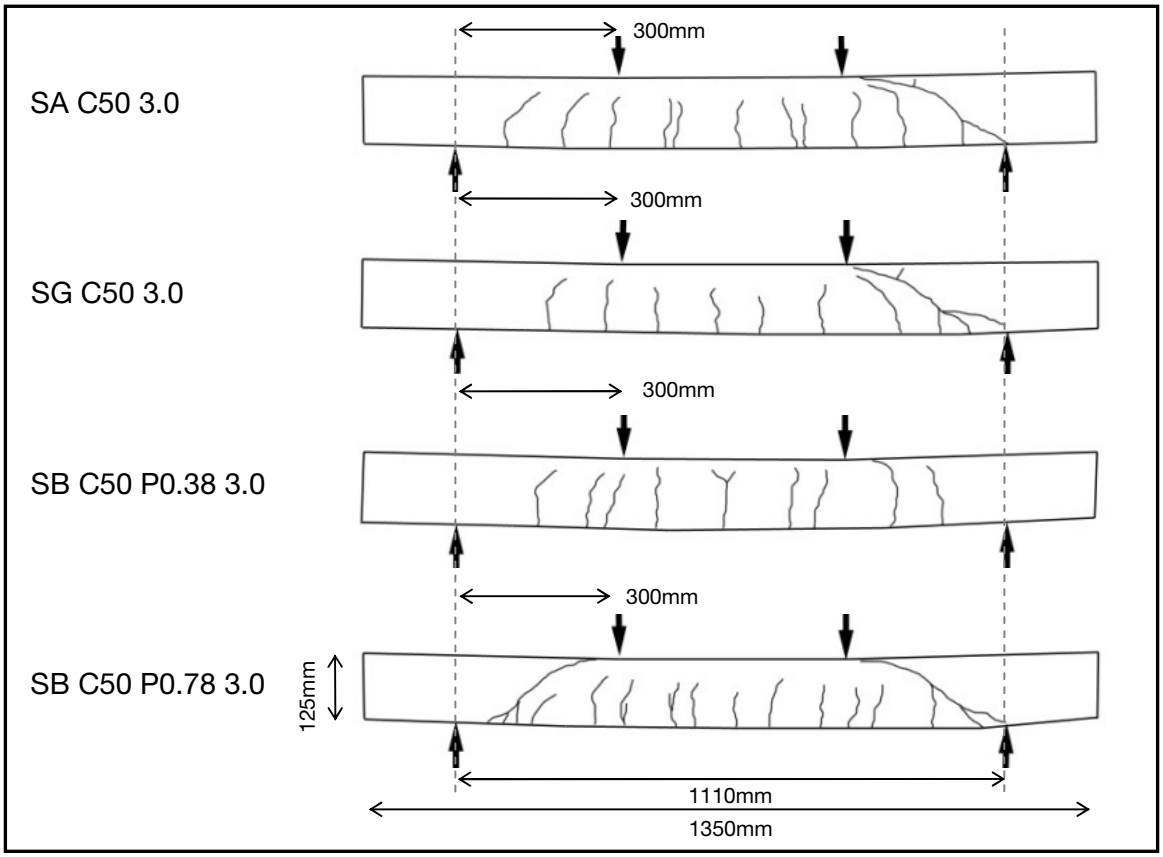

Figure 3-20 Crack pattern for S-series

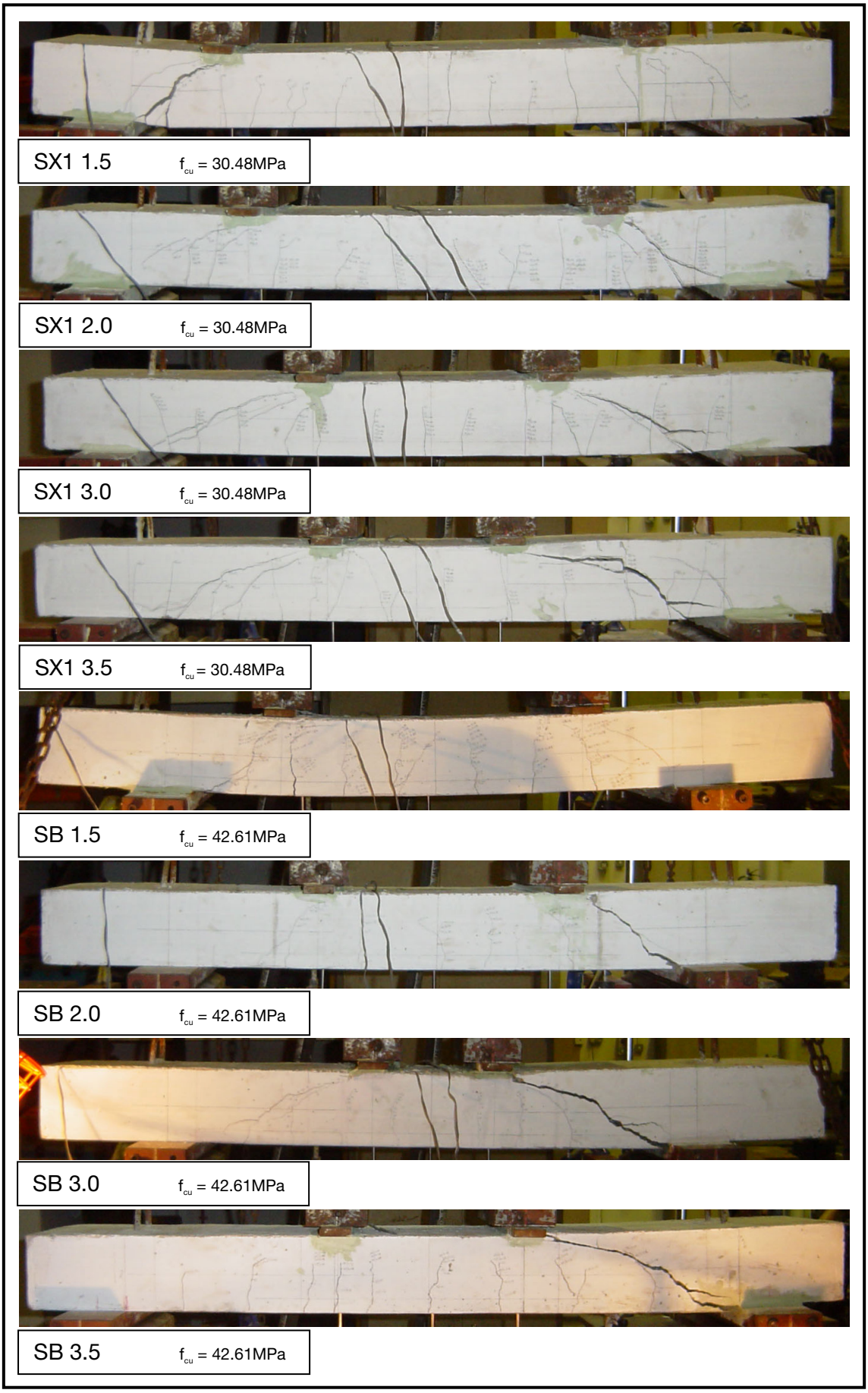

Figure 3-21 Crack patterns after physical failure of SB and SX1 series beams

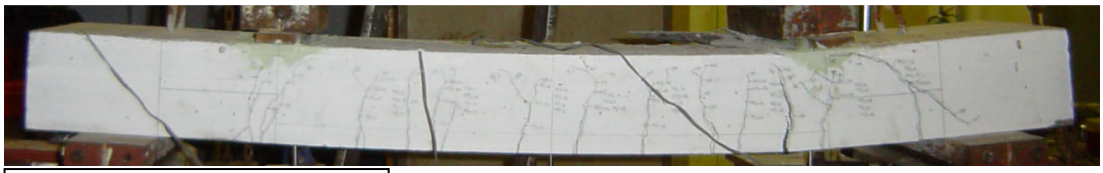

SB C50 1.5 f_{cu} = 47.04MPa

SB C50 2.0 f_{cu} = 47.04

SB C50 3.0 f_{cu} = 47.04MPa

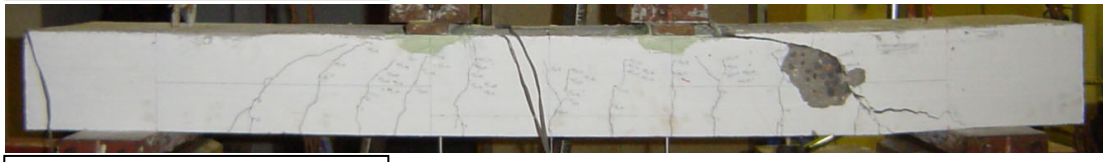

SB C50 3.5 f_{cu} = 47.04MPa

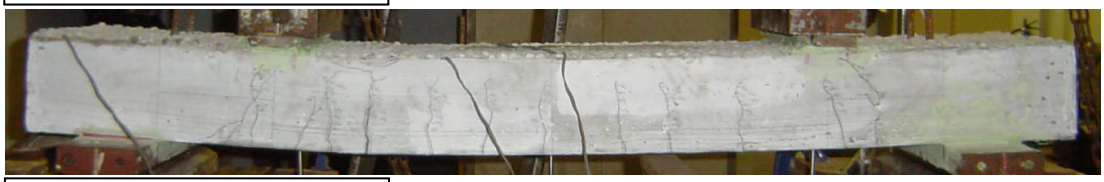

SB C70 1.5 f_{cu} = 69.75MPa

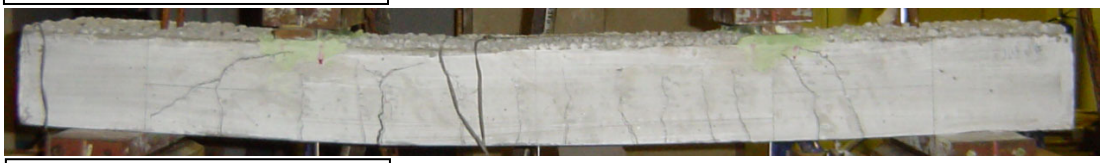

SB C70 2.0 f_{cu} = 69.75MPa

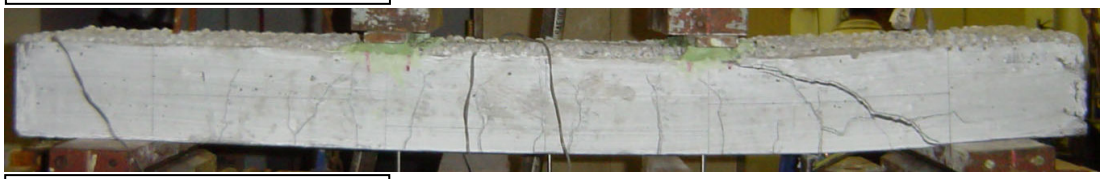

SB C70 3.0 f_{cu} = 69.75MPa

SB C70 3.5 f_{cu} = 69.75MPa

Figure 3-22 Crack pattern after physical failure of SB C50 and SB C70 series beams

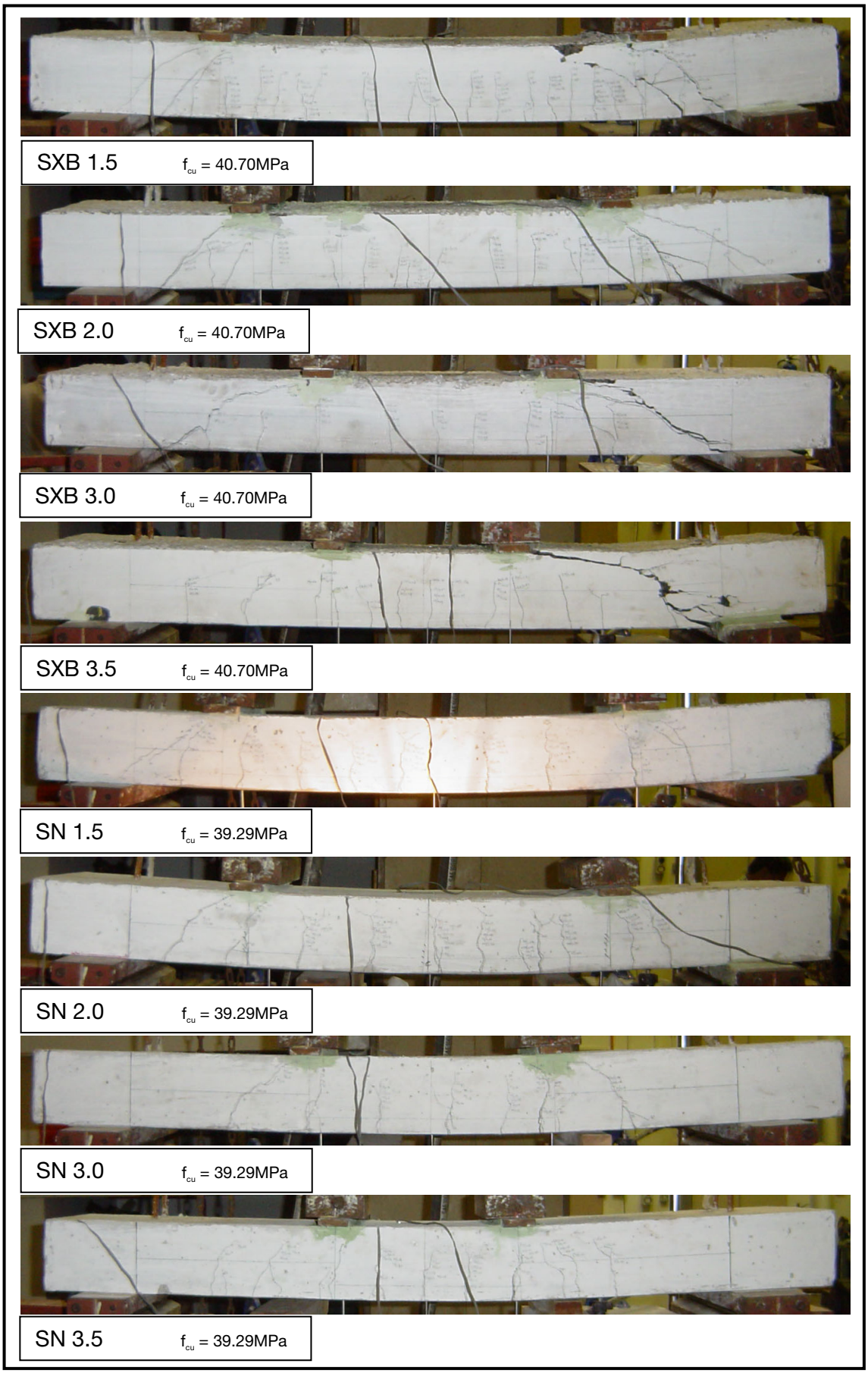

Figure 3-23 Cracking patterns after physical failure of SXB and SN series beams

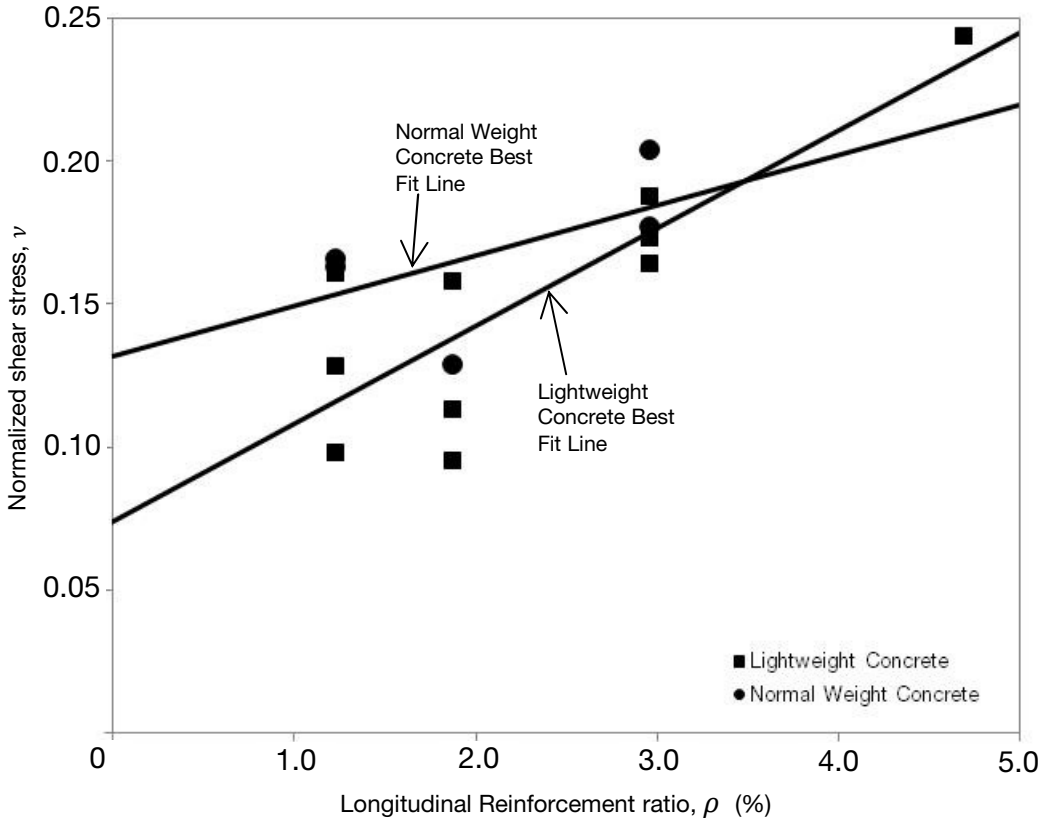

Figure 3-24 Normalized ($\sqrt{f'_c}$) shear stress at diagonal cracking to longitudinal reinforcement ratio for R-series beams without transverse reinforcement

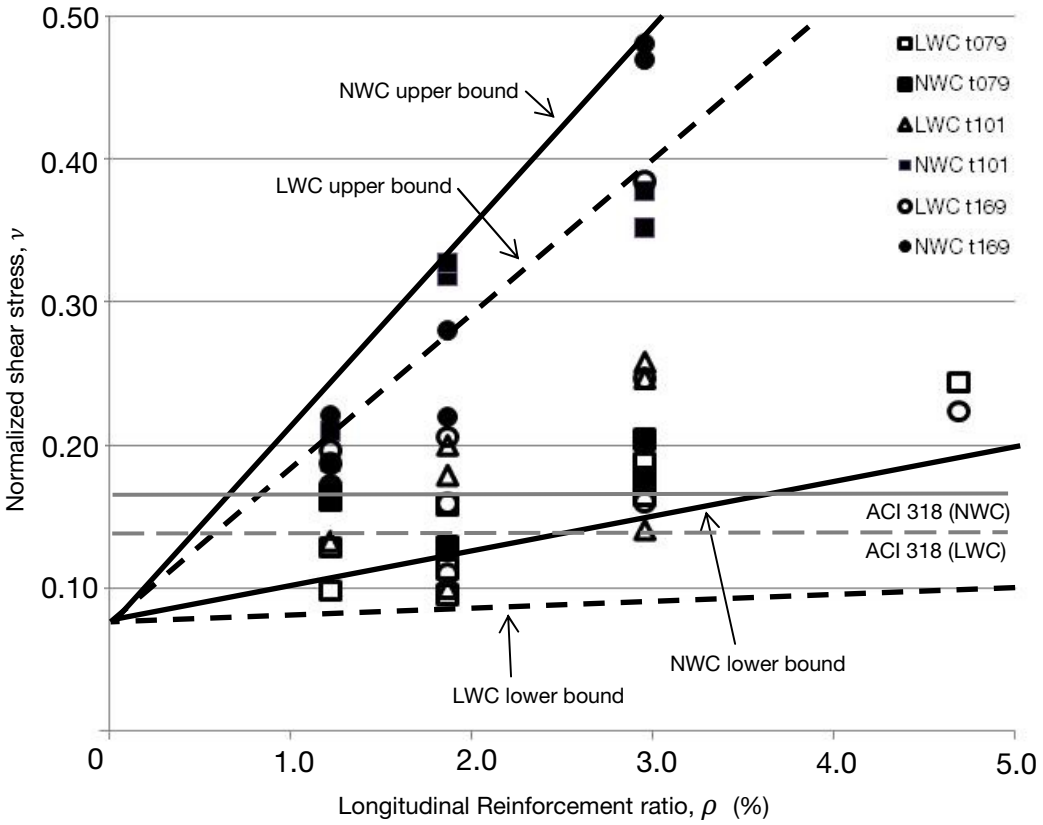

Figure 3-25 Normalized ($\sqrt{f'_c}$) shear stress at diagonal cracking to reinforcement ratio for varying transverse reinforcement

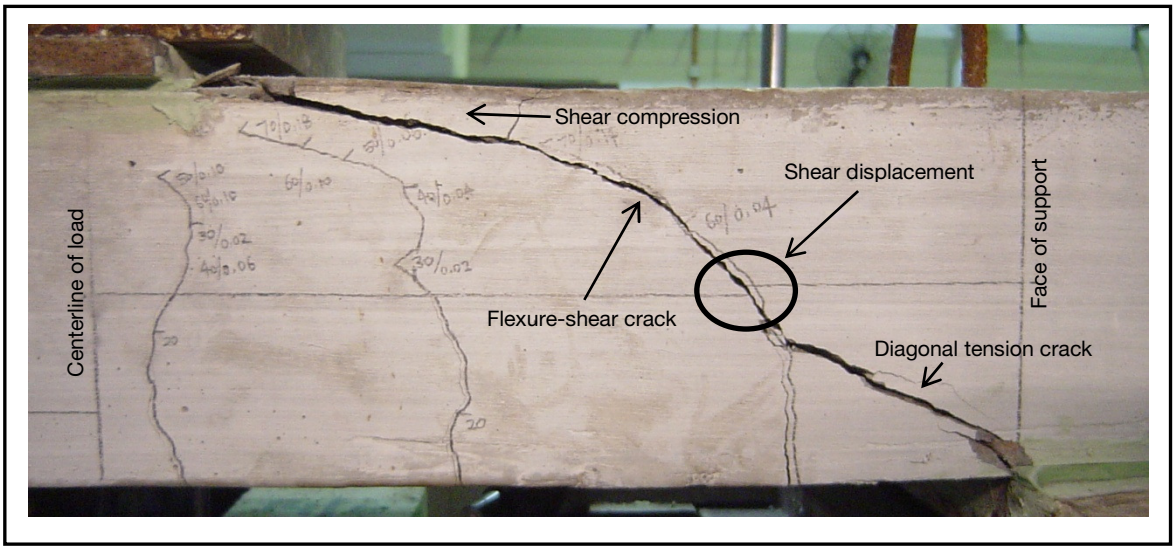

Figure 3-26 Typical crack pattern of lightweight concrete beam

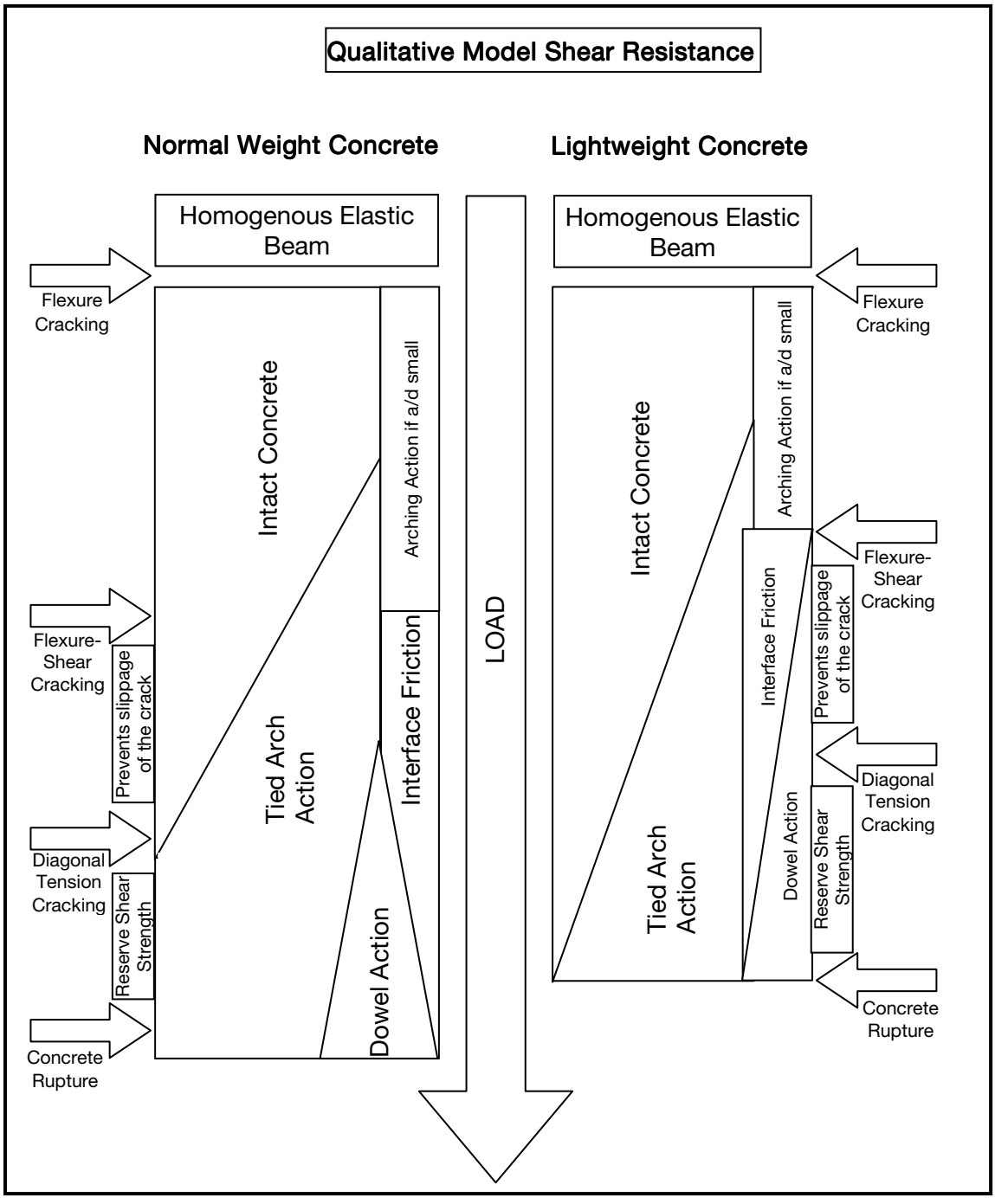

Figure 3-27 Qualitative model of shear resistance mechanisms

This page intentionally left blank for pagination.

Chapter 4 Shear Strength of Lightweight Concrete Beams without Transverse Reinforcement

In the preceding chapter, the cracking modes developed through the loading history of lightweight concrete beams without transverse reinforcement was keenly observed. The appearance of the various modes of cracking revealed the mechanisms involved in resisting shear. Here the strength of the lightweight concrete beams tested earlier are analyzed and the strength of the beams are predicted by a new prediction equation. Comparison with code predictions are also discussed increasing the confidence level as well as exposing weaknesses in the design approach.

4.1 Load-Deflection Response

Figure 4-1 shows the shear force to mid-span deflection of normal weight concrete beams. All four specimens in the S-series had a flexural mode of failure with wide vertical flexural cracks forming below the loading points. These wide cracks are characteristic of elongation of the reinforcement into the plastic region as confirmed by the attached strain gauges. The load-deflection curve also exhibits large plastic deformations as the steel yields and has considerable ductility. As the control test and comparison benchmark to lightweight concrete, the flexural failure mode of all the 4 specimens test indicate that BS 8110 code provisions for shear remain conservative when applied to normal weight concretes made with regular dense rock based aggregates.

Meanwhile, Figure 4-2 shows the shear force to mid-span deflection response of SB-series. In this test series, only the specimen tested with a shear span-to-depth ratio of 1.5 failed in flexure. The other 3 specimens loaded at larger shear span-to-depth ratios produced a shear failure mode with wide inclined cracks extending from

the loading point at the top of the section to the support point at the bottom of the section. Shear failure was sudden and without warning. The two specimens tested at shear span-to-depth ratios of 3.0 and 3.5 also exhibited dual peaks in the shear force to mid-span deflection response. As the load was increased, the section suddenly developed a major shear crack often extending from the face of support to the face of the loading point. This caused the load to suddenly decrease and the mid-span deflection to increase sharply. However, once the system re-stabilized, the section continued to resist load as it once again increased until ultimate failure occurred at a shearing force slightly higher than the first peak. This saw tooth shape is an artifact of the displacement control mode used by the hydraulic actuator in applying the load.

Prior to failure, both SN-series and SB-series exhibit similar responses. Both have a more or less linear response until the mid-span deflection approaches 5 mm. Although the compressive strength of the lightweight concrete is slightly higher than the normal weight concrete, nevertheless, some of the test specimens continued to fail in shear while none of the normal weight concrete specimens did so.

Meanwhile, SX1-series specimens were unintentionally pre-cracked due to material shrinkage. Cracks were vertical and through the depth of the member. As such, no visible change in slope in the shear force to mid-span deflection curves (Figure 4-3), characteristic when first cracking occurs is observed. In this test series, all 4 specimens exhibited shear failures with diagonal shearing cracks leading to ultimate failure. Foamed concrete specimens at higher shear span-to-depth ratios also showed the saw tooth pattern of lightweight aggregate concrete. However the drops when the shear cracks formed were smaller but happened more frequently before final failure. That foamed concrete is weaker and more brittle as compared to lightweight aggregate concrete is expected considering that there are no aggregates in the foamed concrete to contribute to resisting shear via interface friction.

The next test series in the one-way slab experimental program involves lightweight aggregate-foamed concrete (Figure 4-4). In this concrete, some lightweight aggregates are added to the foamed concrete to provide greater strength and to try to improve the shear resistance via interface shear. The test results indicate that this material behaves somewhere in between that of lightweight aggregate concrete and foamed concrete. While foamed concrete had shear failure at shear span-to-depth ratio of 1.5, the lightweight aggregate foamed concrete showed a flexural failure similar to that of lightweight aggregate concrete. At the other end of the scale, at shear span-to-depth ratio 3.5, lightweight aggregate concrete had a sudden shear failure while lightweight aggregate foamed concrete showed some ductility similar to foam concrete before ultimately failing in shearing mode.

Figure 4-5 shows the shear force to mid-span deflection response of a SB C50-series. Unlike the previous grade of lightweight concrete, SB C50-series is categorized as a high-strength lightweight concrete. The shear capacity of the section is expected to increase as the concrete strength increases. However, it can be observed that the increase in shear capacity is only marginal at shear span-to-depth ratio 3.0 and 3.5 over the SB-series (Figure 4-2). However, at shear span-to-depth ratio of 2.0, the ultimate shear capacity is much higher than its SB-series counterpart.

As the lightweight concrete strength is increased to 70 MPa, the test specimens start to exhibit behavior similar to the grade 40 normal weight concrete, SN-series. All specimens in this series except SB C70 3.5 at shear span-to-depth ratio 3.5 failed in flexural mode, with the specimens achieving similar ultimate moment capacities and mid-span deflections to SN-series. As is characteristic of a shear failure, the failure of SB C70 3.5 was sudden and brittle. The failure mode of

SB C70 3.0 was atypical in that ultimate flexural mode was achieved with tension steel having yielded and elongated into the plastic range. While other specimens with ultimate flexural failures continue to elongate until the load drops, or the steel ruptures, SB C70 3.0 suddenly ruptured along a shear compression crack, which was the final collapse mechanism. The saw tooth behavior is also observed in this test series with both tests at shear span to depth ratio 3.0 and 3.5 exhibiting this.

4.2 Shear Strength

In beam elements without transverse reinforcement, i.e. slabs, the failure criteria adopted by the reinforced concrete design codes is the shearing force that causes the formation of a critical diagonal tension crack. This value is taken as the usable design ultimate load because insufficient knowledge is available on the redistributions of forces at cracking and the ability of a section to reach equilibrium after redistribution. In addition to that the long term behavior of a diagonally cracked beam is unknown.

Some experimental subjectivity arises from adoption of these criteria since the formation of a critical diagonal tension crack is dependent on the observer. As such, the little available data would be expected to have a larger scatter when compared to continuously logged data. In this test, a critical diagonal crack is judged to have occurred when an inclined crack forms below the mid depth line of the test specimen. Test results are summarized in Table 3-7 earlier.

Figure 4-6 shows the shear force at diagonal cracking of the test beams with four different types of concrete at 40 MPa while Figure 4-7 shows lightweight aggregate concrete at different compressive strengths. Lightweight aggregate-foamed concrete and foamed concrete fail at a lower shear force when compared to lightweight aggregate concrete and normal weight concrete. This result is expected

since the cellular nature of the microstructure is expected to be significantly weaker under tension. All the concrete types indicate a trend towards lower shear capacities as the shear span-to-depth ratio increases. The shear span-to-depth ratio is related to $^{V}/_{M}$ for cases other than point loads. When the moment is large compared to the shear forces, tensile forces affect the magnitude of principle tension thus reducing the shear capacity. Larger values of shear span-to-depth ratios also results in wider flexural cracks which disrupts shear transfer within the member.

At low shear span-to-depth ratios, some amount of shear enhancement from arching action is expected. However for all the lightweight concrete beams at 40 MPa, this enhancement is not observed compared to normal weight concrete which registered a two fold increase in load prior to the onset of diagonal cracking. This shear enhancement resurfaces once the compressive strength of concrete increases to 50 MPa as shown in the Figure 4-7. The amount of shear enhancement gained from arch action does not appear to be significant with SB C70-series only being marginally stronger. This trend continues until convergence at shear span-to-depth ratio of 3.5.

Although the onset of cracking is taken as the usable design ultimate load, members are still able to resist increasing loads. This is sustained by continuous redistributions of loads between the resistance mechanisms. The amount of additional load sustainable though is unpredictable. This test revealed that foamed concrete, while cracking at low levels was able to sustain 2.5 times the cracking load prior to shear-compression failures. Similarly, lightweight aggregate foamed concrete was able to resist comparable levels. On the other hand lightweight aggregate concrete SB C70-series could sustain no more than 1.5 times. At shear span-to-depth ratios of 3.5, this margin evaporates with all types of concrete failing soon after

the onset on diagonal cracking. Figure 4-8 shows the margin of for all specimens between onset of diagonal cracking to ultimate failure.

4.3 Prediction of Shear Capacity

An accepted rational physical model of shear resistance does not yet exist due to the complex nature of the shear failure mechanism in reinforced concrete beams without transverse reinforcement. Engineers have relied on empirical equations derived from statistical regression of experimental data. While this approach has served engineers well, care needs to be taken when applying these empirically derived predictions to cases not represented in the underlying data set used for regression. This is particularly true for lightweight concrete since the body of experimental data of reinforced lightweight concrete is an order of magnitude less than data for normal weight reinforced concrete.

A clear example is in the application of Mphonde and Frantz's (1984) regression equation. This equation was developed from a data set normal weight concrete ranging from 21 MPa to 103 MPa at shear span-to-depth ratios of 3.0 to 3.6 and was found to give a better statistical representation of concrete shear strengths compared to the ACI 318 code equation including Zsutty (1971). However when Mphonde and Frantz's (1984) equation was applied to lightweight coarse aggregate concrete with normal weight fine aggregate test beams at comparable shear span-to-depth ratio the predicted values were more than 50% higher than the values measured in this test.

Shear tests on lightweight concrete beams has thus far been focused on verifying the applicability and suitability of code equations and provisions for lightweight concrete. These equations and provisions in the codes were themselves simplistically derived by applying a reduction factor to the underlying normal weight

concrete equations after tests on lightweight concrete. With that in mind, a better predictor of shear capacity in lightweight concrete is desirable.

Based on a parametric model of Russo *et al.* (2005), coefficients of regression were developed for lightweight concrete based on the test results herein. The parametric equation was evolved from earlier work by Bazant and Kim (1984) and was derived to the form shown in equation 4-1 below. Derivation of the equation is detailed in Russo *et al.* (2005) and is not reproduced here. The benefit of starting with a parametric model is in that the variables affecting the shear resistance are analytically derived while the exponents defining the behavior are statistically fitted with available test data.

$$v_{uc} = k_0 k_1 \xi \left[\rho^{0.5-p-m} {f'_c}^{q} + k_2 \rho^{1-m-z} {f_{yl}}^{1-z} \left(\frac{a}{d}\right)^{-s-1} \right] \quad (4\text{-}1)$$

The size effect term, ξ, is given by Bazant and Kim (1984) as equation 4-2 below, where d_a is the maximum size of aggregate used. This value is capped at unity since size effect compromises large sections while not enhancing small sections.

$$\xi = \frac{1+\sqrt{5.08/d_a}}{\sqrt{1+d/(25d_a)}} \leq 1 \quad (4\text{-}2)$$

The s value meanwhile is given by the equation below:

$$s = s_0 + s_1 \frac{a}{d} \quad (4\text{-}3)$$

From the analytical derivation of the equation, the differential equation used is only valid if value of s_0 is more than 0.135 times larger than s_1. Constants that need to be fitted to experimental data are; k_1, k_2, p, q, z, s_0, and s_1.

$$s_0 > 0.135\, s_1 \quad (4\text{-}4)$$

The first stage in fitting the constants of this parametric model is to derive the interpolation function for the moment lever arm based on classical beam theory. Only the results for lightweight aggregate concretes from the S-series were used for this purpose so as not to mix the different behaviour types of normal weight concrete, lightweight aggregate concrete and foamed concrete. Results from foamed concrete and lightweight-foamed concrete was also not fitted to the parametric equation as there were insufficient data points generated in this test program.

All shear span-to-depth ratios were included to increase the number of cracking load data points. Although arch effect in short beams and beam effect in slender beams leads to significant differences in behaviour (Kani 1966), this difference mainly affects ultimate shear values while shear cracking loads remains relatively unaffected by shear span-to-depth ratios (Rebeiz 1999). Separating the two data sets and fitting the constants on each would also lead to a discontinuity in the application of the equations at a certain shear span-to-depth ratio which is undesirable. This discontinuity is taken care of by an interpolation function based on the originating differential equation. Values for j_0 were individually calculated based on the modular ratio and longitudinal reinforcement ratio using equation 4-5.

$$j_0 = 1 - \frac{\sqrt{(np)^2+2np}-np}{3} \tag{4-5}$$

This form of the equation is unnecessarily complicated and can be just as well represented by and in equation of the form shown in equation 4-6 below as suggested by Russo *et al.* (2005).

$$j_0 = \mathrm{k_0}\rho^{-\mathrm{m}} \tag{4-6}$$

Iteratively selecting values of k_0 and m until the coefficient of variation is minimized was carried out. This yielded the values of $k_0 = 0.985$ and $m = 0.005$. After

calculating size effect term, ξ, the constants k_1, k_2, p, q, z, s_0, and s_1 remains to be determined. This was accomplished by iterative methods, again with the aim of minimizing the coefficient of variation (standard deviation / mean) of experimental to calculated shear stress values. At the i^{th} iteration, the coefficient of variation was minimized with a value of 0.129 and the constants determined to be $k_1 = 1.4$, $k_2 = 0.42$, $p = 0.05$, $q = 0.4$, $z = 0.013$, $s_0 = 0.4$, and $s_1 = 0.83$. Substituting these constants into equation 4-1 and simplifying yeilds equation 4-7 below.

$$v_{uc} = 1.38\xi\left[\rho^{0.44}{f'_c}^{0.4} + 0.42\rho^{0.98}{f_{yl}}^{0.99}\left(\frac{a}{d}\right)^{-1.4-0.83a/d}\right] \quad (4\text{-}7)$$

This constants s_0, and s_1 satisfy the inequality in equation 4-4. Comparing the coefficients derived for lightweight concrete with Russo *et al.* (2005) coefficients for normal weight concrete based on a data set of 917 beams shows that the coefficients derived here have similar relative values as presented in Table 4-1 below. Equation 4-7 can be simplified to the form below without significant sacrifice of accuracy. With the simplifications, the coefficient of variation increases to 0.136. The predictions of this equation was compared with observed results of independently tested beams of the R-series and other test data from the literature, good correlation was obtained. The comparison is shown in Figure 4-9.

$$v_{uc} = 1.38\xi\left[\sqrt{\rho f'_c} + 0.42\rho f_{yl}\left(\frac{a}{d}\right)^{-1.4-0.83a/d}\right] \quad (4\text{-}8)$$

In this comparison, the cube compressive strengths from the R-series were converted to equivalent cylinder strengths for Equation 4-8 by multiplying cube strengths by a 0.93 factor. Shear span-to-depth ratios throughout the R-series was 3.0 while the size effect factor was as suggested by Bazant and Kim (1984). The yield strength of tensile reinforcing bars are also different for R-series at 460 N/mm^2 while the yield strength of hard drawn wires of the S-series are tested to be 590 N/mm^2.

While Russo *et al.* (2005) developed a parametric equation (equation 4-9) based on a governing differential equation of a beam under shear and bending, Reineck (1991) derived a rational mechanical model of shear resistance for beams without shear reinforcement. This mechanical model is based on Kani's tooth model (1964) that discretises the concrete between shear cracks into wedges that resemble teeth. Individual shear resistance mechanisms as detailed in ACI445 are applied individually and finally rearranged for combined shear resistance of the member. Derivation of the mechanical model is not reproduced here but its salient points are discussed.

$$V_c = \frac{0.4 b_w d f_{ct} + V_{du}}{\left[1 + 0.16 \frac{f_{ct}}{f_c} \lambda \left(\frac{a}{d} - 1\right)\right]} \tag{4-9}$$

where: $\lambda = \frac{f_c}{E_s \rho} \frac{d}{\Delta n_u}$

In the Reineck's model, a significant portion of shear stresses are taken to be resisted by dowel action and by interface shear of the beam. This is consistent with experimental results and observation where lightweight concrete with smoother crack faces develop diagonal cracking at lower loads.

The contribution of dowel action used in the equation is given as

$$V_{du} = \frac{6}{f_c^{1/3}} b_n d_b f_{ct} \tag{4-10}$$

However, Equation 4-10 above is a function of the reinforcement bar diameter. For design, a lower bound value of dowel resistance is proposed since the bar diameter is as yet undetermined. The lower bound value of dowel resistance is given by Equation 4-11 below.

$$\frac{V_{du}}{b_w d f_c} = 1.4 \frac{\rho^{8/9}}{f_c^{2/3} d^{1/3}} \tag{4-11}$$

Experimental values from this test series were input into the formula to compare with the measured values. Good agreement was found between the experimental results and the values predicted by the equation for values of shear span-to-effective depth larger than 2.0. Since the equation was derived from kinematic considerations and is a function of the critical crack width where shear friction breaks down, the predicted values are for ultimate shear, rather than diagonal cracking load as predicted by Russo *et al.* (2005). Test values from beams with shear span-to-depth ratio less than 3.0 were also omitted since the basis of the mechanical model is not valid for a discontinuous region near the supports since a complete "tooth" cannot develop. The shorter span may also lead the contribution of dowel action to shift from a concrete splitting dowel failure mode to a crushing of concrete and yielding of the bar dowel failure mode (Vintzeleou and Tassios 1986).

4.4 Comparison with Code Predictions

For practical purposes, the load at which diagonal cracking first occurs is taken to be the shear failure load regardless of the ultimate shearing load which may be higher than the cracking load (Taylor and Brewer 1963). As such, code equations used to predict the shear capacity of a member is indicated as the onset of diagonal cracking of the beam. Diagonal cracking values are predicted because the extent to which a member can continue resisting shear after the onset of diagonal cracking is uncertain and dependent on loading configurations and local material properties. This was discussed in the preceding section.

For reinforced concrete members without transverse reinforcement, shearing forces are resisted by five mechanisms, *i.e.* uncracked concrete and flexural compression zone, interface shear transfer, dowel action of the longitudinal reinforcement, arch action and residual tensile stresses transmitted directly across cracks. The relative contributions of each mechanism are thought to be affected by a

host of factors with isolation of individual proportions non-trivial. Taking into account the complex nature of shear resistance, ACI 318-05 combines these contributions together as v_c, the shear capacity of a concrete members without transverse reinforcement, which is also referred to as the 'concrete contribution'.

The code proposes two empirical equations to predict this concrete contribution in equations 11-3 and 11-5 of the code. Joint ACI-ASCE Committee 426 suggests the latter equation not be used for reasons laid out by MacGregor and Wight (2005). The former equation (shown in Metric and U.S. Customary units as equation 4-12 and 4-13 respectively) meanwhile gives a reasonable lower bound value for shear resistance.

$$v_c = \frac{\sqrt{f'_c}}{6} b_w d \qquad \text{(MPa)} \qquad (4\text{-}12)$$

$$v_c = 2\sqrt{f'_c} b_w d \qquad \text{(psi)} \qquad (4\text{-}13)$$

When applied to sand-lightweight concrete, ACI 318-05 prescribes a 0.85 reduction factor on shearing capacities computed from Equation 4-12. Alternatively, if the tensile splitting strength of the concrete is specified, the 0.85 reduction can be omitted by replacing values of $\sqrt{f'_c}$ in Equation 4.2 with $f_{ct}/6.7$. This empirical equation only considers the tensile strength of concrete which is assumed to be related to the compressive strength by a square root relationship or by $f_{ct}/6.7$.

From tests carried out on the one-way slab specimens, equation 11-3 of the ACI Building code (Equation 4-12) was able to satisfactorily predict the shear capacities of all the lightweight concrete specimens at all compressive strengths up to shear span to-depth ratios of 3.5 (see Figure 4-10). The alternative method of substituting with $f_{ct}/6.7$ also produced similar prediction to the 0.85 reduction factor for lightweight aggregate concrete except in the SB C50-series series where

experimental values of beams test at shear span to-depth ratios above 3.0 fell below the predictions.

While the 0.85 reduction factor is satisfactory for lightweight aggregate concrete, this reduction factor cannot be applied for foamed concrete. Using the alternative method yielded much better results with predictions close to experimental values indicating that although foamed concrete is able to achieve similar compressive strengths, the tensile strength and shearing capacity is much lower than normal weight concrete and lightweight aggregate concrete. This is not entirely unexpected since the assumption that $\sqrt{f'_c}$ is proportional to the tensile strength of concrete is only a first approximation. Using values of $f_{ct}/6.7$ however, indirect tensile capacity of the material can be obtained which is expected to give closer results when compared to a correlation.

Nevertheless, tensile splitting strengths of lightweight concrete has some draw backs. Most importantly, this material property is not normally specified which may lead to problems of quality concrete. ACI 213R-03 also mentioned that cylinder splitting tests are not suitable on field concrete. As such, the material supplier should provide these design values to the designer and verify that it is reproducible for a given mix. Drying of the test cylinders also affects the tensile splitting strengths with a wide scatter of results observed as compared to continuously moist cured specimens.

The British Standard BS8110 meanwhile gives the shear strength of reinforced lightweight concrete members as 0.8 times the normal weight concrete strength (equation 4-14). The maximum shear stress permitted is also limited to $0.64\sqrt{f_{cu}}$ or 4 N/mm^2 whichever is smaller.

$$v_{c,lwc} = 0.8 \times 0.79 \left(\frac{100A_s}{b_v d}\right)^{1/3} \left(\frac{400}{d}\right)^{1/4} \left(\frac{f_{cu}}{25}\right)^{1/3} \frac{1}{\gamma_m} \quad (4\text{-}14)$$

This limiting value – with and without the lightweight concrete modifications – is superimposed on the shear force mid-span deflection curves for lightweight concretes tested in the S-series (Figure 4-1 to Figure 4-5 and Figure 4-11 to Figure 4-12). The code specified material safety factor, γ_m which is 1.25 for shear was instead set at unity for the comparison. This material safety factor accounts for uncertainty in the material behaviour and is added on top of the design equation which by definition should be a lower bound predictor.

The maximum deflection limit prescribed by BS8110 is also superimposed on figures above. This serviceability limit is governed by restricting the allowable deflection to span length over 250 *i.e.* $^{L}/_{250}$, or 4 mm in the case of the S-series. Without the need for more rigorous deflection calculations, the code provides a series of basic span-depth ratios within which the upper bound deflections do not exceed this serviceability limit. In cases where the loading to the horizontal member is larger than 4 kN/m^2, the basic span-depth ratio is reduced by 15% for lightweight concrete. This reduction accounts for the lower Young's modulus of lightweight concrete that leads to increased deflections as well as the mitigating effect of lower self weights.

Figure 4-1 to Figure 4-5 and Figure 4-11 to Figure 4-12, for lightweight concretes shows that the onset of diagonal cracking for the test specimens are compatible with the design equation of BS8110. The design equation without any modifications gives a lower bound value for onset of diagonal cracking in lightweight concretes with predictions as good as that for normal weight concrete (Figure 4-13). Similarly, no diagonal cracking occurs before the beam deflection has exceeded the serviceability limits.

If this result is viewed in isolation, the case for the removal of the lightweight modification factor is justified since the equation without any modifications gives lower bound values with the safety margins comparable to that of the reference normal weight concrete tests. However, the post-peak behavior gives a different view of lightweight concrete. The reference normal weight concrete was able to continue resisting the increasing load and develop a flexural mode of failure, whereas the lightweight concrete specimens failed with brittle shear mode. Based on this observation, it is prudent to maintain the code modification factor for lightweight concrete since the implicit safety between the onset of diagonal cracking in normal weight concrete to ultimate load is larger than that of lightweight concrete.

Meanwhile for foamed concrete and lightweight aggregate foamed concrete, shear cracking in the beams occurred at loads lower than indicated in the design equations as well as at deformations within the serviceability limits. The performance of lightweight aggregate-foamed concrete is better than foamed concrete with cracking developing at the code limits unlike foamed concrete that failed prematurely. This means that the British design code cannot be safely extrapolated to foamed concrete and lightweight aggregate foamed concrete as yet.

When put in the context of ACI 318-05 predictions, this result implies that the code equation gives a very conservative prediction for normal weight concrete and a accurate prediction of lightweight concrete. A reduction factor for lightweight concrete would then be appropriate to ensure similar margins of safety.

4.5 Implicit safety factor

From the results of this experimental study, it was found that design equations for normal weight concrete and lightweight concrete were adequate for predicting the diagonal cracking load, the failure criteria adopted for these members. However the

reserve strength of normal weight concrete remain very high such that flexural capacity was exhausted prior to shear rupture as seen in the S-series of tests. Lightweight concretes instead had shear rupture of the beam occurring prior to exhaustion of its flexural capacity.

For members without transverse reinforcement, there may thus be a loss in the implicit safety factor of the member. The British Code, BS8110 applies a shear safety factor of 1.25 which is higher than the flexural safety factor due to the relative uncertainty of shear behavior. However, this safety factor was judged against the large body of experimental evidence derived from normal weight concrete tests. The provisions for lightweight concrete were developed and verified by a limited number of lightweight concrete beam tests which show that a 0.8 reduction factor on the code equations is satisfactory in predicting the cracking of lightweight concrete.

While lightweight concrete beams perform well at service loads as observed from this test, designers should be aware that when designing lightweight concrete members near to its strength limits, the material may not be able to evolve sufficient shear resistance beyond service loads. This may lead to physical shear failures precipitating prior to ductile flexural failures.

4.6 Conclusion

Diagonal cracking of concrete is random and its location cannot be accurately predicted. The mechanism resisting shear is a highly complex and indeterminate leading to the usefulness of empirical equations in guiding safe design of concrete structures being of vital importance.

No noticeable difference in cracking patterns was observed between the different types of lightweight concretes tested which cannot be attributed to the compressive strength of the concrete. This is not entirely unexpected since the

cracks propagate through the aggregates inferring that the aggregate shape should have no impact on the properties and behavior of hardened concrete.

Using the diagonal cracking and ultimate shear capacity data generated from this test program, a prediction equation was derived for shear strength of lightweight concrete beams based on the parametric behavior model of Russo *et al.* (2005). This equation was then tested against the results of a set of rectangular lightweight concrete beams and found to be in good agreement across the range of parameters tested.

Comparison of the performance of these lightweight high-strength concrete beams against design equations of the American Concrete Institute and the British Standards Institute show that the equations can be used with confidence. Diagonal cracking of lightweight concrete beams only occur beyond the design loads and deflection limits imposed. However, caution should be exercised when considering the behavior of lightweight concrete beams beyond service loads as the physical shear capacity of the material may be exhausted prior to its flexural capacity.

Table 4-1 Coefficients from Equation 4-7, Equation 4-8, and Russo *et al.* (2005)

Coefficients	k_0k_1	0.5-p-m	q	k_2	1-m-z	1-z	-s-1	COV
NWC	1.13	0.40	0.39	0.50	0.83	0.89	-1.2-0.45a/d	N/A
LWC	1.38	0.44	0.40	0.42	0.98	0.99	-1.4-0.83a/d	0.129
LWC *(simplified)*	1.38	0.50	0.50	0.42	1.00	1.00	-1.4-0.83a/d	0.136

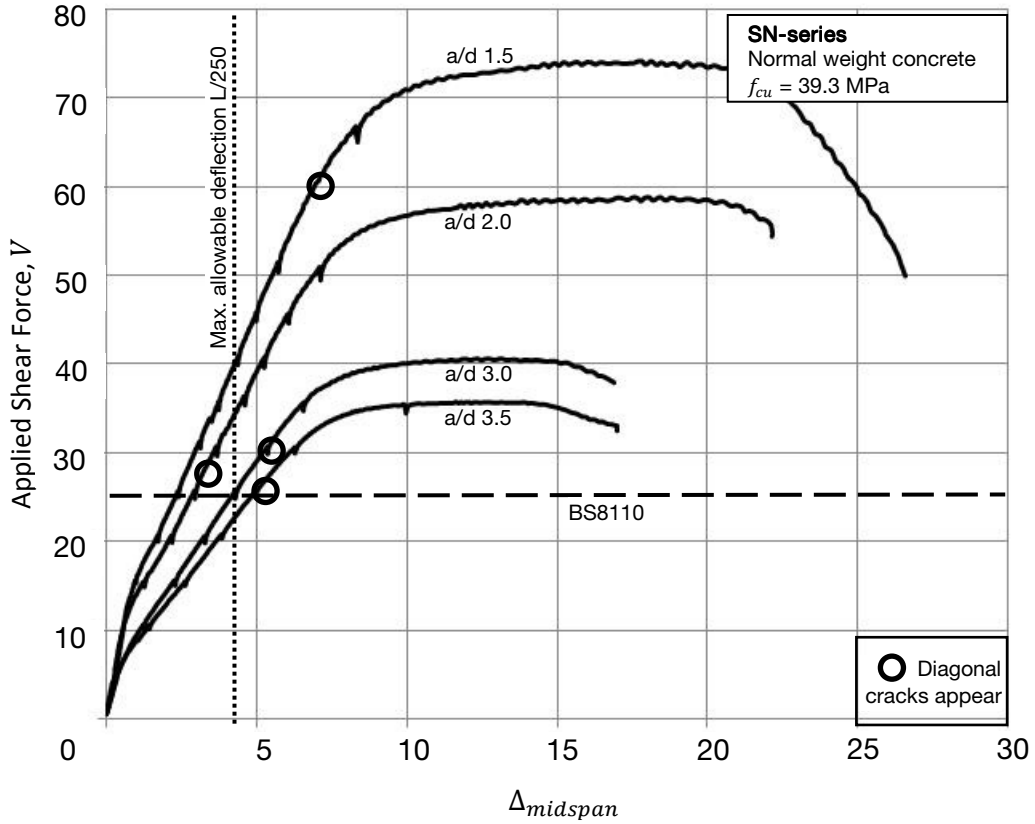

Figure 4-1 Shear force – midspan deflection curve for SN-series

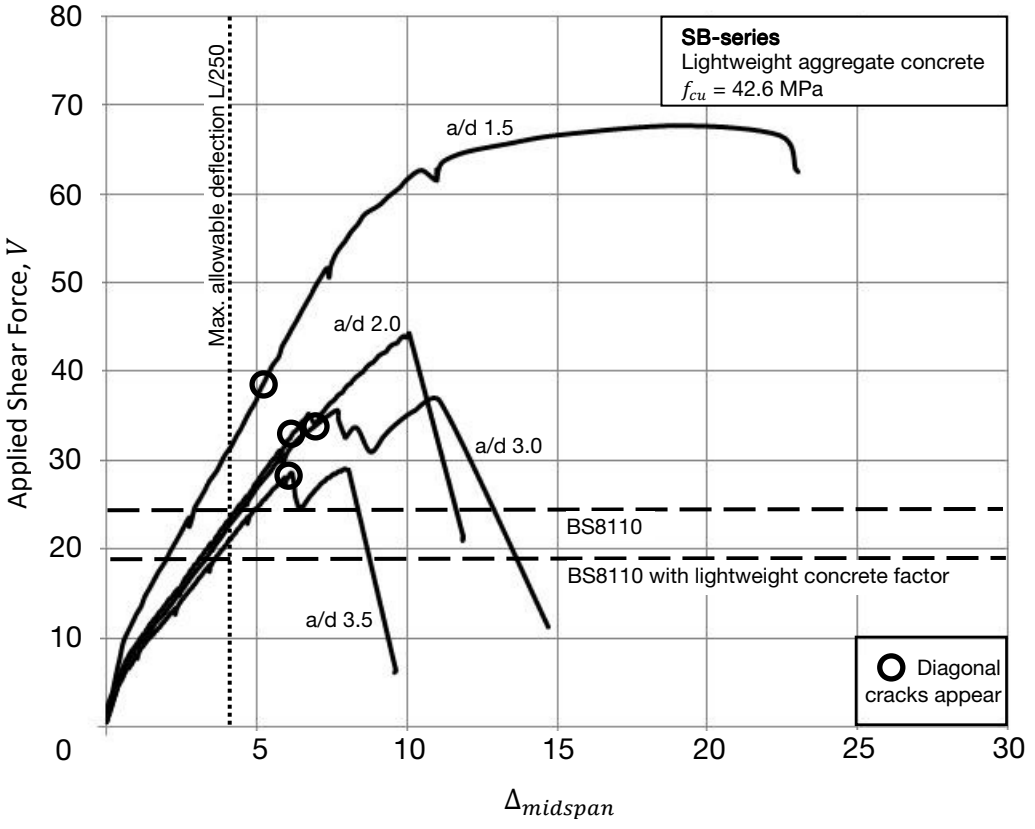

Figure 4-2 Shear force – midspan deflection curve for SB-series

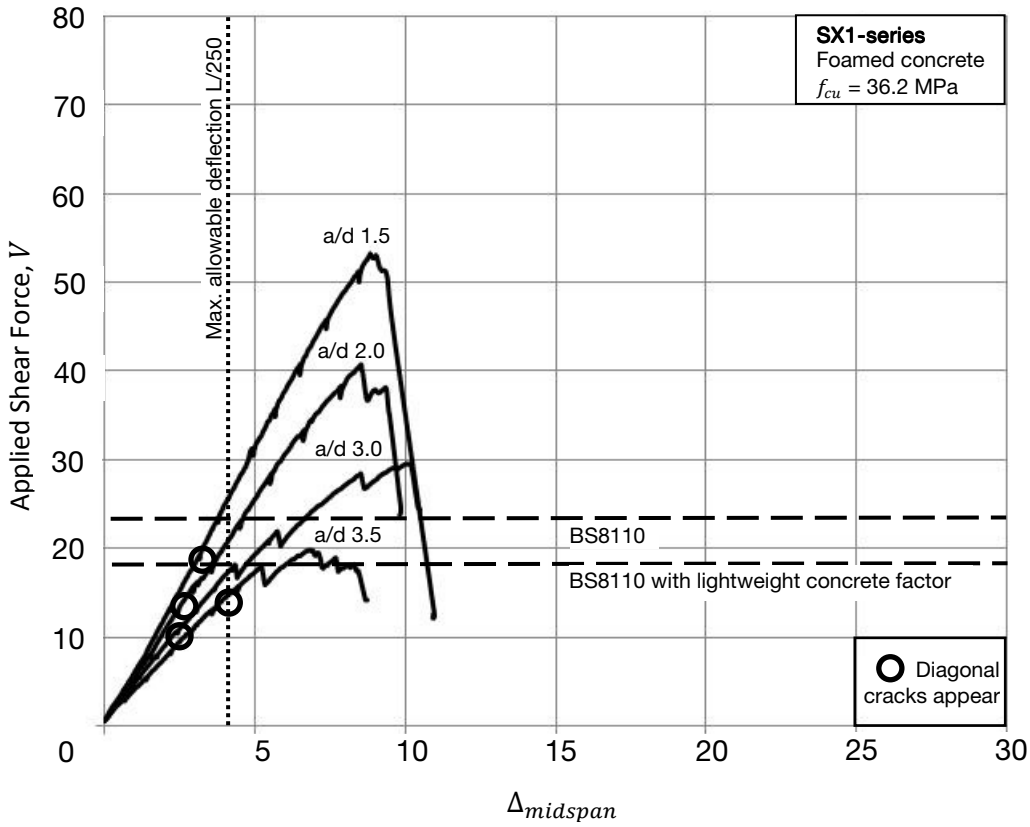

Figure 4-3 Shear force – midspan deflection curve for SX1-series

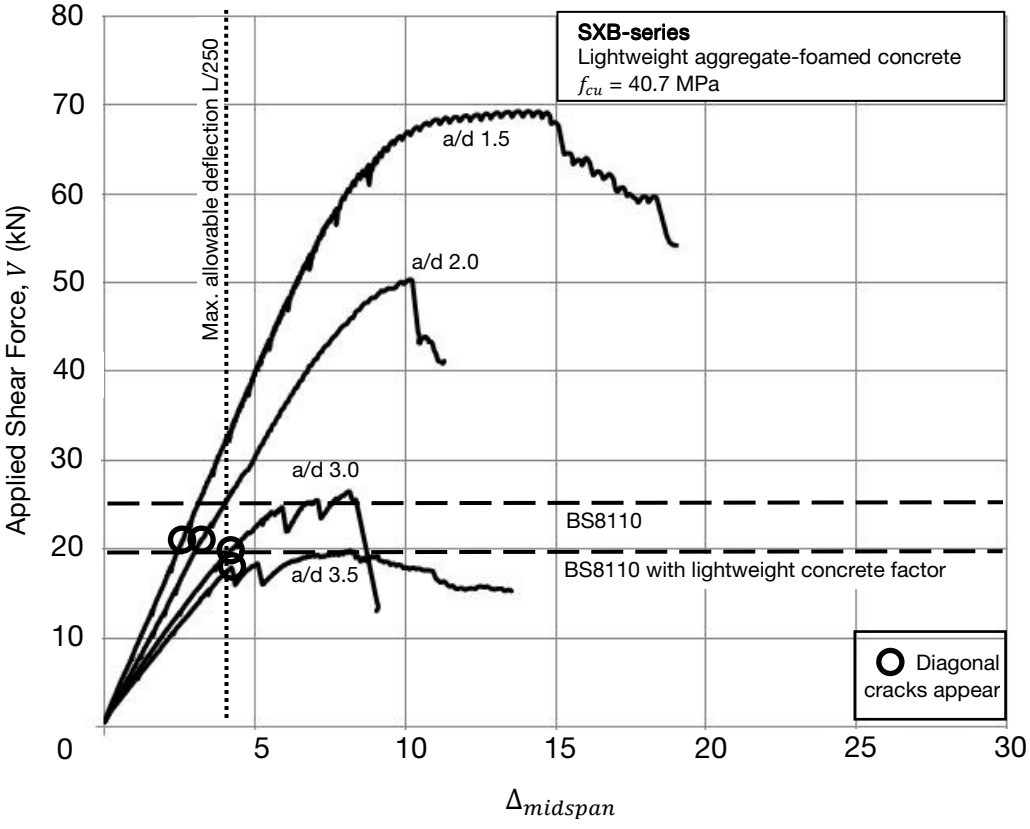

Figure 4-4 Shear force – midspan deflection curve for SXB-series

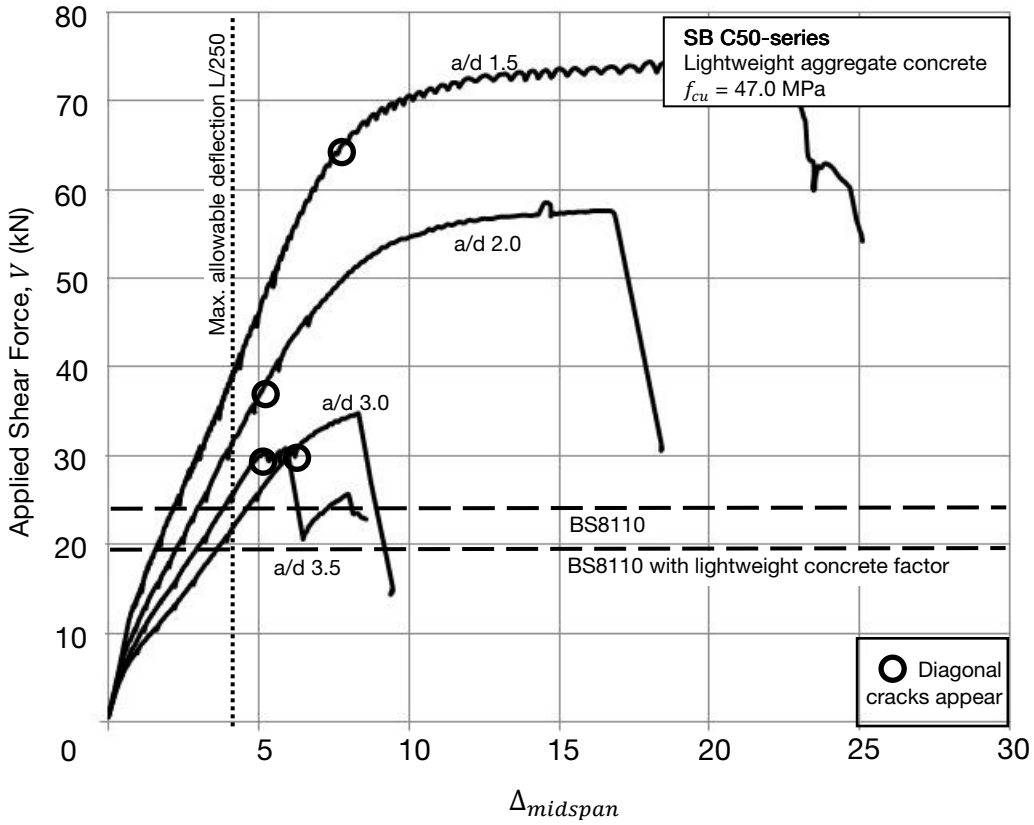

Figure 4-5 Shear force – midspan deflection curve for SB C50-series

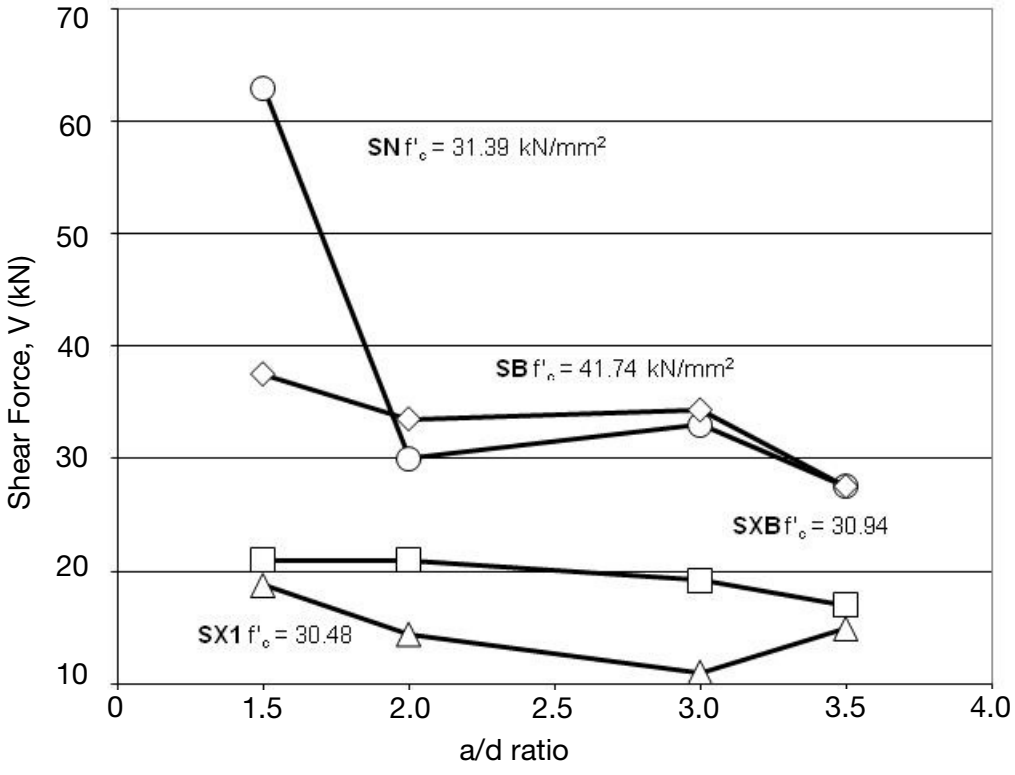

Figure 4-6 Shear force at diagonal cracking

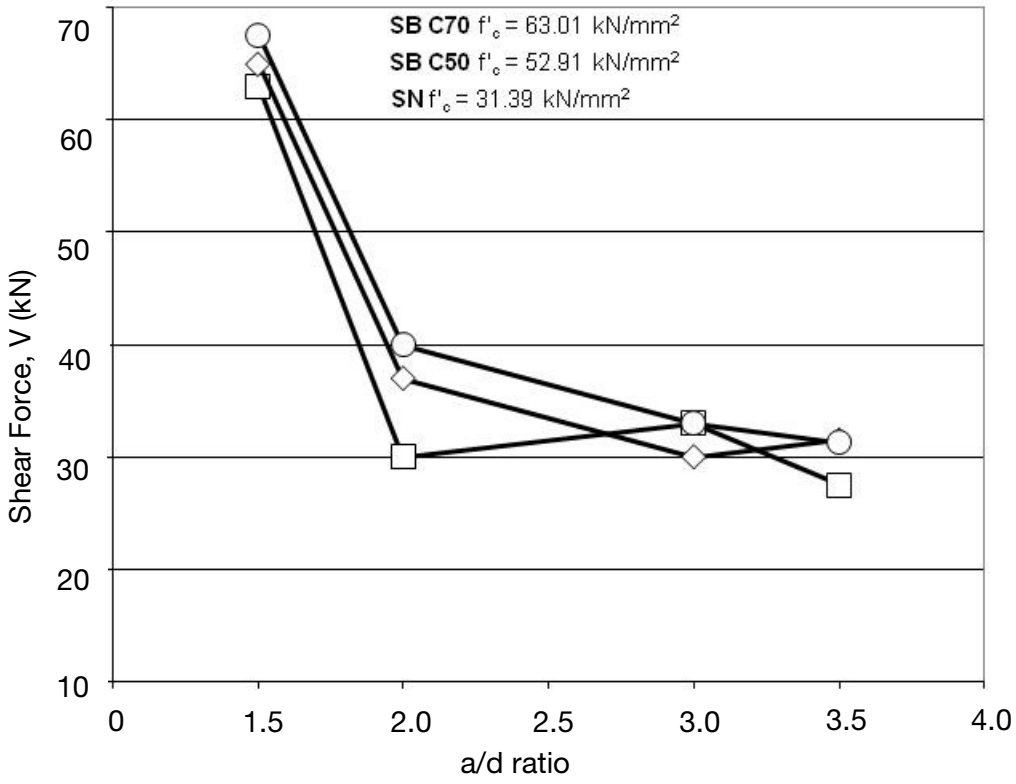

Figure 4-7 Shear force at diagonal cracking

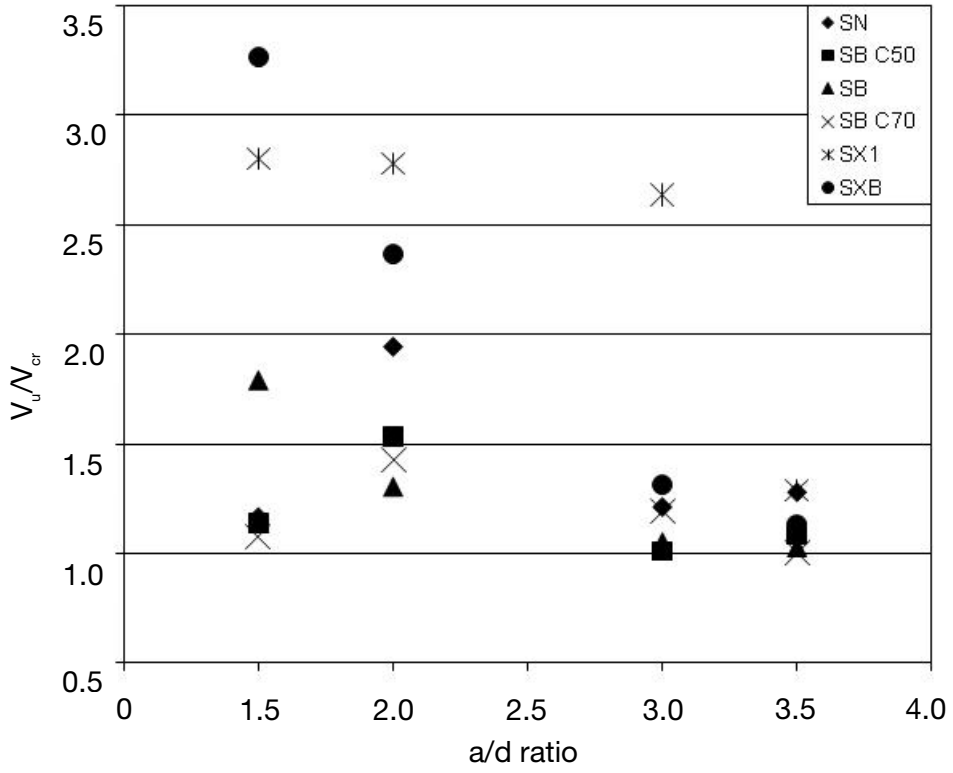

Figure 4-8 Shear at ultimate-shear at diagonal cracking ratio S-series

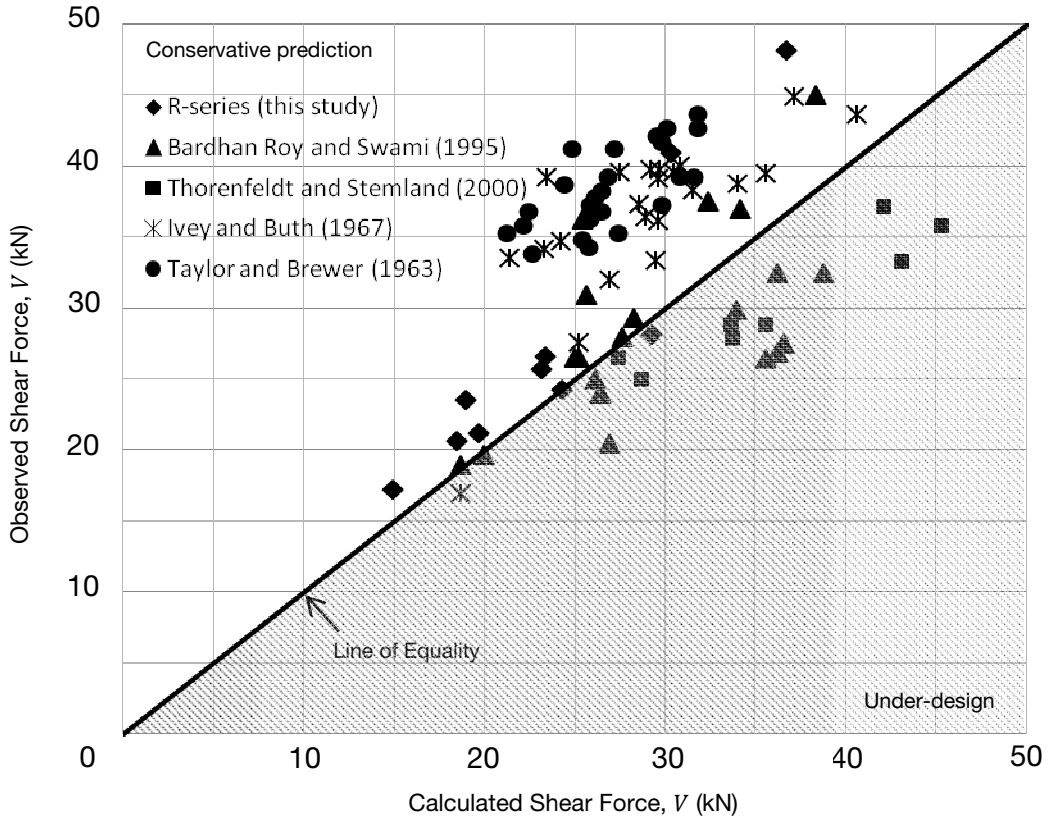

Figure 4-9 Comparison of observed and calculated shear force at ultimate physical failure for R-series beams without transverse reinforcement and data from the literature using equation 4-8

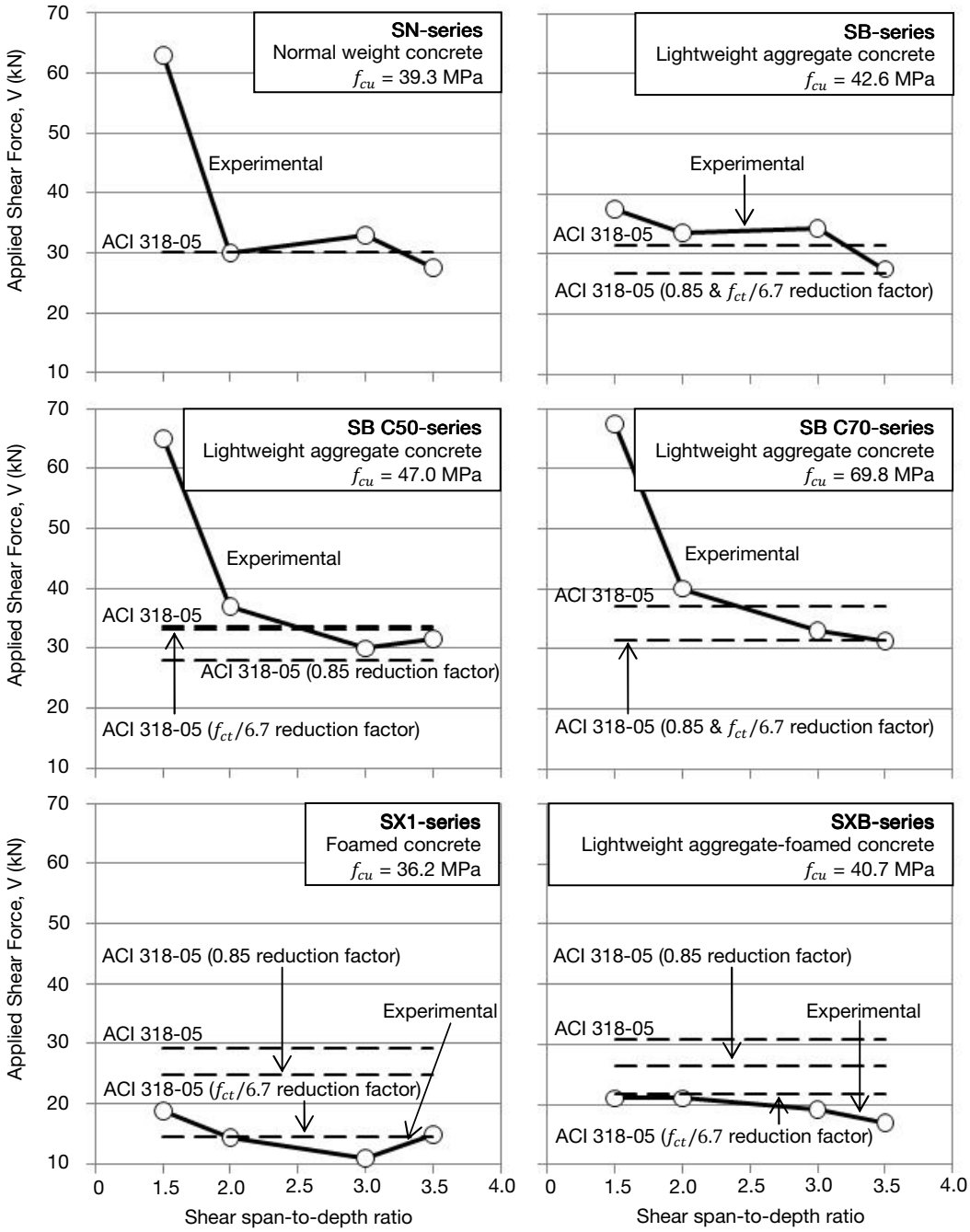

Figure 4-10 Comparison lightweight concrete with ACI 318-05 code prediction

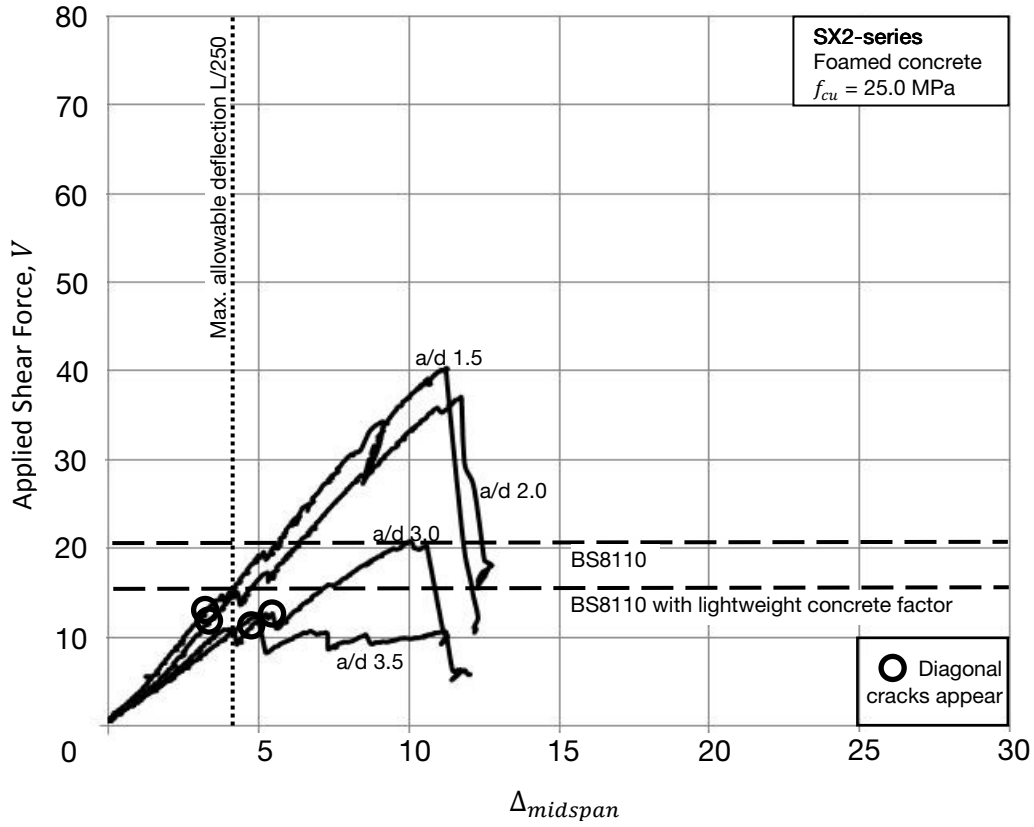

Figure 4-11 Shear force – midspan deflection curve for SX2-series

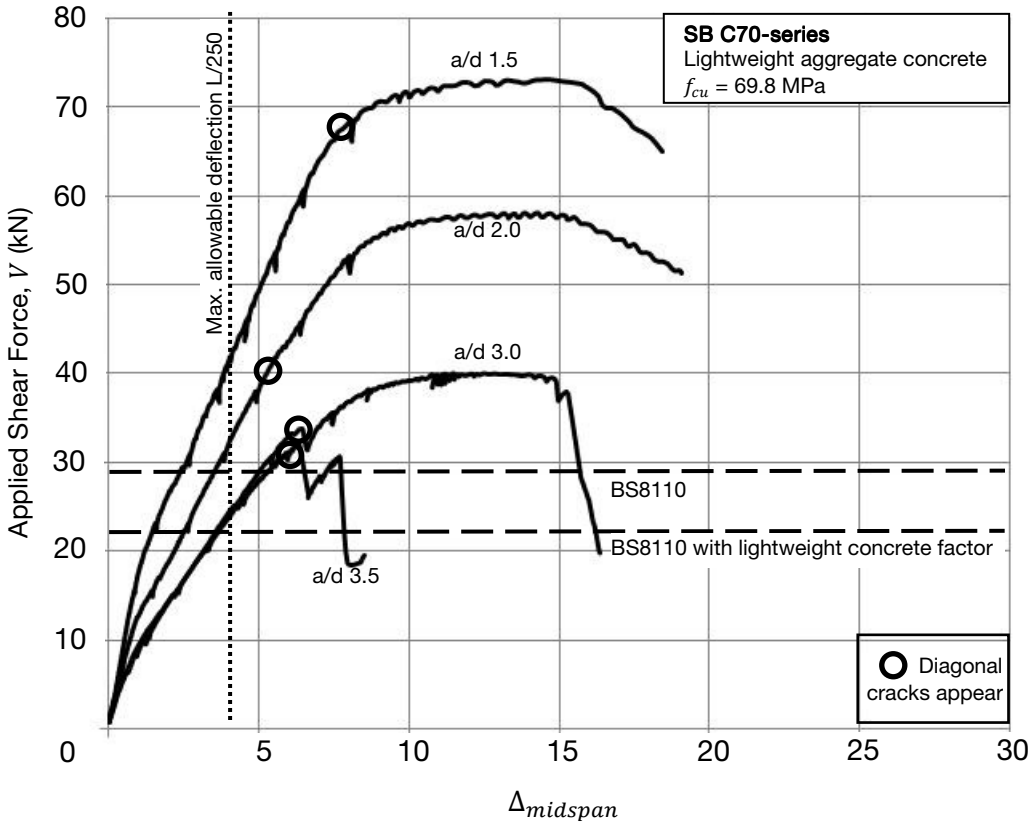

Figure 4-12 Shear force – midspan deflection curve for SB C70-series

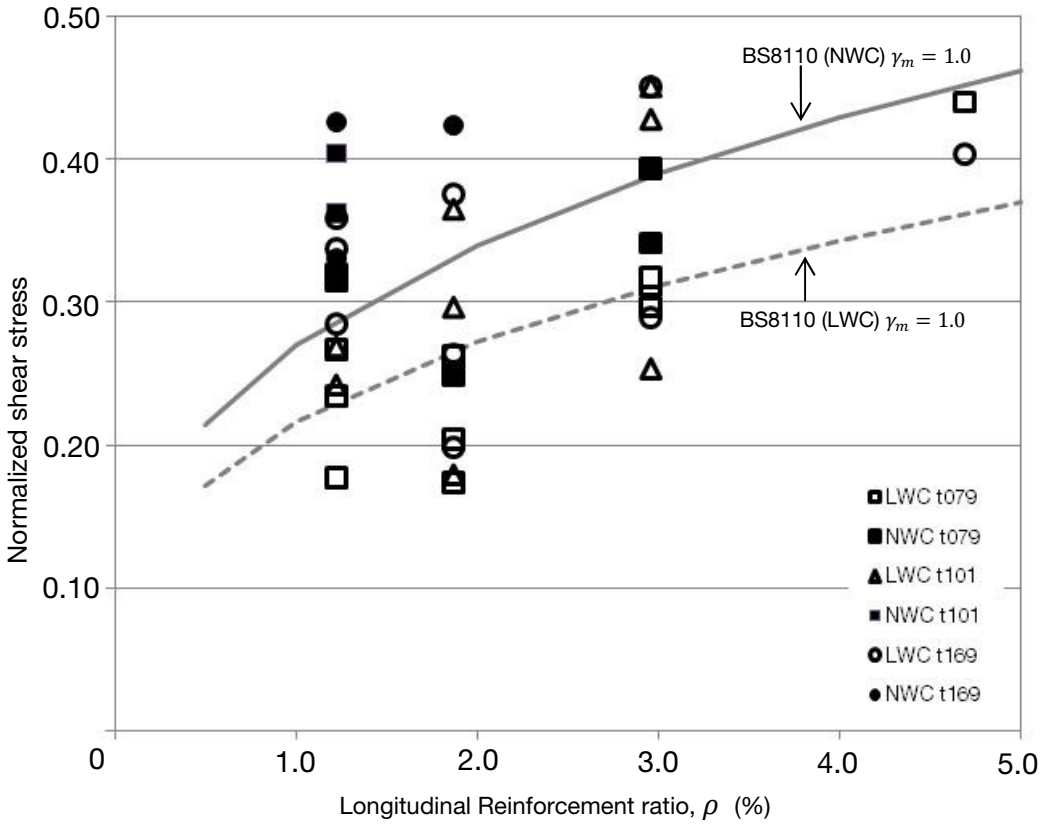

Figure 4-13 Normalised ($\sqrt[3]{f_{cu}}$) shear stress at cracking to reinforcement ratio for varying transverse reinforcement

Chapter 5 Rectangular Lightweight Concrete Beams with Transverse Reinforcement

The R-series of test beams included a second phase of lightweight concrete beams reinforced with transverse steel that allows a completely different mechanism of shear resistance to develop. The presence of transverse steel arrests the development of shear cracks and allows tensile stresses to be carried across the crack interface. As such, truss action is able to develop where the arrangement of longitudinal and transverse steel together with hypothetical inclined concrete struts form a truss like system.

A mathematical solution to model shear behavior in reinforced concrete that simultaneously satisfies the physical limitations of material properties, deformation compatibility, and force equilibrium remains elusive. However, methods such as compression field theory, modified compression field theory adopted by the Canadian design code, and the variable angle truss model, adopted by Eurocode 2 comes close to being the final solution (MacGregor and Wight 2005).

In this section, the results of the second part of the R-series of test beams are presented and analyzed by comparing with the code predictions of ACI 318 and BS8110, both of which use empirical design approaches, and with the Eurocode 2 that uses the rationally derived variable angle truss model.

5.1 Experimental Program and Test Beam Preparation

The experimental program for the R-series with transverse reinforcement is shown in Table 5-1 below. This part of the R-series consists of 38 rectangular beams cast with lightweight aggregate concrete made from 3 different types of lightweight coarse aggregate and a reference normal weight concrete. The normal weight concrete beams were tested in duplicate. Natural sand was used in all concretes as fine

aggregate as its' substitution with lightweight fine aggregate was observed by ACI committee 213 (ACI213R-03) to provide diminishing returns in that the reduction of weight does not offset the loss in material performance. This is further aggravated by the lightweight fine aggregate's water absorbing properties which complicates control of mix water. Foamed concrete and lightweight aggregate foamed concrete were excluded from this phase of study until further material development to address shrinkage cracking could be performed.

The beams were prepared in the same manner as the R-series test beams in Section 3.1 above. Throughout the test program, only the steel reinforcement was varied with longitudinal tensile steel ranging from 1.06% to 3.93% and R6 transverse reinforcement arranged with center to center spacing ranging from 170 mm to 50 mm. Transverse reinforcement for R-series test beams were in the form of closed links. The 6 mm diameter smooth, mild steel links were tack weld shut to prevent opening of the links. Bar lapping at the mouth of the links were placed alternately left and right in the flexural compression zone. In the longitudinal direction, the links were arranged to be symmetrical about the centre line of the longitudinal bars and correspond to the spacing being a multiple of the effective depth, *d*.

Testing and instrumentation method of these R-series test beams with transverse reinforcement and the material properties are identical to that presented in Section 3.3 and Section 3.4 earlier. Casting and testing of these beams were carried out at the same time as the R-series beams discussed in preceding sections. Material properties of the concrete used are presented in Table 3-6.

5.2 Crack Propagation and Patterns

Cracking within the R-series can be classified into six types; flexure tension cracks, flexure-shear cracks, diagonal tension cracks, dowel cracks, shear compression

cracks, and flexural compression cracks are discussed in Chapter Three above. While the order of each crack's appearance and pattern is largely the same, dowel cracks do not always occur as truss action is able to develop with the presence of transverse reinforcement. These steel bars act as vertical ties of a hypothetical truss providing equilibrium to a diagonal concrete strut, without which dowel cracking/splitting ensues.

The final cracking patterns of the lightweight concrete beams tested are shown in Figure 5-1 to Figure 5-5. All the lightweight concrete developed more extensive cracking that had closer spacing compared to normal weight concrete. At higher loads, numerous inclined cracks formed within the shear zones. The angle of these inclined cracks was also tend to be steeper to the horizontal at low longitudinal reinforcement ratios compared to shallow inclines at higher longitudinal ratios.

5.3 Ultimate Failure Modes

From the tests of rectangular beams, a variety of ultimate failure modes were observed. These failure modes ranged from diagonal tension failures, flexural yielding of steel reinforcement, and shear compression failures.

Diagonal tension failures and shear compression failures are brittle modes. The former is typically accompanied by complete rupture of the concrete if no shear reinforcement is provided. This failure mode is characterized by wide diagonal cracks which are widest in the flexural tensile zone of the beam.

Shear compression failures occur when the combined compression stresses caused by shear and flexure exceed the compression capacity of the concrete. The concrete will proceed to crush with tensile cracks appearing perpendicular to the direction of compression stresses. This failure mode is characterized by diagonal cracks that are wider in the flexural compression zone rather than in the flexural

tensile zone. It may also be accompanied by spalling of concrete in the extreme compression fibers.

When nominal links were provided at 125 mm spacing, the shear capacity of the sections were significantly improved. At low longitudinal reinforcement ratios, the nominal shear links provided sufficient additional shear capacity such that the flexural capacity of the section could be realized. However, as the flexural capacity increases with increasing longitudinal reinforcement, shear failure modes begin to precipitate indicating that the shear capacity of the section is near the flexural capacity. At intermediate longitudinal reinforcement ratios, the combination of flexural compression and shear compression was sufficiently high to cause shear compression failures. Meanwhile, at high longitudinal reinforcement ratios, diagonal tension failures occurred instead.

This indicates that the longitudinal reinforcement ratio plays a role in affecting the shear failure mode either through dowel action or from an increased stiffness of the steel reinforcing bars. With a larger longitudinal reinforcement ratio, the section will develop larger flexural compression stresses to withstand higher loads. These higher loads also result in higher shear stresses. While the transverse reinforcement ratio is kept constant, it has been observed that a shear compression failure mode occurs at intermediate longitudinal reinforcement ratios. It would be expected that as the longitudinal reinforcement ratio increases, with the additional compressive stresses, a similar shear compression failure would occur. However, diagonal tensile failures occurred instead.

After the peak load is applied to the test specimens, all the beams approached a load plateau where the beam was able to continue sustaining a reduced load while the displacements continued to increase. This plateau was observed to occur after the concrete has ruptured indicating that the shear

resistance mechanism in effect is not the intact concrete of the flexural compression zone, interface friction, nor residual tensile stresses. These shear stresses must thus be transmitted via dowel action of the main longitudinal bars, by bearing of concrete in the flexural compression zone, and tied arch action.

5.4 Ultimate Loads

The various ways a beam develops ultimate failure was discussed in the preceding section. With the exception of beams without links i.e. T0.00, flexural yielding of longitudinal tensile steel was the limiting property governing the ultimate load for beams with 1.06% reinforcement regardless of concrete type. These beams can sustain an applied moment of 23 kN.m which agrees well with its 25 kN.m calculated capacity using the simplified rectangular stress block of BS8110 with material factors set at unity. Considering the geometry and specimen cross section, the moment capacity corresponds with an applied shear force of 38 kN ($v = 1.1$ N/mm^2) which is within its shear capacity since shear failure did not occur before that. Although diagonal cracking develops, they are quickly arrested by the links allowing loading to progress until typical flexural failure.

At 1.61% tension steel, RN normal weight concrete beams continue to experience yielding of longitudinal tensile steel as its ultimate failure mode. The applied shear force approaches 55 kN as did the RE-series of lightweight concrete beams. This applied shear force corresponds with a bending moment of 33 kN.m which compares favorably with the calculated moment capacity of 36 kN.m. However, RD-series lightweight concrete developed premature shear failures prior to exhausting its tensile capacity while steel in the RF-series began yielding but the beam did not have sufficient ductility for a fully ductile tension failure instead having a shear failure shortly after yielding of steel. This is an indication that the flexural

capacity and shear capacity of the member is close to each other for the specific beam.

When the longitudinal tensile steel is increased to 2.51%, the calculated bending moment also increases to 55 kN.m requiring the hanger bars in the compression zone to be mobilized as compression reinforcement. Only RN normal weight concrete beams were able to approach these calculated values. Even then, the RN-series did not display a fully ductile failure with a distinct peak and compression failure of the steel and crushing of concrete. Lightweight concrete beams meanwhile failed prematurely in shear indicating that the shear strength of lightweight concrete is less than an equivalent normal weight concrete beam.

Typically, as the moment capacity of the beam is increased through more longitudinal tensile steel, lightweight concrete beams will exceed its shear capacity first. In this regards, ultimate diagonal tension failures tend to occur at lower loads compared to ultimate shear compression failures. The former type of failures were observed to occur for beams with transverse reinforcement spaced more than 0.75 time effective depth, d apart. Once the spacing was reduced to 0.5d and smaller, diagonal tension failures ceased to precipitate although shear compression failures still form.

These shear compression failures occur in the flexural compression zone of the beam within the shear span close to the loading plate. Crushing of concrete in this zone is not unexpected since the largest combined flexure compression and compression in the diagonal compression strut coincides at that location. However, once the link spacing was further reduced to 0.3d, shear failures no longer happens with test beams achieving it full flexural capacity including the flexurally over-reinforced beams (P3.93). Nevertheless, regardless of transverse reinforcement

configuration, all beams developed diagonal tension cracks prior to the ultimate failure loads.

5.5 Deflections at Ultimate

Beam displacements are a function of geometry and material properties and is typically governed by its flexural behavior with shearing action contributing negligible deformation. Load-displacement curves are specific to a given geometry and may be generalized across different geometries by converting to moment-curvature curves instead. In this experimental program, all the R-series beams had the same geometry and loading configuration and thus load-displacement curves are compared for simplicity.

Throughout the tests, it has been observed that lightweight concrete consistently initiates shear cracking at lower deflections compared to normal weight concrete regardless of links provided. The initiation of shear cracking also shows little variation with and without the presence of stirrups whereas normal concrete exhibits an increased displacement at cracking when links are provided. With normal weight concrete being able to develop twice the displacements of lightweight concrete at cracking, a different shear resistance mechanism may be at work when transitioning from normal weight concrete to lightweight concrete. This is also contrary to normal weight concrete having a higher stiffness and elastic modulus.

In the load – deflection curves below (Figure 5-6 to Figure 5-23), the region of adequate performance is bounded by the deflection limit on the horizontal axis, and the ultimate calculated load on the vertical axis. If the calculated shear capacity is lower than the cracking load, then the design remains adequate even if cracking initiates prior to breaching the strength limits.

A displacement characteristic of greater concern is the lack of ductility in lightweight aggregate concrete. The topic of lightweight aggregate concrete ductility has been explored in-depth by Lim H. S. (2007) and is beyond the scope of this study. However, it is clear from the results herein that lightweight concrete may initiate shear failure after the longitudinal tensile steel has yielded but before it has adequately deformed into the ductile zone. This observation has negative implication on lightweight concrete member design so far as to point out that implicit safety factors are compromised since warnings of impending failure from exaggerated deformations is not realized. Nevertheless, where sufficient shear capacity was available to avoid premature shear failures, both normal weight concrete and lightweight aggregate concrete occurred at comparable displacements. This is not unexpected since flexural failure is governed by yielding of steel which would be the same provided the concrete has sufficient compressive strength to initiate said flexural yielding of steel.

5.6 Comparison with BS8110 and Eurocode 2

The British Standard, BS8110 uses an empirical approach to design the shear resistance of structural elements. This approach assumes the shear capacity of a beam is the sum of a concrete contribution and a contribution from transverse steel (See equation 1-1). The concrete contribution is derived from the shear carrying capacity of a beam without transverse reinforcement as discussed in Chapter 4. However, it is now clear the failure mechanism of beams with transverse reinforcement is different from those without transverse reinforcement. As such the concrete contribution given in the design code has no rational meaning (Chana 1987).

Nevertheless, this approach has been able to yield design values that approximate the actual strength of a section although the underlying mechanisms are

different. The code approach thus continues to produce safe reinforced concrete design through minimum detailing and curtailment requirements and has been verified by extensive experience and experimental campaigns.

When applied to lightweight aggregate concrete, BS8110 reduces the concrete contribution of lightweight concrete by a factor of 0.8. The transverse steel portion is kept the same. A comparison of the code predictions using material safety factors set at unity and experimental results are shown in Figures 5-6 to 5-23.

It was found that code predictions compared to the normal weight concrete was reasonably accurate and able to produce economical and safe designs. In beams where links were provided, the flexural capacity of the section was realized in full including the ductile post-peak regions. Only in beams with 2.51% longitudinal reinforcement and links spaced at 125 mm did a shear failure occur in the normal weight concrete beams tested. The physical failure of RN P2.51 T0.26 occurred at loads 35% higher than the predicted shear capacity of the section.

When applied to lightweight concretes, BS8110 continues to produce calculated shear capacities that accurately predict the strength of the section. However, the reserve shear strength between the predicted value and actual physical failure of the beam may be compromised with a typical section only able to develop 10% reserve shear strength beyond calculated ultimate value. While this reserve shear strength does not directly impact the design method of the code, it may cause some sections to develop premature shear failures before the full ductility of a flexural failure can be realized.

The design method of the Eurocode 2 meanwhile is based on the rationally derived rotating angle truss model rather than the empirical method of the BS8110. The code gives the shear strength of members containing transverse reinforcement

as shown in equation 5-1 below which is the tensile capacity of the links under truss action. The angle of the inclined struts, θ, is taken between 22° and 45° with the former being the typical angle to maximise transverse reinforcement economy.

$$V_{Rd,s} = \frac{A_{sw}}{s} z f_{ywd} cot\theta \tag{5-1}$$

While equation 5-1 give the tensile capacity of the truss and is independent of the concrete strength and type, values of $V_{Rd,s}$ should not exceed the compressive strength of the diagonal concrete strut in the truss model. The maximum compressive strength of the concrete strut is given as equation 5-2 below.

$$V_{Rd,max} = \alpha_{cw} b_w z \nu_1 {}^{f_{cd}}/_{(\cot\theta + \tan\theta)} \tag{5-2}$$

The term α_{cw} is a coefficient taking account of the state of the stress in the compression chord which in the case of non prestressed concrete is unity. The strength reduction factor for concrete cracked in shear, v_1 is given as equation 5-3 below and as equation 5-4 for lightweight concrete.

$$v_1 = 0.6\left(1 - {}^{f_{ck}}/_{250}\right) \tag{5-3}$$

$$v_{l,1} = 0.5\left(1 - {}^{f_{ck}}/_{250}\right) \tag{5-4}$$

The design compressive strength meanwhile is given as equation 5-6 with the coefficient taking account of long term effects on the compressive strength and of unfavorable effects resulting from the way the load is applied, α_{cc} being unity for normal weight concrete and 0.85 for lightweight concrete.

$$f_{cd} = \alpha_{cc} {}^{f_{ck}}/_{\gamma_c} \tag{5-5}$$

Assuming the angle of the compression strut as 22° and the lever arm as 0.9d, the shear capacity of R-series test beams are calculated using material safety factors set at unity and are tabulated in Table 5-2. From this rational variable angle truss model, the only effect of using lightweight concrete is in a reduction of the capacity of the concrete strut.

From Figure 5-24, it can be seen that the design equation given by Eurocode 2 is able to produce good predictions of the shear strength of a section with transverse reinforcement. In this figure, only data pairs from test beams that developed a shear failure mode were included. Data values from beams that precipitated a flexural failure mode were discarded and not plot in Figure 5-24. Table 5-2 summarizes the shear capacity calculated with Eurocode 2 provisions and the experimentally measured values. It can be seen that the shear capacity of the section is governed by the steel yielding when the compressive strength of concrete increases, *e.g.* in the RE series, while crushing of the concrete struts will be the limiting value in concretes with lower strengths.

When the link spacing is large, the code approach implies that truss action is not able to develop effectively since the compression struts will have to be very shallow and there would be insufficient steel to develop meaningful contribution. As such the calculated shear capacity of the truss model with shear links is as low as 27 kN for links spaced at 200 mm center to center while the strength of the compression strut is calculated to be as high as 84 kN. In effect, the measured shear strength of the section is intermediate between the steel contribution and the concrete strength at 55 kN. Calculating the shear capacity of the section using the equation for sections without transverse reinforcement may be more accurate considering shear resistance mechanisms for sections without transverse reinforcement can develop between the links.

5.7 Conclusion

Three types of lightweight coarse aggregates were tested and while all the lightweight concretes with lightweight coarse aggregate and natural sand developed more extensive cracking than normal weight concrete, there was no discernable difference in cracking between the various lightweight coarse aggregates used. Variations in the shear strength and crack propagation between the lightweight concretes can be adequately attributed to the difference in compressive strengths between the lightweight aggregate concretes.

From the results of the test on 38 rectangular beams with transverse reinforcement, it was found that both BS8110 and Eurocode 2 produces safe and economical designs for lightweight concrete. However, when lightweight concrete was compared to normal weight concrete of this test, some loss in reserve shear strength beyond that calculated by the code was obvious. Nevertheless, this does not affect the design philosophy except that designers should be cognizant of the potential loss in ductility when designing shear critical lightweight concrete members.

Table 5-1 Experimental program R-series

No.	Ref. Number	Target Compressive Strength	Longitudinal Reinforcement		Transverse Reinforcement			Shear span to Effective Depth Ratio	Parameters				
			Ratio (bh) %	Bars	Ratio	Spacing	Spacing (multiples of effective depth)		*f'c*	*agg*	*ρL*	*ρT*	*a/d*
1	RD P1.06 T0.26	40	1.06	2 T13	0.26	125	0.75	3.0		IV	II	I	
2	RD P1.61 T0.26	40	1.61	2 T16	0.26	125	0.75	3.0		V	II	II	
3	RD P2.51 T0.26	40	2.51	2 T20	0.26	125	0.75	3.0		VI	II	III	
4	RD P1.06 T0.39	40	1.06	2 T13	0.39	90	0.5	3.0		VII	III	I	
5	RD P1.61 T0.39	40	1.61	2 T16	0.39	90	0.5	3.0		VIII	III	II	
6	RD P2.51 T0.39	40	2.51	2 T20	0.39	90	0.5	3.0		IX	III	III	
7	RE P1.61 T0.16	40	1.61	2 T16	0.16	200	1.2	3.0				V	
8	RE P2.51 T0.16	40	2.51	2 T20	0.16	200	1.2	3.0				VI	
9	RE P1.61 T0.19	40	1.61	2 T16	0.19	170	1.0	3.0				V	
10	RE P2.51 T0.19	40	2.51	2 T20	0.19	170	1.0	3.0				VI	
11	RE P1.61 T0.26	40	1.61	2 T16	0.26	125	0.75	3.0		V		V	
12	RE P2.51 T0.26	40	2.51	2 T20	0.26	125	0.75	3.0		VI		VI	
13	RE P1.06 T0.39	40	1.06	2 T13	0.39	90	0.5	3.0		VII	V	IV	
14	RE P1.61 T0.39	40	1.61	2 T16	0.39	90	0.5	3.0		VIII	V	V	
15	RE P2.51 T0.39	40	2.51	2 T20	0.39	90	0.5	3.0		IX	V	VI	
16	RE P3.93 T0.39	40	3.93	2 T25	0.39	90	0.5	3.0			V	VII	
17	RE P1.61 T0.48	40	1.61	2 T16	0.48	70	0.4	3.0				V	
18	RE P2.51 T0.48	40	2.51	2 T20	0.48	70	0.4	3.0				VI	
19	RE P2.51 T0.64	40	2.51	2 T20	0.64	50	0.3	3.0				VI	
20	RE P3.93 T0.64	40	3.93	2 T25	0.64	50	0.3	3.0				VII	
21	RF P1.06 T0.26	40	1.06	2 T13	0.26	125	0.75	3.0		IV	VII	VIII	
22	RF P1.61 T0.26	40	1.61	2 T16	0.26	125	0.75	3.0		V	VII	IX	
23	RF P2.51 T0.26	40	2.51	2 T20	0.26	125	0.75	3.0		VI	VII	X	
24	RF P1.06 T0.39	40	1.06	2 T13	0.39	90	0.5	3.0		VII	VIII	VIII	
25	RF P1.61 T0.39	40	1.61	2 T16	0.39	90	0.5	3.0		VIII	VIII	IX	
26	RF P2.51 T0.39	40	2.51	2 T20	0.39	90	0.5	3.0		IX	VIII	X	
27	RN P1.06 T0.26	40	1.06	2 T13	0.26	125	0.75	3.0		IV	X	XI	
28	RN P1.61 T0.26	40	1.61	2 T16	0.26	125	0.75	3.0		V	X	XII	
29	RN P2.51 T0.26	40	2.51	2 T20	0.26	125	0.75	3.0		VI	X	XIII	
30	RN P1.06 T0.39	40	1.06	2 T13	0.39	90	0.5	3.0		VII	XI	XI	
31	RN P1.61 T0.39	40	1.61	2 T16	0.39	90	0.5	3.0		VIII	XI	XII	
32	RN P2.51 T0.39	40	2.51	2 T20	0.39	90	0.5	3.0		IX	XI	XIII	

Table 5-2 Comparison with Eurocode 2 design

No.	Ref. Number	Coefficient for concrete cracking, v_1	Maximum compression strut strength, kN	Maximum shear strength of yielding links, kN	Shear strength prediction of Eurocode 2, kN	Observed shear force at shear failure, kN	Observed shear force at flexure failure, kN
1	RD P1.06 T0.26	0.458	54.9	43.8	43.8 (s)	-	39.2
2	RD P1.61 T0.26	0.458	54.7	43.4	43.4 (s)	42.8	-
3	RD P2.51 T0.26	0.458	53.8	42.9	42.9 (s)	52.9	-
4	RD P1.06 T0.39	0.458	54.9	60.8	54.9 (c)	-	35.1
5	RD P1.61 T0.39	0.458	54.7	60.2	54.7 (c)	46.7	-
6	RD P2.51 T0.39	0.458	53.8	59.5	53.8 (c)	53.8	-
7	RE P1.61 T0.16	0.431	84.9	27.1	27.1 (s)	56.5	-
8	RE P2.51 T0.16	0.431	84.0	26.8	26.8 (s)	64.3	-
9	RE P1.61 T0.19	0.431	84.9	27.1	27.1 (s)	55.9	-
10	RE P2.51 T0.19	0.431	84.0	31.5	31.5 (s)	65.7	-
11	RE P1.61 T0.26	0.431	84.9	43.4	43.4 (s)	-	57.5
12	RE P2.51 T0.26	0.431	84.0	42.9	42.9 (s)	67.4	-
13	RE P1.06 T0.39	0.431	85.7	60.8	60.8 (s)	-	37.5
14	RE P1.61 T0.39	0.431	84.9	60.2	60.2 (s)	-	55.5
15	RE P2.51 T0.39	0.431	84.0	59.5	59.5 (s)	-	81.6
16	RE P3.93 T0.39	0.431	82.7	58.7	58.7 (s)	99.6	-
17	RE P1.61 T0.48	0.431	84.9	77.4	77.4 (s)	-	56.0
18	RE P2.51 T0.48	0.431	84.0	76.5	76.5 (s)	-	81.5
19	RE P2.51 T0.64	0.431	84.0	84.0	84.0 (s)	-	86.1
20	RE P3.93 T0.64	0.431	82.7	105.6	82.7 (c)	-	116.7
21	RF P1.06 T0.26	0.425	91.4	43.8	43.8 (s)	-	39.7
22	RF P1.61 T0.26	0.425	90.6	43.4	43.4 (s)	53.4	-
23	RF P2.51 T0.26	0.425	89.6	42.9	42.9 (s)	55.1	-
24	RF P1.06 T0.39	0.425	91.4	60.8	60.8 (s)	-	39.0
25	RF P1.61 T0.39	0.425	90.6	60.2	60.2 (s)	57.8	-
26	RF P2.51 T0.39	0.425	89.6	59.5	59.5 (s)	61.5	-
27	RN P1.06 T0.26 A	0.476	166.3	43.8	43.8 (s)	-	31.9
28	RN P1.61 T0.26 A	0.476	164.9	43.4	43.4 (s)	-	48.1
29	RN P2.51 T0.26 A	0.476	163.0	42.9	42.9 (s)	-	76.5
30	RN P1.06 T0.39 A	0.476	166.3	60.8	60.8 (s)	-	32.6
31	RN P1.61 T0.39 A	0.476	164.9	60.2	60.2 (s)	-	51.9
32	RN P2.51 T0.39 A	0.476	163.0	59.5	59.5 (s)	-	76.1
33	RN P1.06 T0.26 B	0.476	166.3	43.8	43.8 (s)	-	30.9
34	RN P1.61 T0.26 B	0.476	164.9	43.4	43.4 (s)	-	48.2
35	RN P2.51 T0.26 B	0.476	163.0	42.9	42.9 (s)	-	78.4
36	RN P1.06 T0.39 B	0.476	166.3	60.8	60.8 (s)	-	33.7
37	RN P1.61 T0.39 B	0.476	164.9	60.2	60.2 (s)	-	49.0
38	RN P2.51 T0.39 B	0.476	163.0	59.5	59.5 (s)	-	81.1

Note: (s) denotes steel governs (c) denotes concrete governs
Angle of inclined concrete strut assumed to be 22°

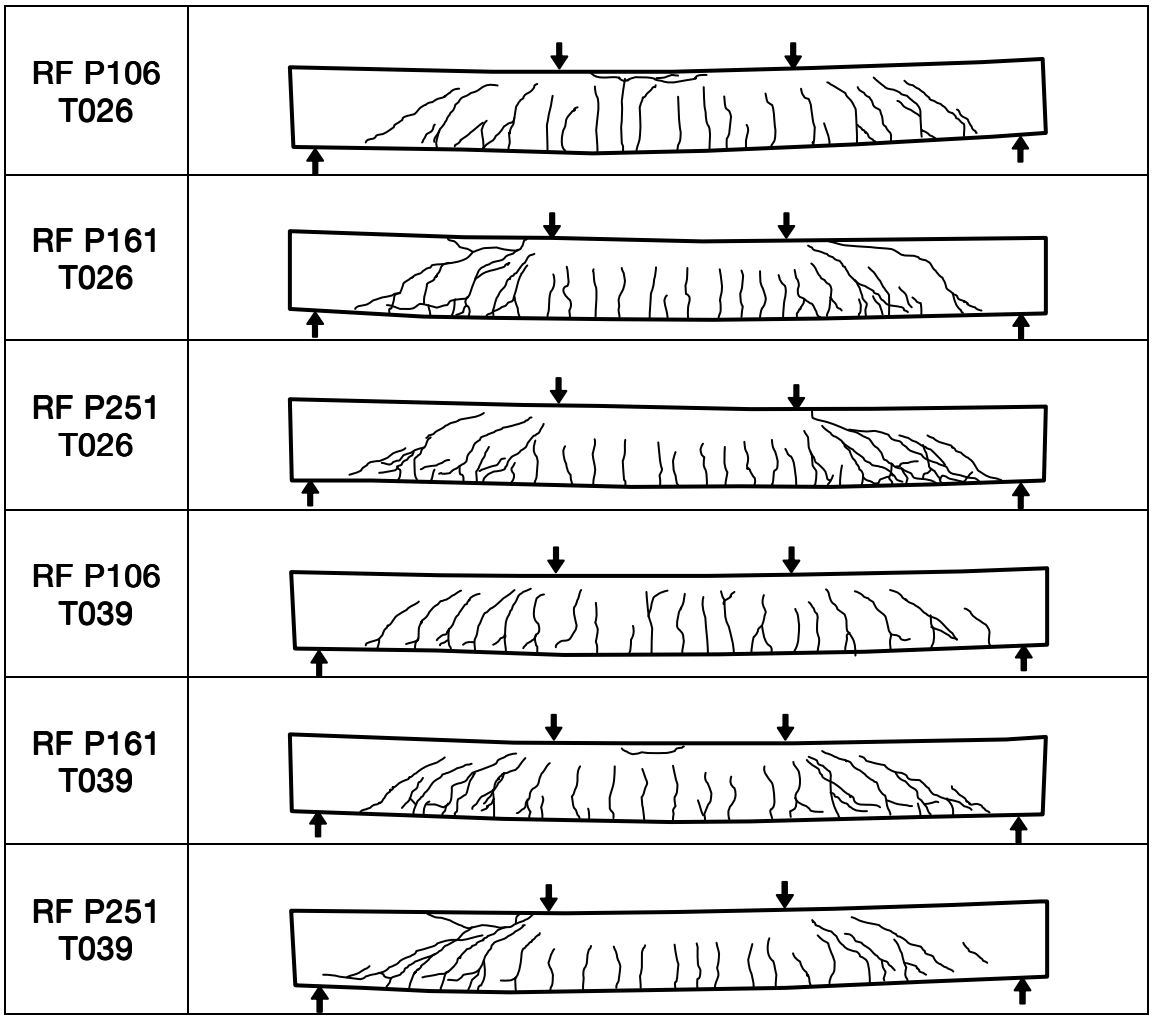

Figure 5-1 RF-series cracking pattern

RD P106 T026	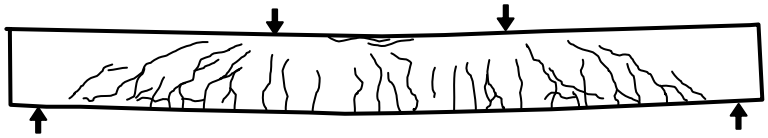
RD P161 T026	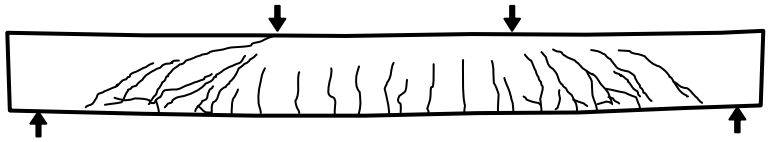
RD P251 T026	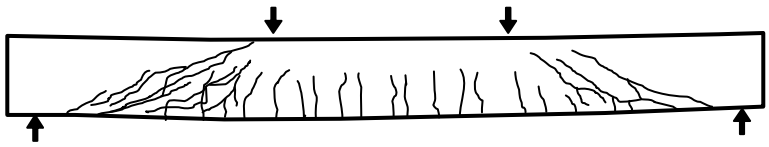
RD P106 T039	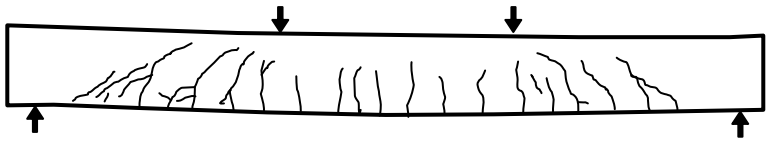
RD P161 T039	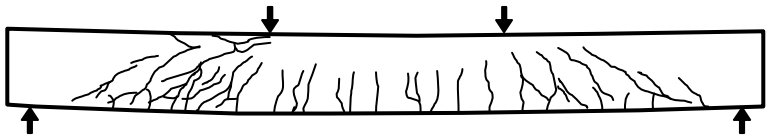
RD P251 T039	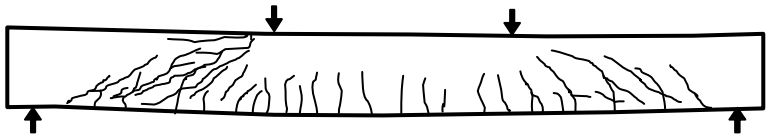

Figure 5-2 RD-series cracking pattern

RE P161 T016	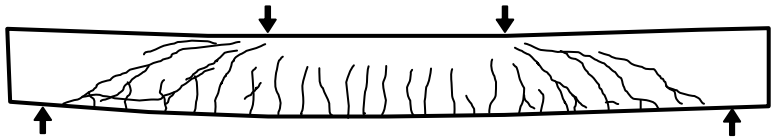
RE P251 T016	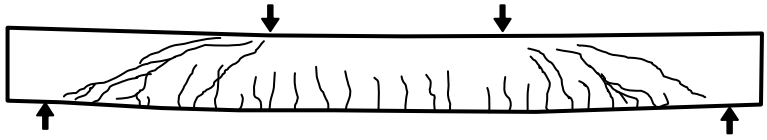
RE P161 T019	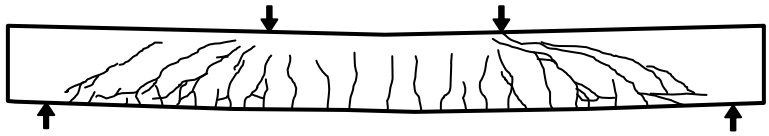
RE P251 T019	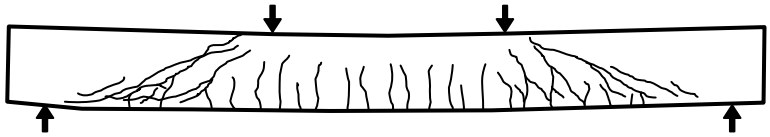
RE P161 T026	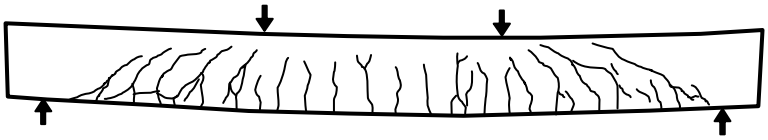
RE P251 T026	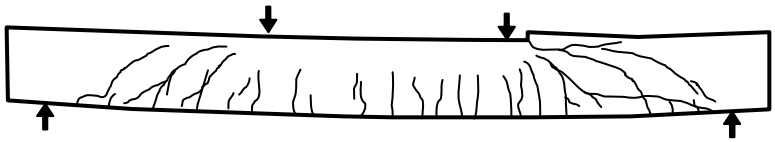
RE P106 T039	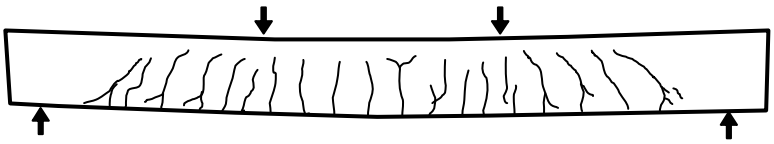
RE P161 T039	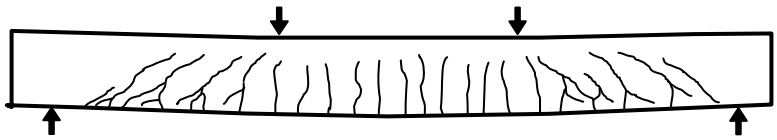

Figure 5-3 RE-series cracking patterns

RE P251 T039	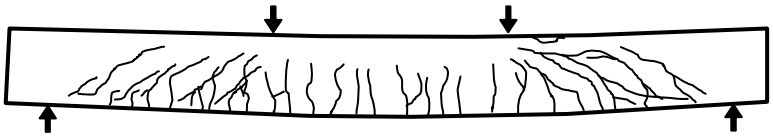
RE P393 T039	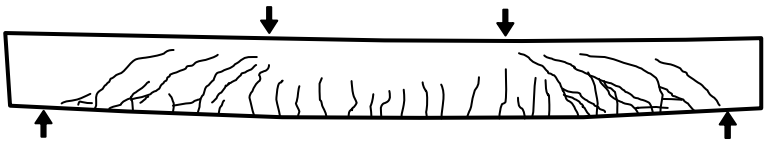
RE P161 T048	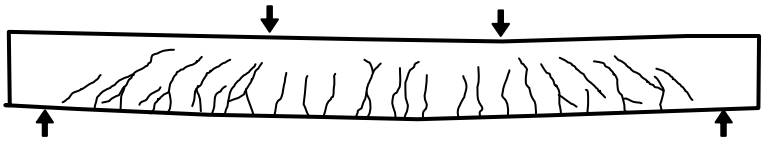
RE P251 T048	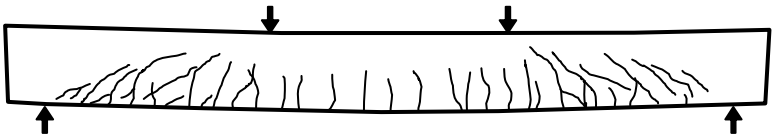
RE P251 T064	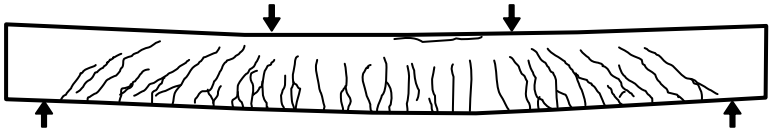
RE P393 T064	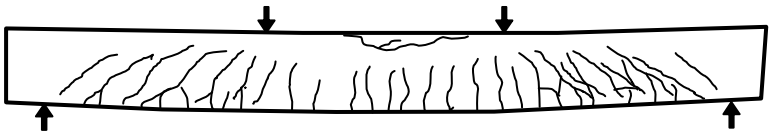

Figure 5-4 RE-series cracking patterns (continued)

RN P106 T000	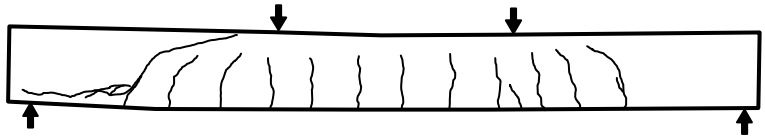
RN P251 T000	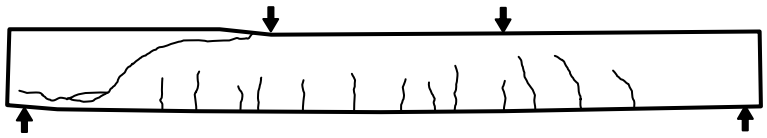
RN P106 T039	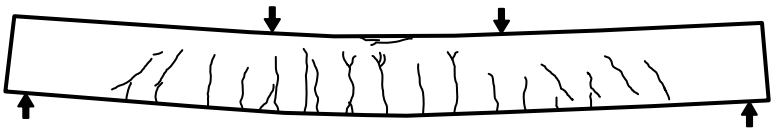
RN P161 T000	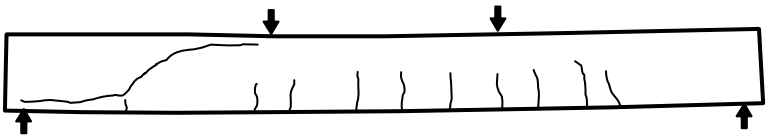
RN P161 T039	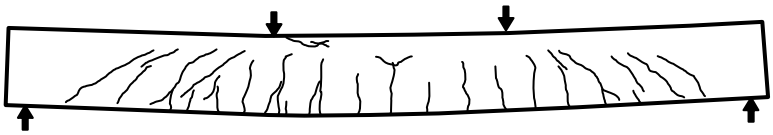
RN P251 T000	

Figure 5-5 RN-series cracking pattern

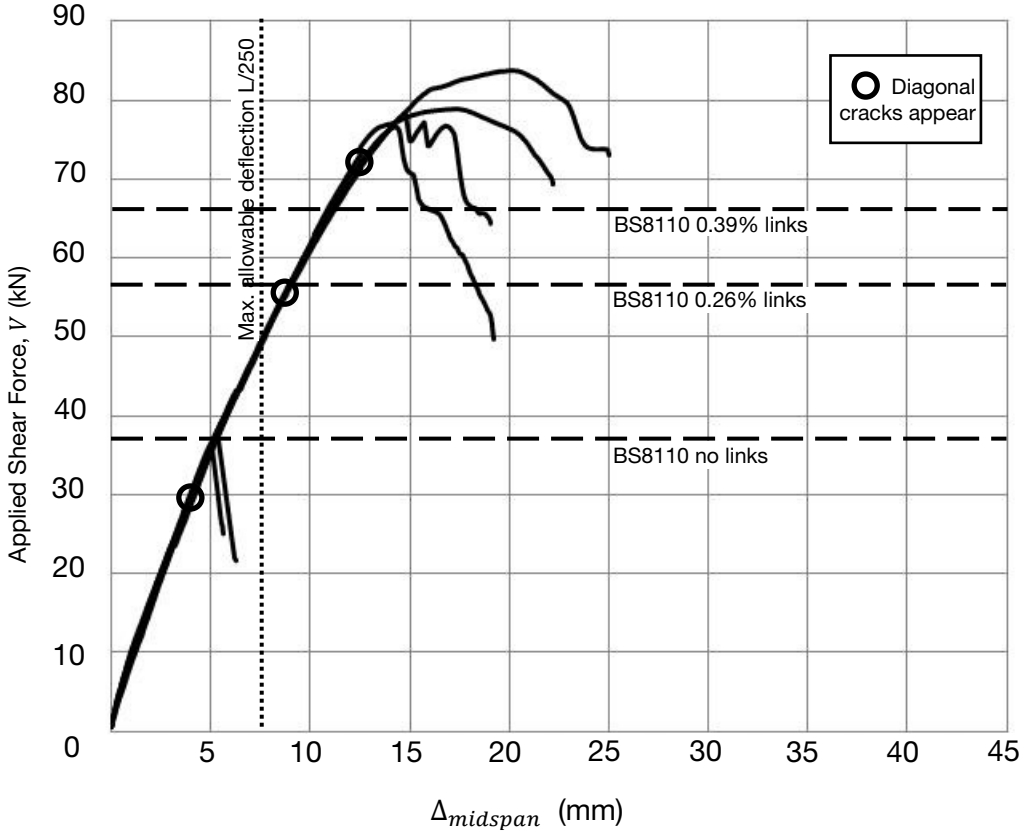

Figure 5-6 Load-deflection curve for RN Series at 2.51% steel

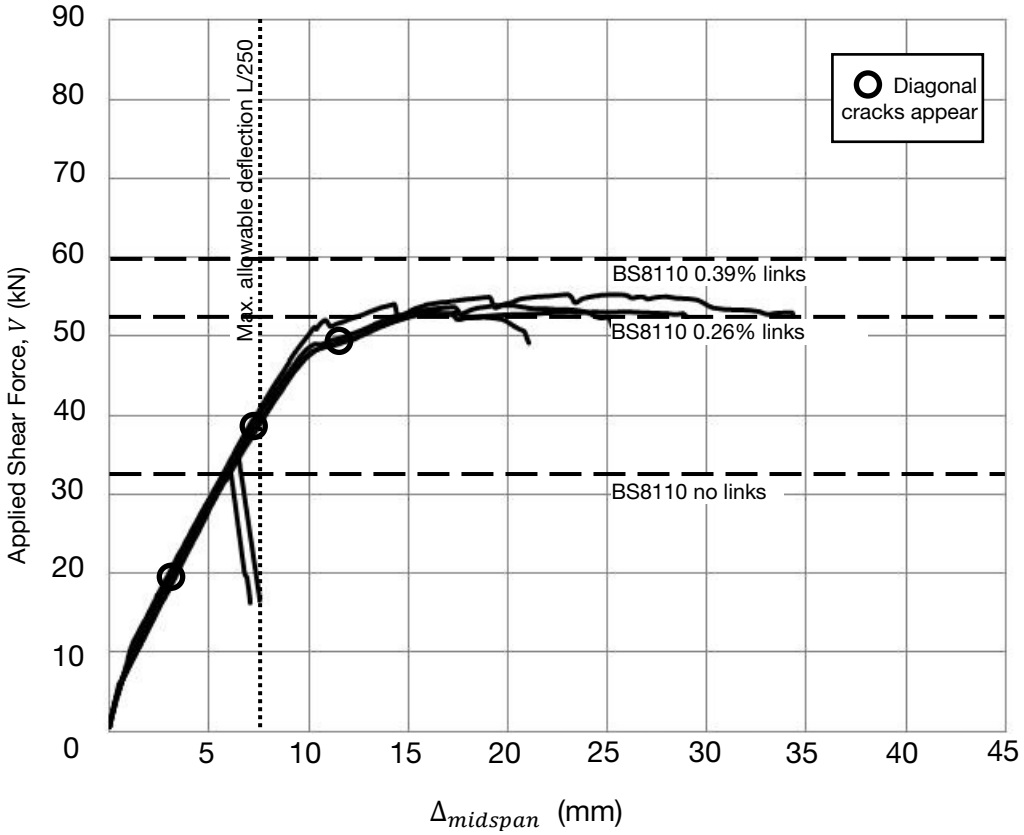

Figure 5-7 Load-deflection curve for RN Series at 1.61% steel

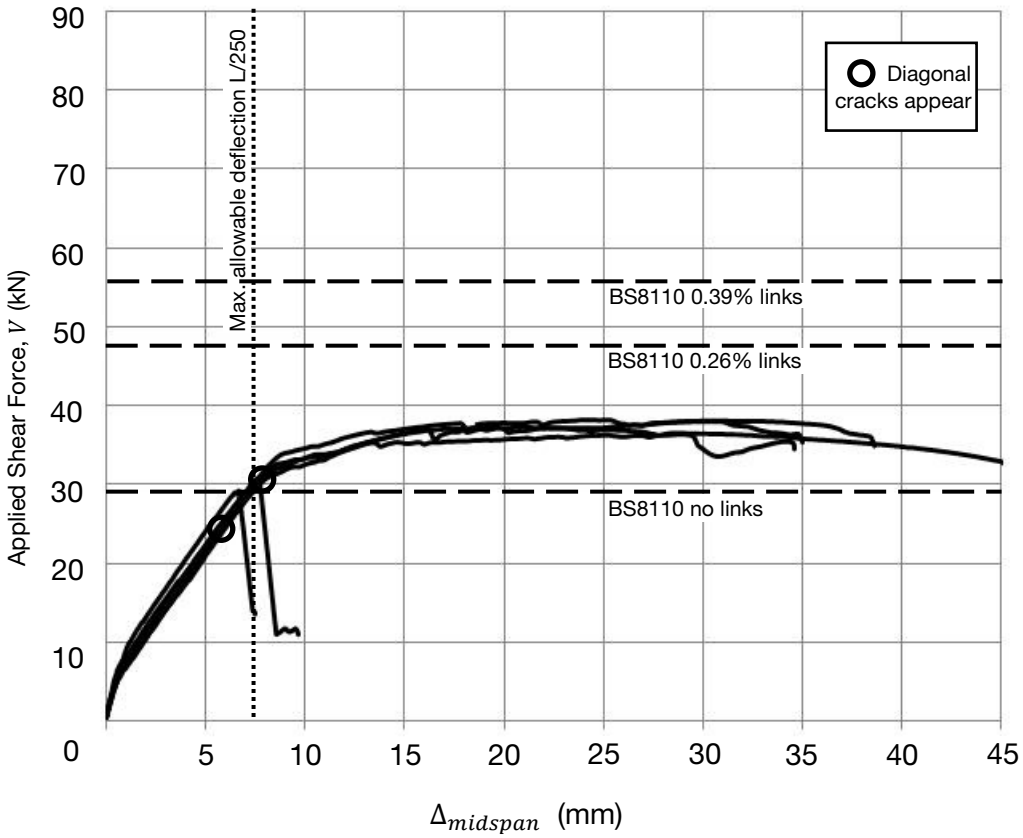

Figure 5-8 Load-deflection curve for RN Series at 1.06% steel

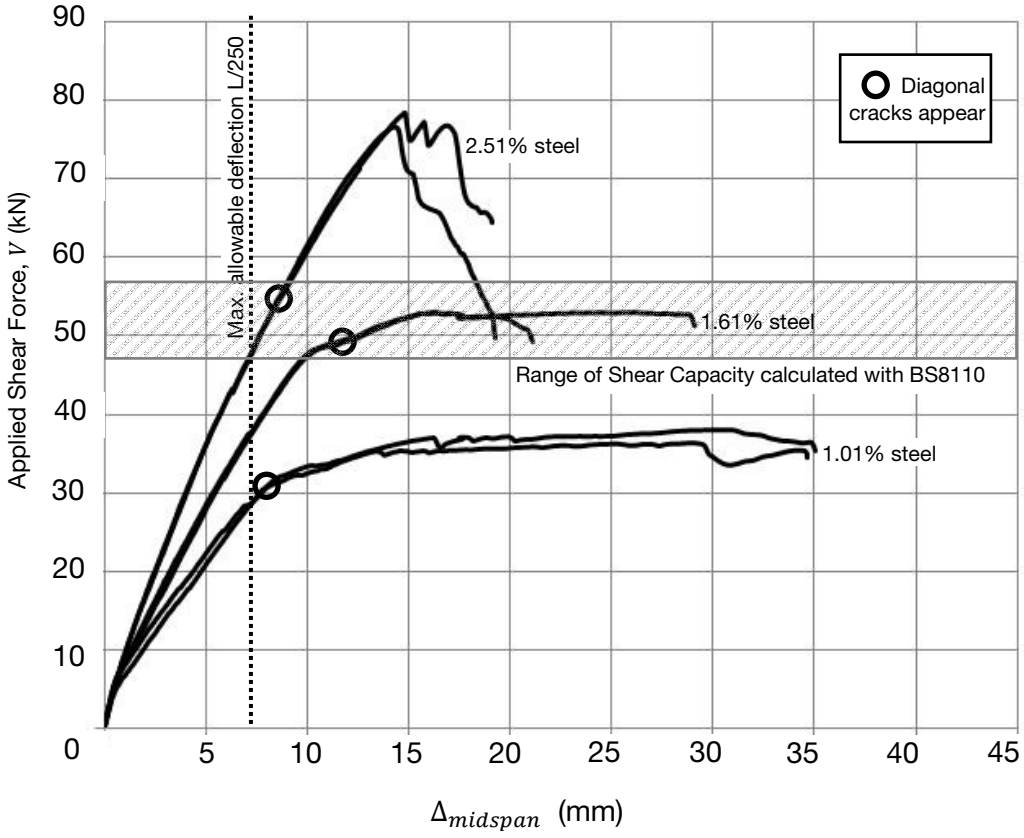

Figure 5-9 Load deflection curve for RN series with 0.26% transverse links

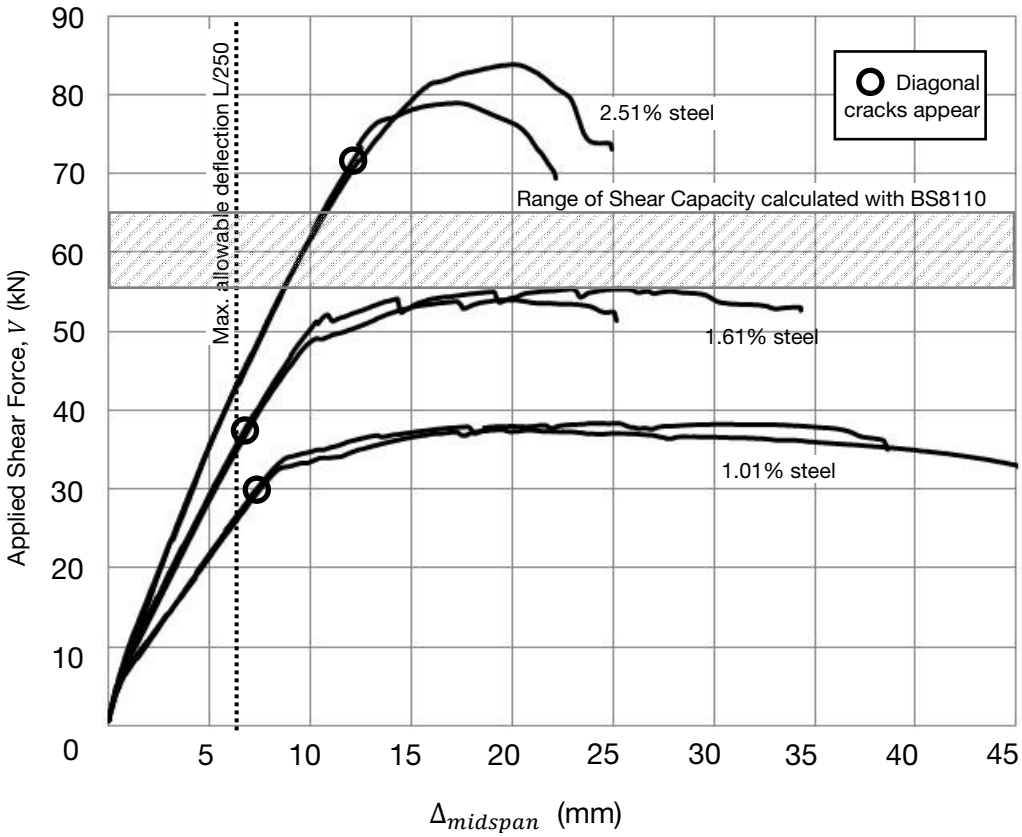

Figure 5-10 Load deflection curve for RN series with 0.39% transverse links

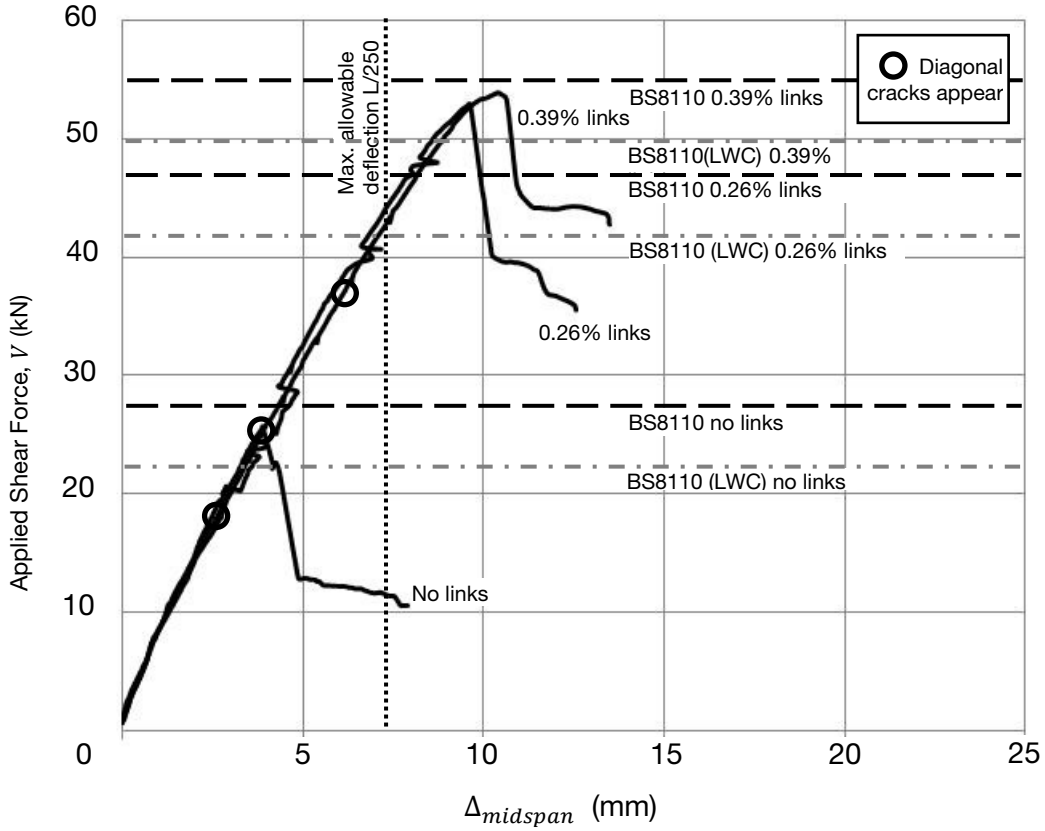

Figure 5-11 Load deflection curve for RD series with 2.51% steel

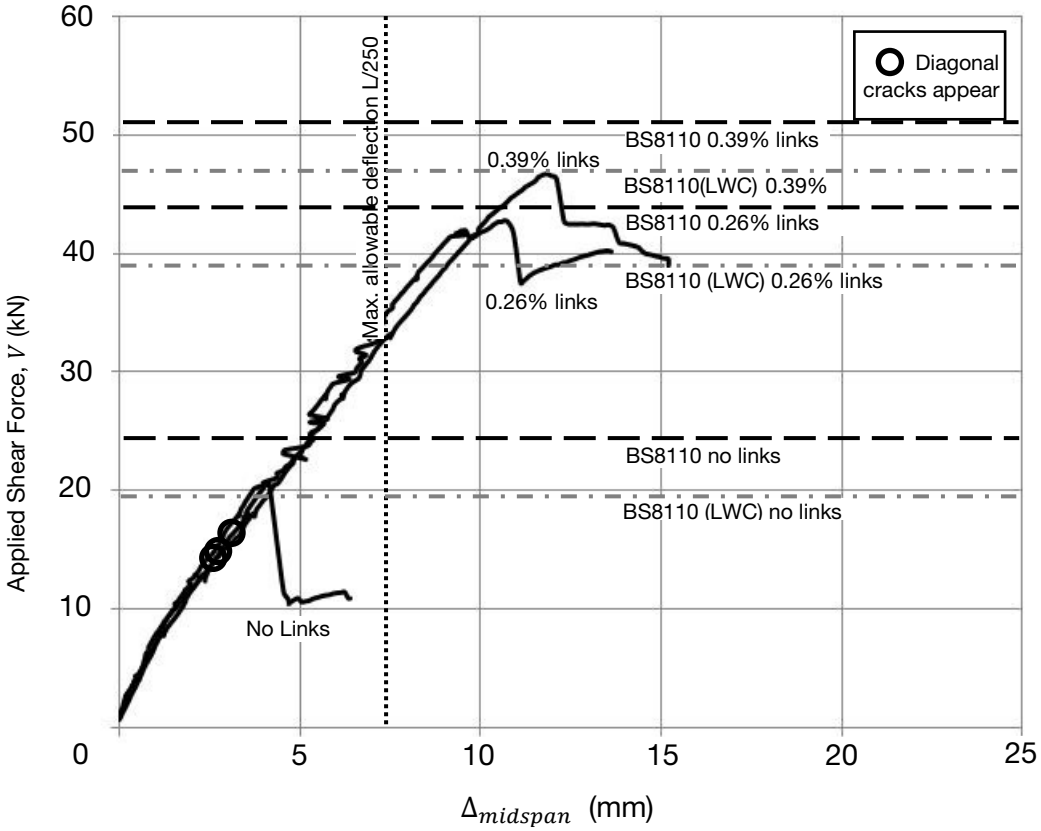

Figure 5-12 Load deflection curve for RD series with 1.61% steel

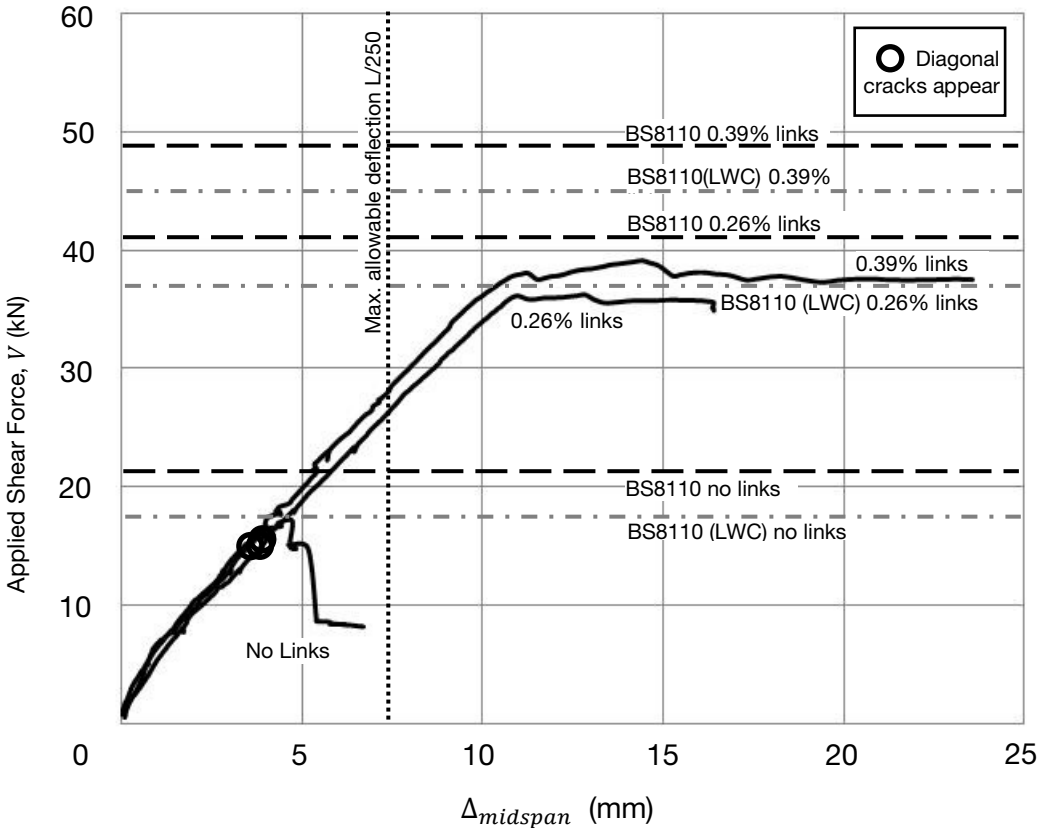

Figure 5-13 Load deflection curve for RD series with 1.06% steel

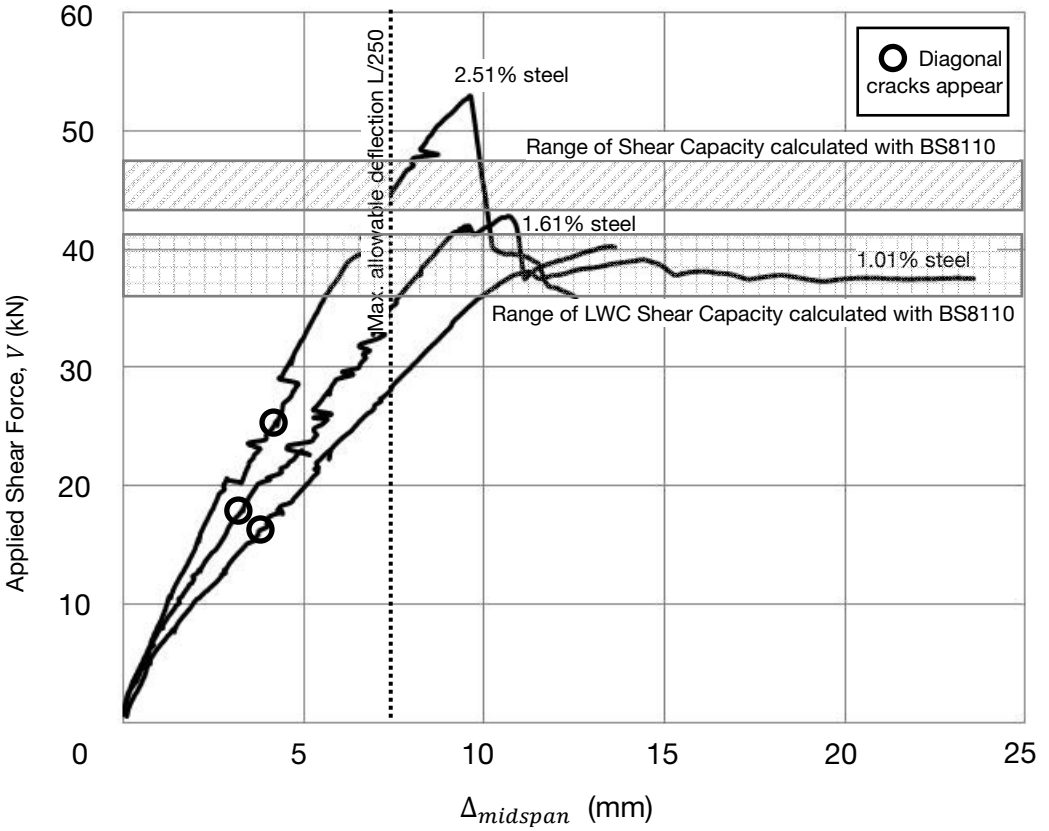

Figure 5-14 Load deflection curve for RD series with 0.26% links

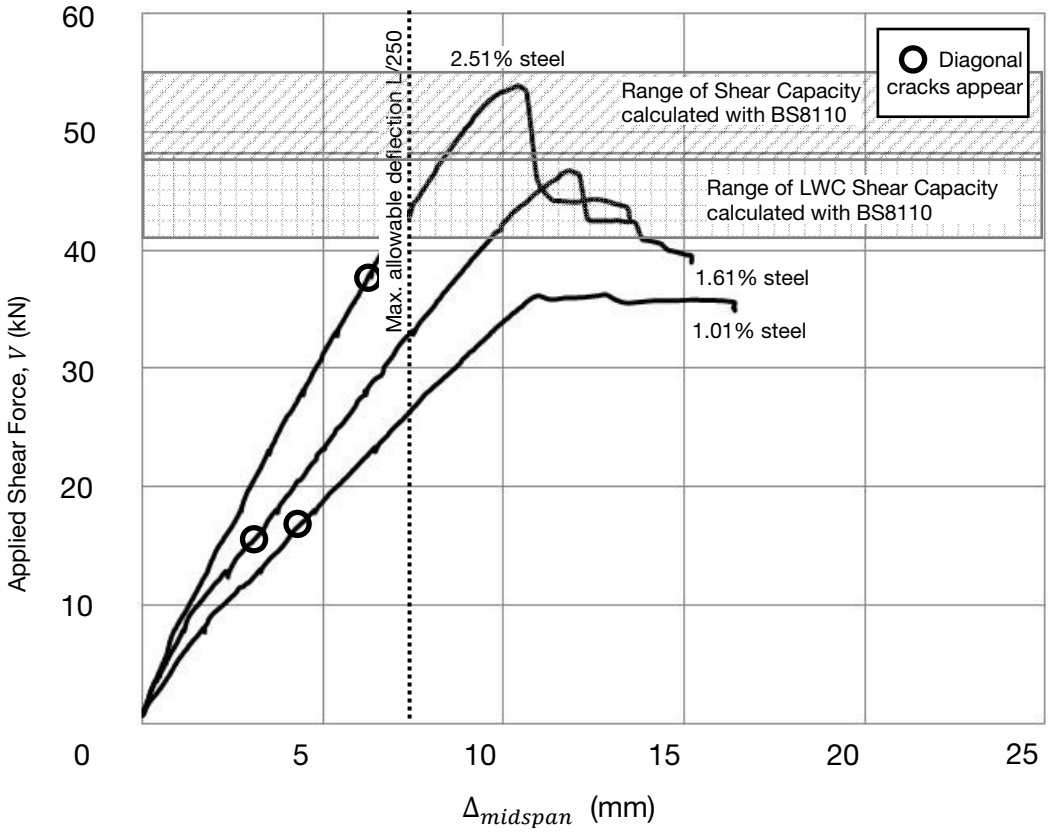

Figure 5-15 Load deflection curve for RD series with 0.39% links

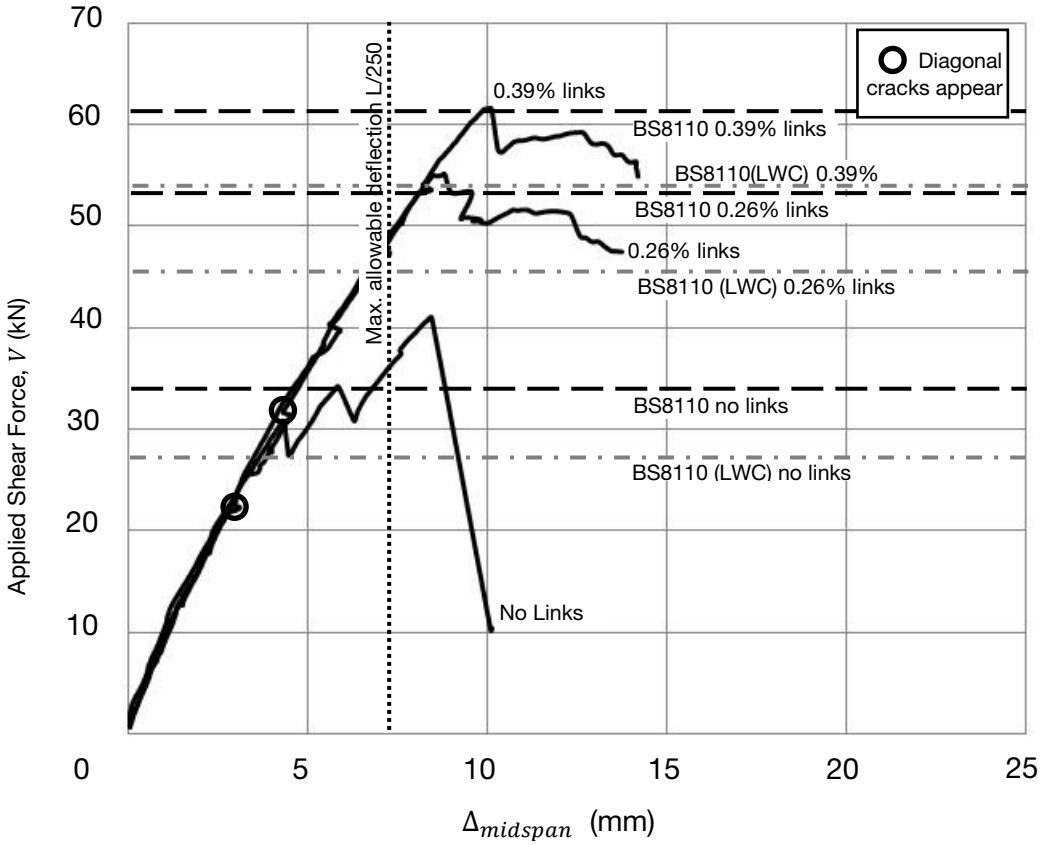

Figure 5-16 Load deflection curve for RF series with 2.51% steel

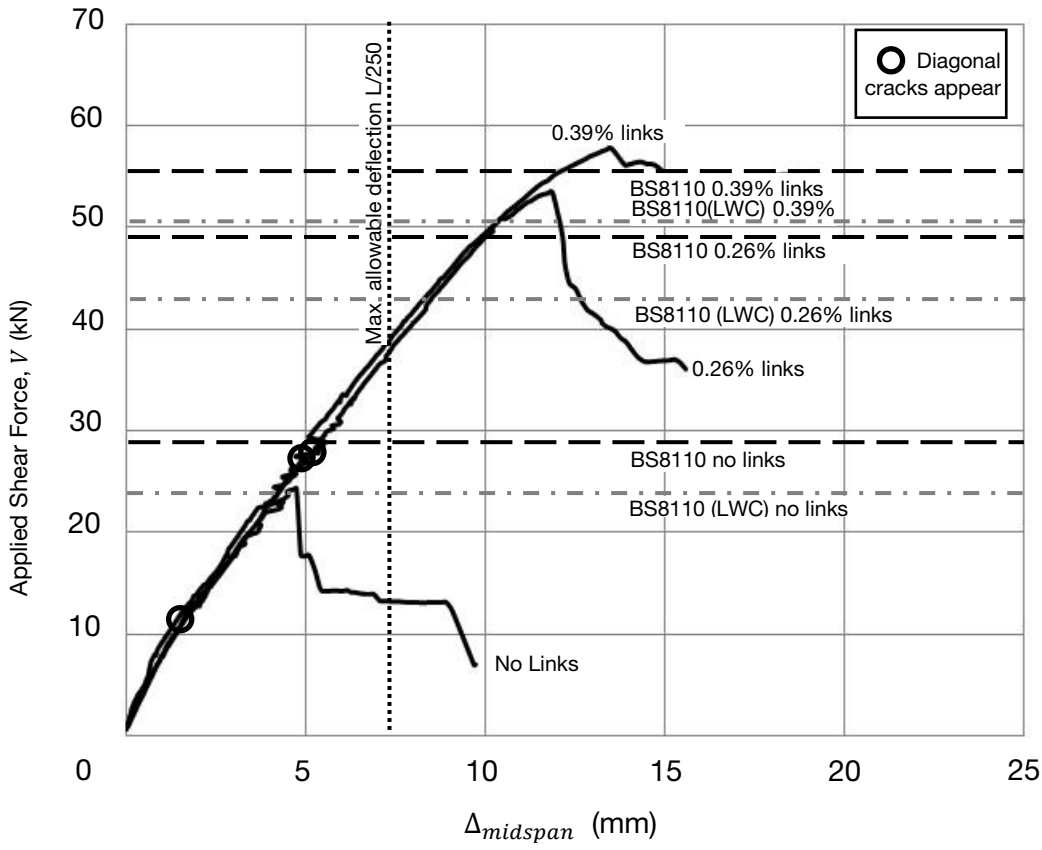

Figure 5-17 Load deflection curve for RF series with 1.61% steel

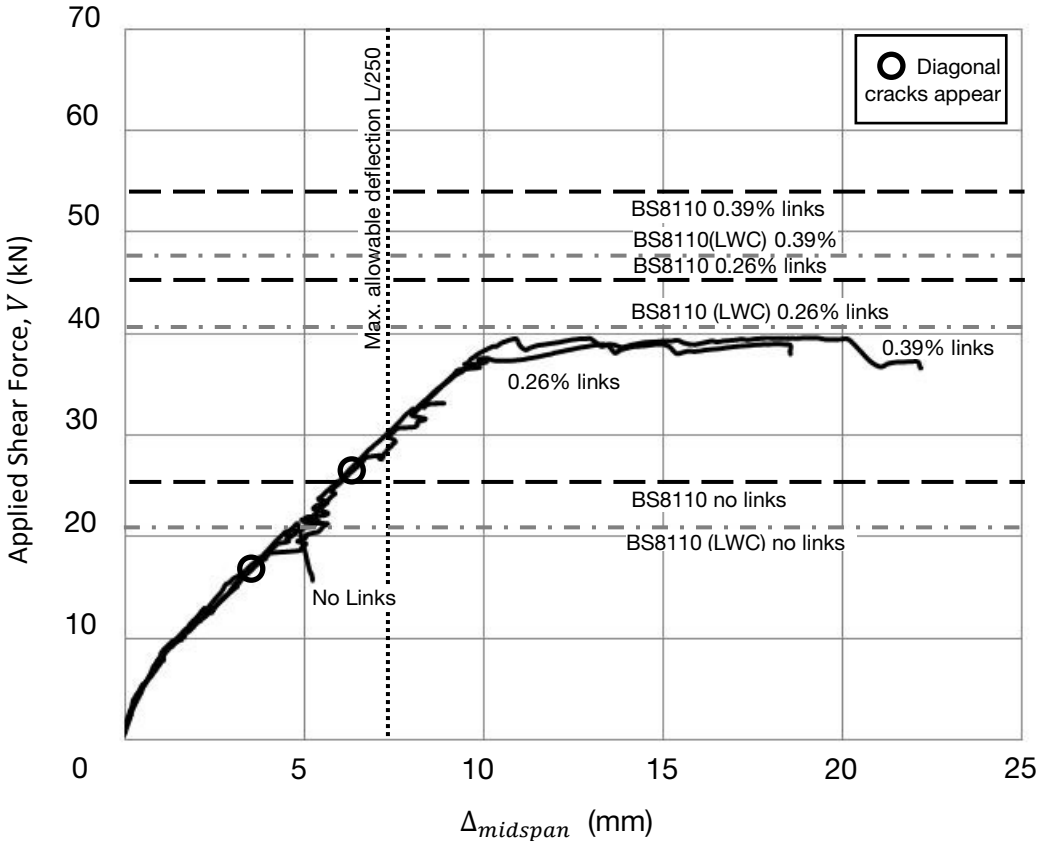

Figure 5-18 Load deflection curve for RF series with 1.06% steel

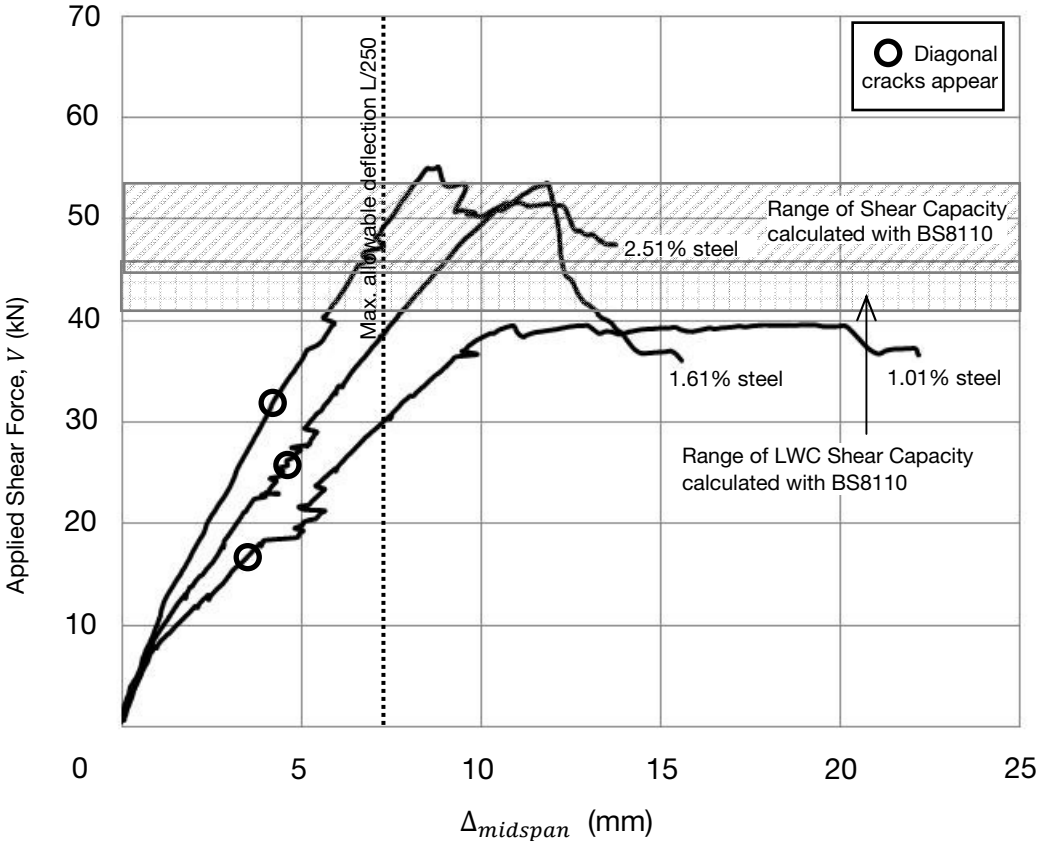

Figure 5-19 Load deflection curve for RF series with 0.26% links

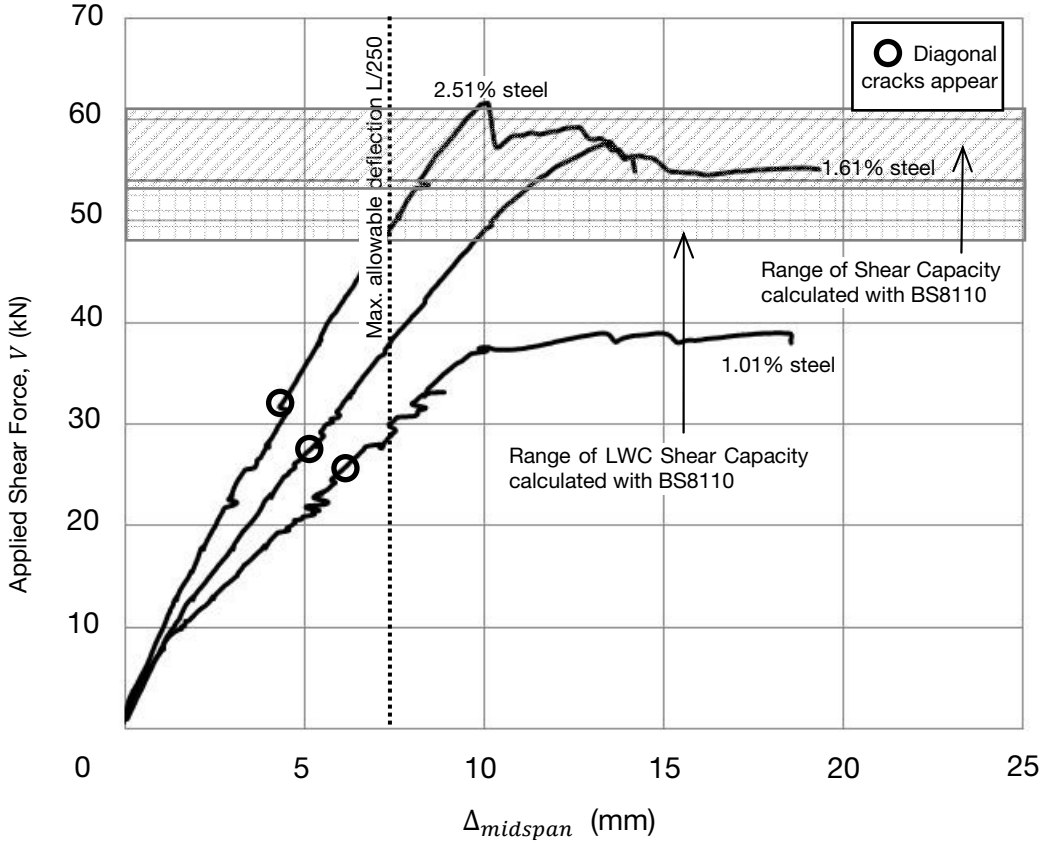

Figure 5-20 Load deflection curve for RF series with 0.39% links

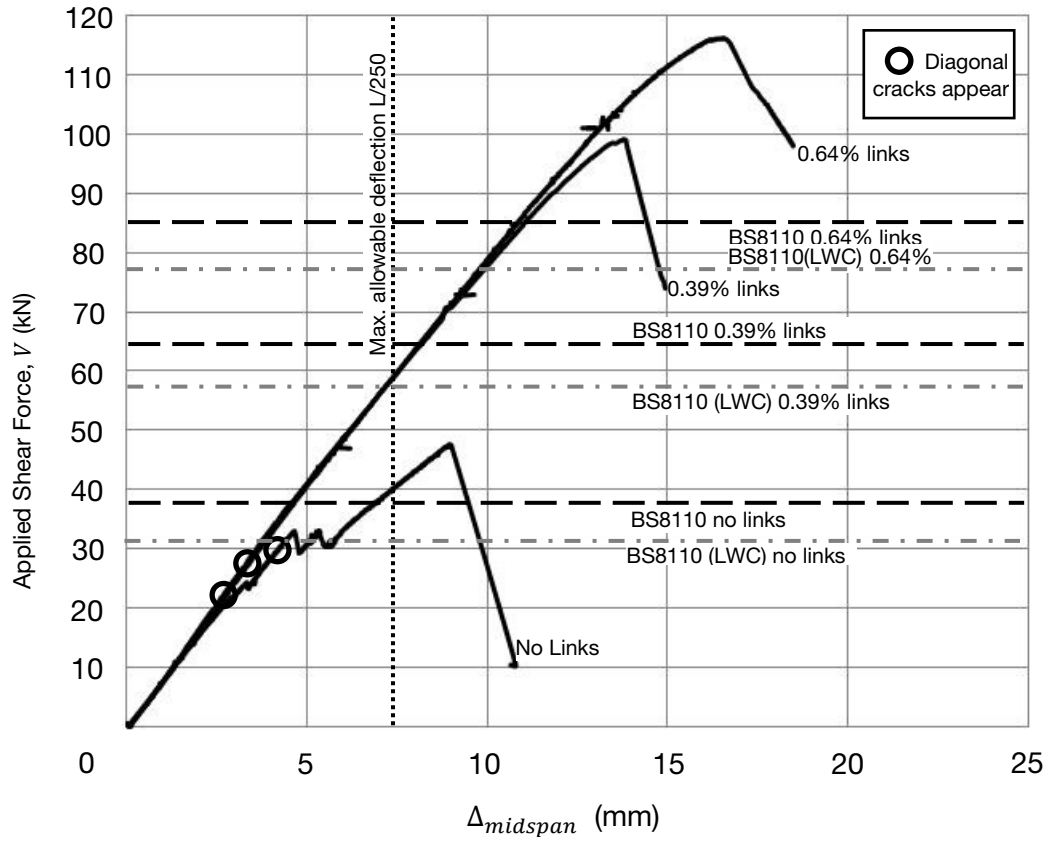

Figure 5-21 Load Deflection curve for RE Series 3.93% Steel

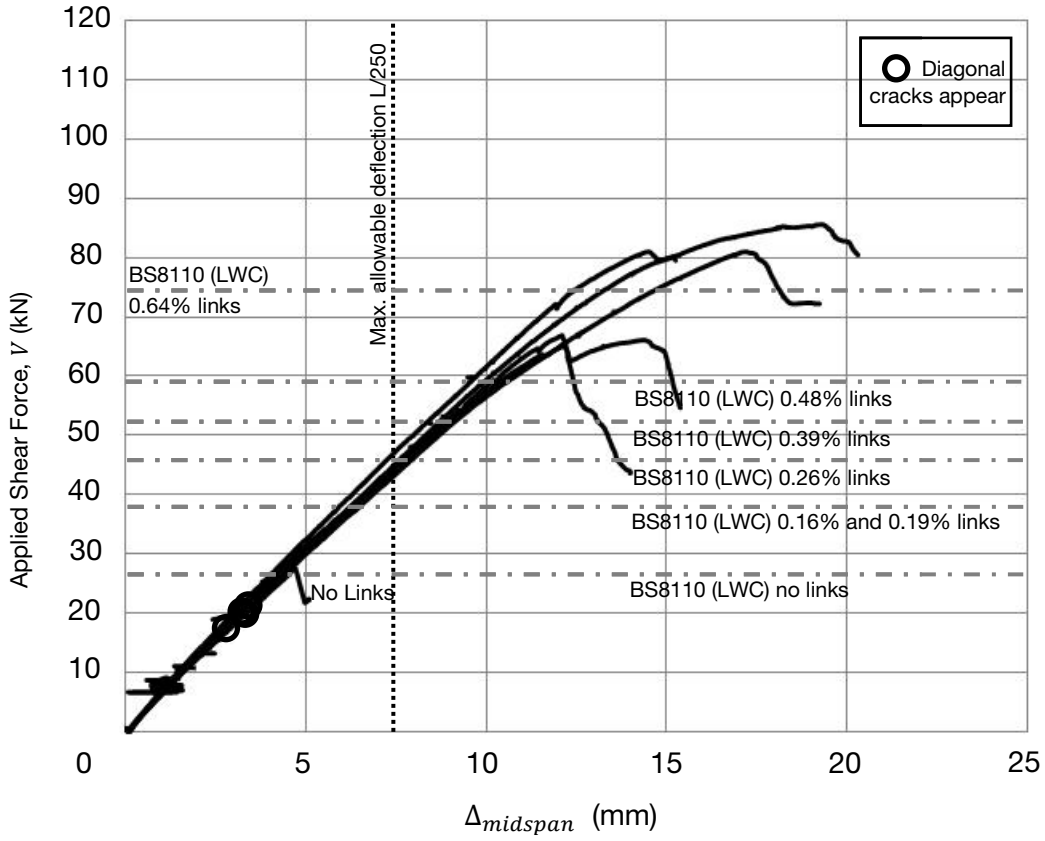

Figure 5-22 Load Deflection curve for RE series 2.51% steel

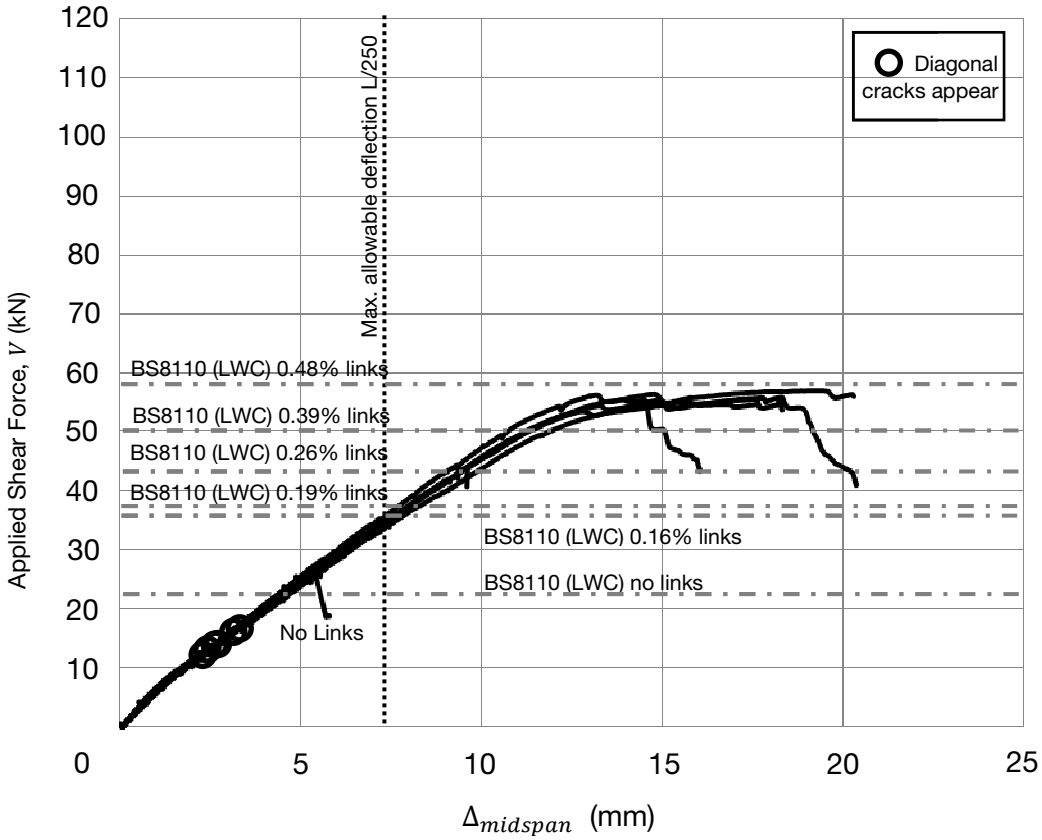

Figure 5-23 Load deflection curve for RE series 1.61% steel

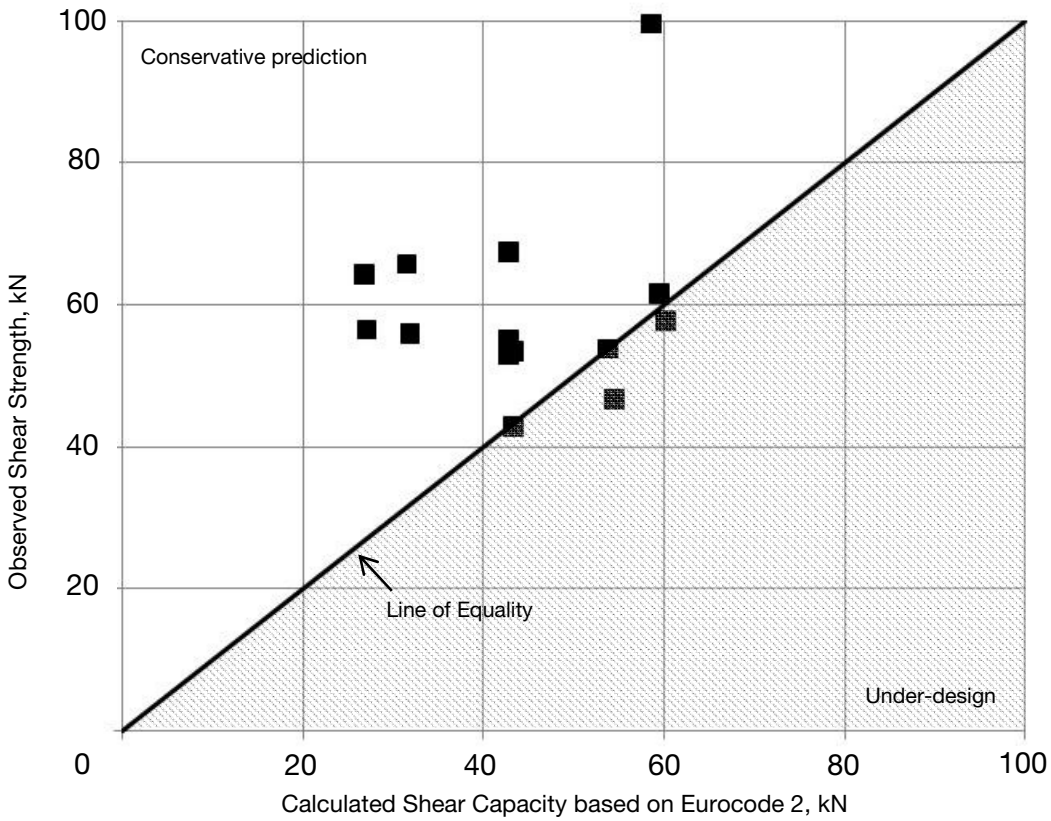

Figure 5-24 Observed shear strength to Eurocode 2 calculated shear strength

This page intentionally left blank for pagination.

Chapter 6 Conclusion

Lightweight concrete with and without aggregates is a high performance material which is advantageous for myriad of applications. It has potential to be used from sophisticated structures like prefabricated high-rise construction and architectural icons, to simple low-cost housing and rapidly erected semi-permanent structures. Successful development and understanding of the material will benefit the sustainability of human civilization as we continue to grapple with finite resources on Earth.

There remains significant lacunae in engineering knowledge with regards to shear response of reinforced concrete. This is especially true of lightweight concrete with and without aggregate which remains a maturing engineering material. While lightweight aggregate concrete has been introduced and successfully used in specialized environments, it has yet to meet mainstream acceptance as an alternative to normal weight concrete. This is not unexpected since civil engineering remains a traditional and conservative profession which has been slow to adopt new methods, materials and technologies requiring some 30 to 40 years prior to acceptance. As an interesting observation, the longest wrought iron bridge span was only constructed in 1816 after the first iron bridge was erected in 1780.

Numerous landmark structures have been built with lightweight aggregate concrete in the last half a century accompanied by a wealth of research and practical experience gained with the material. Research on this concrete has advanced with better understanding of its properties and durability. However, structural performance of lightweight aggregate concrete in shear remains at a performance validation phase with the material being benchmarked against better researched normal weight concrete. With the recent introduction and development of lightweight aggregate-foamed concrete and foamed concrete, the available behavioral range has

increased substantially. It was then an opportune time to take another look at approaches to shear design and failure models/mechanisms which have been hereinto confined to data and observations of normal weight concrete.

Experimental tests and rigorous observations conducted and presented in Chapter Three of this dissertation indicates that design equations and theoretical models developed with normal weight concrete can be generalized and extended to cover lightweight concretes with lightweight coarse aggregate and normal weight sand as well as foamed concrete varieties in a rational manner. There also does not appear to be any weaknesses that can be considered as a significant material deficiency precluding it from structural use. On the contrary, suitable design and detailing rules can be established to account for these weaknesses without compromising safety while simultaneously not mandating provision of large quantities of superfluous steel reinforcement.

While restrictions on lightweight concrete imposed by design codes may be over-conservative in some areas (Birjandi and Clarke 1993, Clarke and Birjandi 1990), the values applied for shear strength of concrete is justified for lightweight aggregate concrete. This is because of the way the design code define failure in shear. Physical rupture of concrete remains consistant between normal weight concrete and lightweight aggregate-normal weight sand concrete, but when considering the onset of cracking, then there is significant loss of reserve shear strength in the latter.

6.1 Conclusion

An experimental test program on lightweight concrete beams and companion reference normal weight concrete beams were tested until failure. Development of cracks in the beams were keenly and rigorously observed with the results presented in Chapter Three. The results were analyzed and compared with empirical equations

in the literature as well as international reinforced concrete building codes. Within the scope of this study, the following conclusions can be arrived at:

6.1.1 Shear transfer mechanism and failure models of lightweight aggregate concrete with normal weight sand, and foamed concrete

1. Lightweight coarse aggregate with normal weight sand concrete beams behaved in similar manner to the reference normal weight concrete beams until onset of diagonal cracking. Thereafter, while normal weight concrete beams were able to continue resisting shear until a flexural mode of physical failure occurred, lightweight aggregate with normal weight sand concrete was unable to develop sufficient resistance and physically failed in a brittle shear mode.

2. Foamed concrete and lightweight coarse aggregate-foamed concrete also responded to loads like normal weight concrete. Diagonal cracking occurred at lower loads than both normal weight concrete and lightweight coarse aggregate with normal weight sand concrete due to its tensile strength being much lower than the reference concrete although having comparable compressive strengths. Nevertheless, after the onset of diagonal cracking, foamed concrete and lightweight coarse aggregate-foamed concrete was able to continue resisting significant amount of shear prior to physical ultimate failure.

3. The ability of foamed concrete and lightweight coarse aggregate-foamed concrete to continue resisting shear after diagonal cracking is due to the irregular and angular cracking plane at macro level compared to the smooth crack surface at the micro level.

4. Diagonal cracking of concrete is random and its location cannot be accurately predicted. The mechanism resisting shear is a highly complex and indeterminate leading to the usefulness of empirical equations in guiding safe design of concrete structures being of vital importance.

5. No noticeable difference in cracking patterns was observed between the different types of lightweight concretes tested which cannot be attributed to the compressive strength of the concrete.

6.1.2 Design methods for lightweight aggregate concrete with normal weight sand beams

1. Comparison of the ultimate limit state and serviceability limit state performance of these high-strength lightweight coarse aggregate – normal weight fine aggregate concrete beams without transverse reinforcement against design equations of the American Concrete Institute and the British Standards Institute show that the equations can be used with confidence.
2. Diagonal cracking of lightweight aggregate with normal weight sand concrete beams without transverse reinforcement only occur beyond the design loads and deflection limits imposed. However, caution should be exercised when considering the behavior of lightweight aggregate with normal weight sand concrete beams without transverse reinforcement beyond service loads as the physical shear capacity of the material may be exhausted prior to its flexural capacity.

3. From the results of the test on 38 rectangular beams with transverse reinforcement, it was found that both BS8110 and Eurocode 2 produces safe and economical designs for lightweight aggregate with normal weight sand concrete beams with transverse reinforcement. However, when compared to

normal weight concrete of this test, some loss in reserve shear strength beyond that calculated by the code was evident. Nevertheless, this does not affect the design philosophy except that designers should be cognizant of the potential loss in ductility when designing shear critical lightweight concrete members such as transfer beams.

6.1.3 Model and prediction equation for shear strength of lightweight aggregate concrete with normal weight sand

1. Using the diagonal cracking and ultimate shear capacity data generated from this test program, a prediction equation was derived for shear strength of lightweight coarse aggregate-normal weight sand concrete beams based on the parametric behavior model of Russo *et al.* (2005). This equation was then tested against the results of a set of rectangular lightweight aggregate concrete beams from the literature and found to be in good agreement across the range of parameters tested.

6.2 Suggestions for Future Work

The shear response of lightweight concrete beams was the main focus of the study reported in this dissertation. Three types of lightweight concrete was tested including lightweight aggregate concrete with lightweight coarse aggregates and normal weight sand, lightweight aggregate-foamed concrete, and foamed concrete. While a large number of lightweight aggregate concrete beams were tested, only a small set of lightweight aggregate-foamed concrete, and foamed concrete beams were prepared. These foam concrete variants were found do have developed shrinkage cracking, an issue that requires further material research to control and mitigate. Measures such as internal curing using water absorbed by lightweight aggregates, and a more rigorous curing regime should be explored.

These foamed concrete materials had good compression strengths and could be developed for use in compression only structures such as domes and arched structures. The lightweight, fast preparation and easy casting can avail itself for use in semi-permanent structures such as disaster relief shelters. Further research into the structural behavior of foamed concretes should be pursued, particularly in durability aspects and creep performance which may be of interest when foamed concrete is used for compression only structures.

Analysis of the experimental results presented here can also be extended to include mathematical expressions of the dowel action of the reinforcing steel as well as of bond characteristics of deformed bars and welded wire mesh on the shear behavior of lightweight concrete beams without transverse reinforcement. The qualitative shear resistance model can also be further extended to lightweight concrete beams with transverse reinforcement. Although reinforced concrete beams with transverse reinforcement are able to develop truss action, nevertheless, understanding of the behavior of the concrete pre-cracking is important to decipher the ultimate behavior with truss action.

The experimental results of the second phase of R-series of tests can also be used as another important data point in continuing efforts to derive a rational theory on the shear strength of reinforced concrete. This experimental program covers a wide range of longitudinal and transverse reinforcement as well as lightweight concrete compressive strengths. Further testing of lightweight concrete beams with rebar cages carefully fabricated and instrumented with strain gauges on links and tested with the deformation on the concrete faces measured may yield further clues as to the behavior of a reinforced concrete member. The range of reinforcement ratios may be expanded to cover longitudinal steels less than 1.06% used in this study.

As cracking of lightweight concrete passes through the aggregate, a sufficiently different characteristic of concrete cracking is generated that can allow further insights and validation of the rational theories. A wider spread of material properties are available when using lightweight aggregates that can expand the range of softened concrete behavior compared with normal weight concretes. Since lightweight concretes have been observed to have fundamentally similar behavior to normal weight concrete, experimental studies on specialized bi-axial tension-compression rigs should be extended to using lightweight aggregate concrete.

This page intentionally left blank for pagination.

References

ACI Committee 213, 2006, “Guide for Structural Lightweight-Aggregate Concrete (ACI213R-03),” American Concrete Institute, Farmington Hills, Michigan, 38 pp.

ACI Committee 318, 2004, “Building Code Requirements for Structural Concrete (ACI 318-05) and Commentary (ACI 318R-05),” American Concrete Institute, Farmington Hills, Michigan, 430 pp.

ACI Committee 363, 2006, “State-of-the-Art Report on High-Strength Concrete (ACI 363R-92),” American Concrete Institute, Farmington Hills, Michigan, 55 pp.

Ahmad, S. H.; Xie, Y.; and Yu, T., 1994, “Shear Strength of Reinforced Lightweight Concrete Beams of Normal and High-Strength Concrete,” *Magazine of Concrete Research*, V.46, No. 166, Mar., pp. 57-66.

Ahmad, S. H.; Khaloo. A. R.; and Poveda A., 1986, “Shear Capacity of Reinforced High-Strength Concrete Beams,”*ACI Journal*, V. 83, No. 2, pp. 297-305.

ASCE-ACI Committee 426, 1973, “The Shear Strength of Reinforced Concrete Members,” *Journal of the Structural Division*, Proceedings of ASCE, V. 99, No. 6, Jun., pp.1091-1187.

ASCE-ACI Committee 445, 1998, “Recent Approaches to Shear Design of Structural Concrete,” *Journal of Structural Engineering*, V. 124, No. 12, Dec., pp. 1375-1417.

ASTM, 2004, “C 496-04 Standard Test Method for Splitting Tensile Strength of Cylindrical Concrete Specimens,” ASTM International, West Conshohocken, United States, 5 pp.

ASTM, 2005, “C 567-05a Standard Test Method for Determining Density of Structural Lightweight Concrete” ASTM International, West Conshohocken, United States, 3 pp.

Bae, Y. H.; Lee, J. H.; and Yoon, Y. S., 2006, “Prediction of Shear Strength in High-Strength Concrete Beams Considering Size Effect,” *Magazine of Concrete Research*, V. 58, No. 4, May, pp. 193-200.

Bardhan-Roy, B. K.; and Swami, R. N., 1995, “Prediction of Shear Strength of Structural Lightweight Aggregate Concrete T-Beams,” *International Symposium on Structural Lightweight-Aggregate Concrete*, Sandefjord, Norway, pp. 117-130.

Bazant, Z. P.; and Kim, J. K., 1984, “Size Effect in Shear Failure of Longitudinally Reinforced Beams,” *ACI Journal Proceedings*, V. 81, No. 5, Sep.-Oct., pp. 456-468.

Belarbi, A; and Hsu, T. T. C., 1994, "Constitutive Laws of Concrete in Tension and Reinforcing Bars Stiffened by Concrete," *ACI Structural Journal*, V. 91, No. 4, pp. 465-474.

Belarbi A., and Hsu, T. T. C., 1995, "Constitutive Laws of Softened Concrete in Biaxial Tension-Compression," *ACI Structural Journal*, V. 92, No. 5, pp. 562-573.

Birjandi, F. L.; and Clarke, J. L., 1993, "Deflection of Lightweight Aggregate Concrete Beams," *Magazine of Concrete Research*, V. 45, No. 162, Mar., pp. 43-49.

British Standards Institute, 1997, "BS 8110-1:1997 Structural use of concrete. Code of practice for design and construction," British Standards Institute, London, 168 pp.

British Standards Institute, 1998, "BS EN 1097-3:1998 Tests for mechanical and physical properties of aggregates. Determination of loose bulk density and voids," British Standards Institute, London, 10 pp.

British Standards Institute, 1998, "BS EN 1097-3:1998 Tests for mechanical and physical properties of aggregates. Part 3: Determination of loose bulk density and voids," British Standards Institute, London, 6pp.

British Standards Institute, 2000, "BS EN 1097-6:2000 Tests for Mechanical and Physical Properties of Aggregates. Part 6: Determination of Particle Density and Water Absorption," British Standards Institute, London, 29 pp.

British Standards Institute, 2008, "BS EN 1097-7:2008 Tests for Mechanical and Physical Properties of Aggregates. Part 7: Determination of the Particle Density of Filler — Pyknometer Method," British Standards Institute, London, 13 pp.

Building and Construction Authority, 2005, "Code of Practice on Buildable Design," Building and Construction Authority, Singapore, 69 pp.

Choi, K. K.; Park, H. G.; and Wight, J. K., 2007, "Shear Strength of Steel Fiber-Reinforced Concrete Beams without Web Reinforcement," *ACI Structural Journal*, V. 104, No. 1, Jan.-Feb., pp 12-21.

Clarke, J. L., 1987, "Shear Strength of Lightweight Aggregate Concrete Beams: Design to BS 8110," *Magazine of Concrete Research*, V.39, No. 141, Dec., pp. 205-213.

Clarke, J. L.; Birjandi, F. K., 1990, "Punching Shear Resistance of Lightweight Aggregate Concrete Slabs," *Magazine of Concrete Research,* V. 42, No. 152, Sep., pp. 171-176.

Clarke, J. L., ed., 1993, "Structural lightweight-aggregate concrete," Blackie Academic and Professional, London, 240 pp.

Chana, P. S., 1987, "Investigation of the Mecahnism of Shear Failure of Reinforced Concrete Beams," *Magazine of Concrete Research*, V.39, No. 141, Dec., pp. 196-204.

Chandra, S.; and Berntsson, L., 2003, "Lightweight Aggregate Concrete," Noyes Publications, Norwich, N.J., 430 pp.

Chung, W.; and Ahmad, S. H., 1994, "Model for Shear Critical High-Strength Concrete Beams," *ACI Structural Journal*, V. 91, No. 1, Jan.-Feb., pp. 31-41.

Centre for Civil Engineering Research and Codes (CUR), 1995, "CUR Report 173 – Structural Behaviour of Concrete with Coarse Lightweight Aggregates," Centre for Civil Engineering Research and Codes, Gouda, the Netherlands, 79 pp.

Collins, M. P., 1978, "Towards a Rational Theory for RC Members in Shear," *Journal of the Structural Division Proceedings of the ASCE*, V. 104, No. ST4, Apr., pp. 649-666.

Dei Poli, S.; Di Prisco, M.; and Gambarova, P. G., 1990, "Stress Field in Web of RC Thin-Webbed Beams Failing in Shear," *Journal of Structural Engineering*, V. 116, No. 9, Sep., pp. 2496-2515.

Elzanaty A. H.; Nilson, A. H.; and Slate, F. O., 1986, "Shear Capacity of Prestressed Concrete Beams Using High-Strength Concrete," *ACI Journal,* V. 83, No. 3, May-Jun., pp. 359-368.

Evans, R. H.; and Dongre, A. V., 1963, "The Suitability of a Lightweight Aggregate (Aglite) for Structural Concrete," *Magazine of Concrete Research*, V. 15, No. 44, Jul., pp. 93-100.

Federation Internationale de la Precontraine (FIP), 1983, "FIP Manual of Lightweight Aggregate Concrete," Halsted Press, New York, 259 pp.

Fenwick, R. C.; and Paulay, T., 1968, "Mechanisms of Shear Resistance of Concrete Beams," *Journal of the Structural Division ASCE*, V. 94, No. 10, pp. 2325-2350.

FIB Task Group 8.1, 1999, "Bulletin 8 Lightweight Aggregate Concrete – Codes and Standards," International Federation for Structural Concrete, Lausanne, Switzerland, 40 pp.

FIB Task Group 8.1, 2000, "Lightweight Aggregate Concrete," International Federation for Structural Concrete, Lausanne, Switzerland.

Finnimore, B., 1989, "Houses from the Factory: System Building and the Welfare State 1942-74," Rivers Oram Press, London, 278 pp.

Gambarova, P. G., 1981, "On Aggregate Interlock Mechanism in Reinforced Concrete Plate it Extensive Cracking," IABSE Colloquium, Zurich, pp. 105-134.

Gerritse, A., 1981, “Design Considerations for Reinforced Lightweight Concrete,” *International Journal of Cement Composites and Lightweight Concrete,* V. 3, No. 1, Feb., pp 57-69.

Gopalaratnam, V. S.; and Shah, S. P., 1985, “Softening Response of Plain Concrete in Direct Tension,” *ACI Journal Proceedings,* V. 82, No. 3, pp. 310-323.

Grutzeck, M. W., 2005, “Cellular Concrete,” in *Cellular Ceramics: Structure, Manufacturing, Properties and Applications*, Scheffler, M.; and Paolo, C. (eds.), Wiley – VCH Verlag, Weinheim, pp. 193-223.

Hamadi, Y. D.; and Regan, P. E., 1980, “Behaviour in Shear of Beams with Flexural Cracks, *Magazine of Concrete Research*,” V. 32, No. 1, pp. 67-77.

Hanson, J. A., 1958, “Shear Strength of Lightweight Reinforced Concrete Beams, *ACI Journal Proceedings,* V. 55, No. 3, pp. 307-404.

Hanson, J. A., 1961, “Tensile Strength and Diagonal Tension Resistance of Structural Lightweight Concrete,” *ACI Journal Proceedings*, V.58, No.1, pp.1-40.

Hanson, J. A., 1968, “Effects of Curing and Drying Environments on Splitting Tensile Strength,” *ACI Journal Proceedings*, V. 65, No. 7, Jul., pp. 535-543.

Head, P. R., 2001, “Construction Materials and Technology: A Look at the Future,” *Proceedings of the ICE*, Civil Engineering, V. 144, Aug., pp. 113-118.

Hognestad, E.; Elstner, R. C.; and Hanson, J. A., 1964, “Shear Strength of Reinforced Structural Lightweight Aggregate Concrete Slabs,” *Journal of th ACI Proceedings*, V. 61, No. 6, Jun., pp. 643-653.

Holland, I., 1995, “Supplement to Model Code 90 for LWA Structural Concrete,” *International Symposium on Structural Lightweight-Aggregate Concrete*, Sandefjord, Norway, pp. 176-179.

Holm, T. A., and Bremner, T. W., 2000, “ERDC/SL TR-0-3 State of the Art Report on High-Strength, High Durability Structural Low Density Concrete for Applications in Severe Marine Environments,” US Army Corp of Engineers, Washington, DC, 116 pp.

Hsu, T. T. C., 1993, “Unified Theory of Reinforced Concrete,” CRC Press, Boca Raton, 313 pp.

Huffington, J. A., 2000, “Development of High-Performance Lightweight Concrete Mixes for Prestressed Bridge Firdsers,” University of Texas at Austin, in ACI213R.

Ivey, D. L., and Buth, E., 1967, “Shear Capacity of Lightweight Concrete Beams,” *ACI Journal Proceedings*, V. 64, No. 10, Oct., pp. 634-643.

The Institution of Structural Engineers (IStructE) and The Concrete Society, 1987, "Guide to the Structural Use of Lightweight Aggregate Concrete," The Institution of Structural Engineers, London, 58 pp.

Jones, M. R.; and McCarthy, A., 2005, "Preliminary Views on the Potential of Foamed Concrete as a Structural Material," *Magazine of Concrete Research*, V. 57, No. 1, Feb., pp. 21-31.

Kani, G. N. J., 1966, "Basic Facts Concerning Shear Failure," Journal of the American Concrete Institute, *Proceedings*, V. 63, No. 6, pp. 675-691.

Keown, P.; Cleland, D. J.; Gilbert, S. G.; and Sloan, D., 2006, "Shear in Reinforced Concrete Continuous Beams," *The Structural Engineer*, V. 84, No. 16, Aug., pp. 24-28.

Kim, W.; and White, R. N., 1991, "Initiation of Shear Cracking in Reinforced Concrete Beams with No Web Reinforcement," *ACI Structural Journal*, V. 88, No. 3, May-Jun., pp. 301-308.

Kim, J. K.; and Park, Y. D., 1996, "Prediction of Shear Strength of Reinforced Concrete Beams without Web Reinforcement," *ACI Materials Journal*, V. 93, No. 3, May-Jun., pp. 213-222.

Kupfer, H.; Mang, R.; and Karavesyrouglou, M.,1983, "Failure of the Shear-zone of R.C. and P.C. Girders – An Analysis with Consideration of Interlocking of Cracks," *Bauingenieur*, V.58, pp. 143-149, in ASCE-ACI 445.

Kupfer, H. B.; and Gerstle, K. H., 1973, "Behavior of Concrete Under Biaxial Stresses," *Journal of the Engineering Mechanics Division*, V. 99, No. EM4, Aug., pp853-866.

Krefeld, W. J.; and Thurston, C. W., 1966a, "Contribution of Longitudinal Steel to Shear Resistance of Reinforced Concrete Beams," *Journal of the American Concrete Institute*, V. 63, No. 3, Mar., pp. 325-344.

Krefeld, W. J.; and Thurston, C. W., 1966b, "Studies of the Shear and Diagonal Tension Strength of Simply Supported Reinforced Concrete Beams," *Journal of the American Concrete Institute*, V. 63, No. 4, Apr., pp. 451-476.

LaRue, H. A., 1946, "Modulus of Elasticity of Aggregates and its Effect on Concrete," *Proceedings* 46, ASTM International, West Conshohocken, pp. 1298-3098, in ACI 213R-03.

Levinson, M., 2006, "The Box: How the Shipping Container Made the World Smaller and the World Economy Bigger," Princeton University Press, Princeton, 276 pp.

Lim H. S., 2007, "Structural Response of LWC Beams in Flexure," Ph.D Thesis Submitted to National University of Singapore, 244 pp.

Lomborg, B., 2001, “The Skeptical Environmentalist : Measuring the Real State of the World,” Cambridge University Press, New York, 515 pp.

MacGregor, J. G.; and Wight, J. K., 2005, “Reinforced Concrete Mechanics and Design, 4th Edition,” Pearson Prentice Hall, Upper Saddle River, N. Jersey, 1132 pp.

Malhotra, V. M., 1976, “No-Fines Concrete - Its Properties and Applications,” *ACI Journal Proceedings*, V. 73, No. 11, Nov., pp. 628-644.

Mander, J. B., 1998, “Shear Controversy,” *Journal of Structural Engineering*, V. 124, No. 12, Dec., pp. 1374.

Mansur, M. A.; Lee, C. K.; and Lee, S. L., 1986, “Anchorage of Welded Wire Fabric Used as Shear Reinforcement in Beams,” *Magazine of Concrete Research*, V. 38, No. 134, Mar., pp. 36-46

Mattock, A. H.; and Hawkings, N. M., 1972, “Research on Shear Transfer in Reinforced Concrete,” *PCI Journal,* V. 17, No. 2, pp. 55-75.

McCormick, F. C., 1967, “Rational Proportioning of Preformed Foam Cellular Concrete,” *ACI Journal*, V. 64, No. 2, Feb., pp. 104-110.

Millard, S. G., and Johnson, R. P., 1984, “Shear Transfer Across Cracks in Reinforced Concrete due to Aggregate Interlock and to Dowel Action,” *Magazine of Concrete Research,* V. 36, No. 126, Mar., pp. 9-21.

Mindess, S.; Young, J. F.; and Darwin, D., 2003, “Concrete, Second Edition,” Prentice Hall, Upper Saddle River, N. Jersey, 644 pp.

Mphonde, A. G.; and Frantz, G. C., 1984, “Shear Tests of High- and Low-Strength Concrete Beams Without Stirrups,” *ACI Journal Proceedings*, V. 81, No. 4, Jul.-Aug., pp. 350-357.

Narayanan, R. S.; and Beeby, A., 2005, “Designer’s Guide to EN1992-1-1 and EN1992-1-2 Eurocode 2: Design of Concrete Structures,” Thomas Telford Publishing, London, 218 pp.

Nassar, A. J., 2002, “Investigation of Transfer Length, Development Length, Flexural Strength and Prestress Loss Trend in Fully Bonded High-Strength Lightweight Prestressed Girders,” Virginia Polytechnic Institute and State University, May, 136 pp., in ACI 213R-03.

Nesbit, J. K., 1966, “Structural Lightweight-Aggregate Concrete,” Concrete Pub., London, 280 pp.

Neville, A. M., 1999, “Properties of Concrete, Fourth Edition,” Longman, Essex, 844 pp.

Niwa, J.; Yamada, K.; Yokozawa, K.; and Okamura, H., 1986, "Revaluation of the Equation for Shear Strength of Reinforced Concrete Beams without Web Reinforcement," Translated from *Proceedings of Japan Society of Civil Engineering*, V. 5, No. 372, 1986-1988.

Okamura, H.; and Higai, T., 1980, "Proposed Design Equation for Shear Strength of R.C. Beams without Web Reinforcement," *Proceedings of the Japan Society of Civil Engineering*, V. 300, pp. 131-141, in ACI 445, 1998.

Owens, P. L., 1993, "Lightweight Aggregates for Structural Concrete," Structural Lightweight Aggregate Concrete, J. L. Clarke, ed., Blackie Academic and Professional, London, pp. 1-18.

Pang, X.; and Hsu, T. T. C., 1995, "Behavior of Reinforced Concrete Membrane Elements in Shear," *ACI Structural Journal*, V. 92, No. 6, pp. 665-679.

Pauw, A., 1960, "Static Modulus of Elasticity of Concrete as Affected by Density," *Journal of the American Concrete Institute. Proceedings,* V. 57, No. 6, Dec., pp. 679-687.

Pfeifer, D. W., 1967, "Sand Replacement in Structural Lightweight Concrete," *ACI Journal Proceedings*, V. 64, No. 7, pp. 384-392.

Philleo, R., 1991, "Concrete Science and Reality," Materials Science of Concrete II, Skalny, J. P. and Mindess, S., eds., American Ceramic Society, Westerville, OH, pp. 1-8.

Ramirez, J. A., 1998, "Recent Approaches to Shear Design of Structural Concrete," *Journal of Structural Engineering*, V. 124, No. 12, Dec., pp. 1374.

Ramirez, J. A.; Olek, J.; and Malone, B. J., 2004, "Shear Strength of Lightweight Reinforced Concrete Beams," *High-Performance Structural Lightweight Concrete*, SP-218, J. P. Ries and T. A. Holm, eds., American Concrete Institute, Farmington Hills, Mich., pp. 69-90.

Regan, P. E., 1993, "Research on Shear: A Benefit to Humanity or a Waste of Time?" *The Structural Engineer*, V. 71, No. 19, Oct., pp. 337-347.

Regan, P. E.; and Arasteh, A. R., 1990, "Lightweight Aggregate Foamed Concrete," *The Structural Engineer*, V. 68, No. 9, May., pp. 167-173.

Regan, P. E.; Kennedy-Reid, I. L.; Pullen, A. D.; and Smith, D. A., 2005, "The Influence of Aggregate Type on the Shear Resistance of Reinforced Concrete," *The Structural Engineer*, V. 83, No. 23, Dec., pp. 27-32.

Reibeiz, K. S., 1999, "Shear Strength Prediction for Concrete Members," *Journal of Structural Engineering*, ASCE, V.125, No. 3, pp.301-308.

Reineck, K. H., 1991, "Ultimate Force of Structural Concrete Members without Transverse Reinforcement Derived from a Mechanical Model," *ACI Structural Journal*, V. 88, No. 5, Sep.-Oct., pp. 592-602.

Reinhardt. H. W.; Cornelissen, H. A. W.; and Hordijk, D. A., 1986, "Tensile Tests and Failure Analysis of Concrete," *Journal of Structural Engineering ASCE*, V. 112, No. 11, pp. 2462-2477.

Russo, G.; Somma, G.; and Mitri, D., 2005, "Shear Strength Analysis and Prediction for Reinforced Concrete Beams without Stirrups," *Journal of Structural Engineering,* V. 131, No. 1, Jan., pp. 66-74.

Salandra, M. A.; and Ahmad, S. H., 1989, "Shear Capacity of Reinforced Lightweight High-Strength Concrete Beams," *ACI Structural Journal*, V. 86, No. 6, Nov.-Dec., pp. 697-704.

Sherwood, E. G.; Bentz, E. C.; and Collins, M. P., 2007, "Effect of Aggregate Size on Beam-Shear Strength of Thick Slabs," *ACI Structural Journal*, V. 104, No 2, Mar.-Apr., pp. 180-190.

Slate, F. O.; Nilson, A. H.; and Martinez, S., 1986, "Mechanical Properties of High-Strength Lightweight Concrete," *ACI Journal*, V. 84, No. 4, Jul.-Aug., pp. 606-613.

Tam, C. T.; Lim, T. Y.; and Lee, S. L., 1987, "Relationship Between Strength and Volumetric Composition of Moist-cured Cellular Concrete," *Magazine of Concrete Research*, V. 39, No. 138, Mar., pp. 12-18.

Taylor, R., 1959, "A note on the Mechanism of Diagonal Cracking in Reinforced Concrete Beams without Shear Reinforcement," *Magazine of Concrete Research*, V. 11, No. 33, Nov., pp. 159-162.

Taylor, R., 1960, "Some Shear Tests on Reinforced Concrete Beams without Shear Reinforcement," *Magazine of Concrete Research*, V. 12, No. 36, Nov., pp.145-154.

Taylor, R.; and Brewer, R. S., 1963, "The Effect of the Type of Aggregate on the Diagonal Cracking of Reinforced Concrete Beams," *Magazine of Concrete Research*, V. 15, No. 44, Jul., pp. 87-92.

Thorenfeldt, E.; Stemland, H.; and Tomaszewicz, A., 1995, "Shear Capacity of Large I-beam," *International Symposium on Structural Lightweight-Aggregate Concrete*, Sandefjord, Norway, pp. 733-744.

Thorenfeldt, E.; and Stemland, H., 2000, "Shear Capacity of Lightweight Concrete Beams without Shear Reinforcement," *Second International Symposium on Structural Lightweight Aggregate Concrete,* Kristiansand, Norway, pp. 244-255.

Tureyen, A. K., and Frosch, R. J., 2003, "Concrete Shear Strength: Another Perspective," *ACI Structural Journal*, V. 100, No. 5, Sep.-Oct., pp. 609-615.

Vintzeleou, E. N.; and Tassios, T. P., 1986, "Mathematical Models for Dowel Action Under Monotonic and Cyclic Conditions," *Magazine of Concrete Research*, V. 38, No. 134, Mar., pp. 13-22.

Vecchio, F. J.; and Collins, M. P., 1986, "The Modified Compression-Field Theory for Reinforced Concrete Elements Subjected to Shear," *ACI Journal Proceedings,* V. 83, No. 2, Mar.-Apr., pp. 219-231.

Walraven, J., 1981, "Fundamental Analysis of Aggregate Interlock," *Journal of the Structural Division,* ASCE, V.108, pp. 2245-2270.

Walraven, J.; and Al-Zubi, N., 1995, "Shear Capacity of Lightweight Concrete Beams with Shear Reinforcement," *International Symposium on Structural Lightweight-Aggregate Concrete*, Sandefjord, Norway, pp. 91-104.

Weber, S.; and Reinhardt, H., 1995, "A Blend of Aggregates to Support Curing of Concrete," *International Symposium on Structural Lightweight-Aggregate Concrete*, Sandefjord, Norway, pp. 662-671.

Wee, T.H., 2005, "Recent Developments in High Strength Lightweight Concrete with and without Aggregates," *Construction Materials: Performances, Innovations and Structural Implications and Mindess Symposium*, Proceedings of Third International Conference, N. Banthia; T. Uomoto; A. Bentur; and S. P. Shah, eds., Vancouver, British Columbia, Canada, 97 pp.

Wesche, K. 1968, "Regulations for Reinforced and Prestressed Lightweight-aggregate Concrete in Various Countries," *International Congress on Lightweight Concrete,* Proceedings of First International Congress on Lightweight Concrete, Brooks, A. E., ed., London, pp. 225-233.

Zararis, P. D.; and Papadakis, G. Ch., 2001, "Diagonal Shear Failure and Size Effect in RC Beams without Web Reinforcement," *Journal of Structural Engineering*, V. 127, No. 7, Jul., pp. 733-742.

Zsutty, T.C., 1971,"Shear Strength Prediction for Separate Categories of Simple Beams Tests," ACI Structural Journal, V. 68, No. 2, pp. 138-143.

-------- END --------